

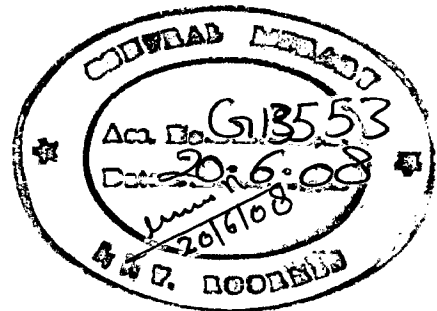
REMOVAL OF LEAD FROM WASTE WATER BY ADSORPTION

A DISSERTATION

*Submitted in partial fulfillment of the
requirements for the award of the degree*
of
MASTER OF TECHNOLOGY
in
CHEMICAL ENGINEERING
(With Specialization in Industrial Pollution Abatement)

By

RAMAMOHANA RAO LATCHIREDDI



**DEPARTMENT OF CHEMICAL ENGINEERING
INDIAN INSTITUTE OF TECHNOLOGY ROORKEE
ROORKEE - 247 667 (INDIA)
JUNE, 2007**

CANDIDATE'S DECLARATION

I hereby declare that the work, which is being presented in the dissertation entitled “**REMOVAL OF LEAD FROM WASTE WATER BY ADSORPTION**” in the partial fulfillment of the requirements of the award of the degree of Master of Technology in Chemical Engineering with specialization in **Industrial Pollution Abatement**, submitted in the **Department of Chemical Engineering of Indian Institute of Technology Roorkee**, under the kind guidance of **Dr. SHRI CHAND**, Professor and Head, Chemical Engineering Department, Indian Institute of Technology Roorkee, Roorkee.

The matter embodied in this dissertation has not been submitted by me for the award of any other degree of this or any other Institute.

Date: 25th June, 2007.

Place: Roorkee.

L. Ramamohana Rao
(RAMAMOHANA RAO LATCHIREDDI)

CERTIFICATE

This is to certify that the above statement made by the candidate is correct to the best of my knowledge and belief.

Shri Chand
25/6/07
(Dr. SHRI CHAND)

Professor & Head,
Department of Chemical Engineering,
Indian Institute of Technology Roorkee,
Roorkee – 247 667 (India).

ACKNOWLEDGEMENT

This is consummated and symbolized not only my efforts but also guidance and vital inputs of different people at crucial junctures in the course of this undertaking to whom I would like to express my gratitude.

I wish to express my deep sense of gratitude and sincere thanks to my loving guide **Dr. Shri Chand** , Professor and Head ,Chemical Engineering Department, IIT Roorkee, for being helpful and a great source of inspiration. His keen interest and constant encouragement gave me the confidence to complete my work. I wish to extend my sincere thanks to for their excellent guidance and suggestions for the successful completion of my dissertation work.

My special thanks are due to Mr. Pradeep Kumar Saini (Research Scholar) for his immense help, kind suggestion and motivation and I am also very thankful to Mr.Arvind and Mr. Dilip (Research Scholars).

I am thankful to Shri Ayodhya Prasad (Senior Lab. Attendant), Pollution Abatement Research Lab, to Shri Sat Pal (I.A.Lab), Lab Technician and other employees of Dept .of Chemical Engineering, IIT Roorkee, Roorkee for their continuous help during the experimental work.

I am greatly indebted to all my friends whose enthusiastic support, encouragement and help, made me come up with this report. Though it is not possible to mention everyone, none can be forgotten for their direct/indirect help.

This report saw the light of the day only due to the encouragement and unflinching support and love of my parents and brother. Utmost thanks are due to the Almighty, for providing me the knowledge and wisdom for the successful completion of this report.

Date: 25th June 2007

(**RAMAMOHANA RAO LATCHIREDDI**)

ABSTRACT

The pollution of water resources due to indiscriminate disposal of heavy metals has been causing worldwide concern for the last few decades. Unlike organic pollutants, the majority of which are susceptible to bio-degradation, heavy metals are non-degradable to harmless end products. They are toxic to aquatic flora and fauna even in relatively low concentrations. Metals, which are significantly toxic to human beings and ecological environments, include arsenic (As), chromium (Cr), copper (Cu), lead (Pb), mercury (Hg), manganese (Mn), cadmium (Cd), nickel (Ni), zinc (Zn) and iron (Fe), etc.

Lead, an element which has been used by man for years, can be regarded as a longstanding environmental contaminant. All the chemicals/compounds containing lead are considered as cumulative poisons that usually affect the gastrointestinal track, nervous system and sometimes both. The chief sources of lead in water are the effluents of processing industries. Apart from this lead is also used in storage batteries, insecticides, plastic water pipes, food, beverages, ointments and medicinal concoctions for flavoring and sweetening. Lead poisoning causes damage to liver, kidney and reduction in hemoglobin formation, mental retardation, infertility and abnormalities in pregnant women etc.

There are several methods for removing toxic/heavy metals from aqueous solutions, such as chemical precipitation, membrane filtration, ion exchange, biosorption and adsorption. Removal of lead from contaminated water bodies has been attempted by several researchers employing a wide variety of techniques. Majority of these are adsorption on various surfaces like activated carbon, peat, goethite mineral, hydrated iron etc.

In the present study laboratory scale experiments have been carried out using the Coconut Jute Activated Carbon (CJAC) and Commercial Activated Carbon (CAC) as adsorbents for the removal of Lead. The present study has been undertaken with the objective to

investigate the suitability of CJAC as a low cost adsorbent for the removal of Lead as replacement of CAC. Batch experiments were carried out to determine the effect of various factors such as contact time, initial concentration, pH, adsorbent dose, adsorbent particle size and temperature on adsorption process.

Kinetic study shows that adsorption of Pb(II) on CJAC and CAC follows the Pseudo-second order kinetics. Langmuir isotherm best-fitted the isotherm data for Pb(II) adsorption on CJAC and CAC at almost all temperatures. However, the error analysis values and the non-linear correlation coefficients, R^2 , are comparable for Langmuir, Temkin isotherms (for CJAC) and Langmuir, Temkin, Redlich-Peterson (for CAC). Adsorption rate increases with increase in temperature for both the adsorbents, showing the endothermic nature of adsorption. From thermodynamic study ΔG^0 , ΔH^0 and ΔS^0 values are also calculated for both adsorbents.

CONTENTS

	Page No.
CANDIDATE'S DECLARATION	i
ACKNOWLEDGEMENT	ii
ABSTRACT	iii
NOMENCLATURE	ix
LIST OF FIGURES	x
LIST OF TABLES	xii
Chapter 1: INTRODUCTION	1
1.1 Lead in Periodic Table	3
1.2 Sources of Lead	4
1.3 Exposure of Lead	6
1.4 Health Hazard Information	8
1.5 Environmental Levels and Standards	10
Chapter 2: GENERAL PROCESSES FOR LEAD REMOVAL	11
2.1 Chemical Precipitation	11
2.2 Ion Exchange	12
2.3 Adsorption	14
2.4 Electrodialysis	15
2.5 Solvent Extraction	15
2.6 Reverse Osmosis	16
2.7 Membrane Separation	17
2.8 Gamma Irradiation	18
2.9 Cementation	18
2.10 Biological	19

Chapter 3:	ADSORPTION FUNDAMENTALS	20
3.1	General	20
3.1.1	Physical Adsorption vs. Chemisorption	20
3.1.2	Intra-particle Diffusion Process	22
3.1.3	Stages in Adsorption Process	22
3.2	Adsorption Isotherms	23
3.2.1	Langmuir Isotherm	23
3.2.2	Freundlich Isotherm	24
3.2.3	Temkin Isotherm	25
3.2.4	Redlich-Peterson isotherm	25
3.3	Adsorption Practices	27
3.3.1	Batch Adsorption Systems	27
3.3.2	Continuous Adsorption Systems	27
3.4	Factors Controlling Adsorption	27
3.4.1	Initial Concentration	28
3.4.2	Temperature	28
3.4.3	pH	28
3.4.4	Contact Time	29
3.4.5	Degree of Agitation	29
3.4.6	Nature of Adsorbent	29
Chapter 4:	LITERATURE REVIEW	32
Chapter 5:	EXPERIMENTAL PROGRAMME	43
5.1	Objective of present study	43
5.2	Preparation of adsorbents	43
5.3	Characterization of Adsorbent	44
5.3.1	Proximate Analysis	44
5.3.2	Density	44
5.3.3	EDS Analysis for Adsorbents	44

5.3.4	Scanning Electron Micrograph (SEM)	44
5.4	Adsorbate	45
5.4.1	Analytical Measurements	45
5.5	Experimental Programme	46
5.5.1	Batch Adsorption Experiments	46
Chapter 6:	RESULTS AND DISCUSSION	48
6.1	General	48
6.2	Characterization of adsorbents	48
6.3	Batch Adsorption Studies	49
6.3.1	Effect of Initial pH	49
6.3.2	Effect of Adsorbent Dose	50
6.3.3	Effect of Initial Concentration	50
6.3.4	Effect of Contact Time	50
6.3.5	Effect of Particle Size	51
6.3.6	Effect of Temperature	51
6.4	Adsorption kinetic study	52
6.4.1	Pseudo-first-order model	52
6.4.2	Pseudo-second-order model	52
6.4.3	Weber-Morris intra-particle diffusion model	53
6.4.4	Bangham's model	54
6.5	Adsorption Equilibrium Study	54
6.5.1	Freundlich and Langmuir isotherms	54
6.5.2	The Temkin isotherm	55
6.5.3	Redlich-Peterson Isotherm	56
6.6	Error Analysis	57
6.6.1	The Sum of the Squares of the Errors	57
6.6.2	The Average Relative Error	58
6.6.3	The Hybrid Fractional Error Function	58
6.6.4	Marquardt's Percent Standard Deviation	58

6.6.5	The Sum of the Absolute Errors	58
6.6.6	Choosing best-fit isotherm based on error analysis	59
6.7	Thermodynamic Study	59
Chapter 7:	CONCLUSIONS AND RECOMMENDATIONS	61
7.1	Conclusions	61
7.2	Recommendations	62
	REFERENCES	64
	APPENDIX-A	67
	APPENDIX-B	80
	APPENDIX-C	105

NOMENCLATURE

C_o	Initial concentration of effluent (mg/l)
C_e	Concentration of adsorbate solution at equilibrium (mg/l)
K	Adsorption rate constant (1/min)
K_A	Langmuir isotherm constant, (l/mg)
K_T	Temkin isotherm constant, (l/mg)
K_F	Freundlich isotherm constant, ((mg/g)/(mg/l) ^{1/n})
$1/n$	Heterogeneity factor, dimensionless
Q_t, q_t	Amount of adsorbate adsorbed per unit amount of adsorbent at time t, (mg/g)
Q_e, q_e	Amount of adsorbate adsorbed per unit amount of adsorbent at equilibrium, (mg/g)
R_L	Separation Factor
k_f	First order rate constant, (1/min)
k_s	Second order rate constant, (g/mg min)
K_{id}	The intra-particle diffusion rate constant
ΔG°	Gibbs free energy, (KJ/mol)
ΔH°	Enthalpy, (KJ/mol)
ΔS°	Entropy, (J/ mol K)
R	Universal gas constant, 8.314 J/mol K
SSE	Sum of the Squares of the Errors
SAE	Sum of the Absolute Errors
ARE	Average Relative Error
HYBRID	Hybrid Fractional Error Function
MPSD	Marquardt's Percent Standard Deviation
CJAC	Coconut Jute Activated Carbon
CAC	Commercial Activated Carbon

LIST OF FIGURES

Fig. No	Title of Figure	Page No.
Fig. 5.1	Calibration curve	45
Fig. B-1	SEM of CJAC before adsorption	80
Fig. B-2	SEM of CJAC after adsorption	80
Fig. B-3	SEM of CAC before adsorption	81
Fig. B-4	SEM of CAC after adsorption	81
Fig. B-5	EDS pattern for CJAC before adsorption	82
Fig. B-6	EDS pattern for CJAC after adsorption	82
Fig. B-7	EDS pattern for CAC before adsorption	83
Fig. B-8	EDS pattern for CAC after adsorption	83
Fig. B-9	Effect of pH_0 on adsorption of lead by CJAC	84
Fig. B-10	Effect of pH_0 on adsorption of lead by CAC	84
Fig. B-11	Effect of adsorbent dose on adsorption of lead by CJAC	85
Fig. B-12	Effect of adsorbent dose on adsorption of lead by CAC	85
Fig. B-13	Effect of agitation time and initial lead concentration on percentage removal by CJAC	86
Fig. B-14	Effect of agitation time and initial lead concentration on percentage removal by CAC	86
Fig. B-15	Effect of agitation time and initial lead concentration on amount adsorbed on CJAC	87
Fig. B-16	Effect of agitation time and initial lead concentration on amount adsorbed on CAC	87
Fig. B-17	Effect of partical size on removal of lead by CJAC	88
Fig. B-18	Effect of partical size on removal of lead by CAC	88

Fig. B-19	Effect of temperature on removal of lead on percent removal by CJAC	89
Fig. B-20	Effect of temperature on removal of lead on percent removal by CAC	89
Fig. B-21	Effect of temperature on removal of lead on amount adsorbed by CJAC	90
Fig. B-22	Effect of temperature on removal of lead on amount adsorbed by CAC	90
Fig. B-23	First order kinetics for removal of lead by CJAC	91
Fig. B-24	First order kinetics for removal of lead by CAC	91
Fig. B-25	Pseudo second order plot for removal of lead by CJAC	92
Fig. B-26	Pseudo second order plot for removal of lead by CAC	92
Fig. B-27	Weber Morris plot for removal of lead by CJAC	93
Fig. B-28	Weber Morris plot for removal of lead by CAC	93
Fig. B-29	Bangham's plot for removal of lead by CJAC	94
Fig. B-30	Bangham's plot for removal of lead by CAC	94
Fig. B-31	Freundlich Isotherm plot for lead with CJAC	95
Fig. B-32	Freundlich Isotherm plot for lead with CAC	96
Fig. B-33	Langmuir Isotherm plot for lead with CJAC	97
Fig. B-34	Langmuir Isotherm plot for lead with CAC	98
Fig. B-35	Temkin Isotherm plot for lead with CJAC	99
Fig. B-36	Temkin Isotherm plot for lead with CAC	100
Fig. B-37	Redlich-Peterson Isotherm plot for lead with CJAC	101
Fig. B-38	Redlich-Peterson Isotherm plot for lead with CAC	102
Fig. B-39	Thermodynamic equilibrium constant values and different temperatures for CJAC	103
Fig. B-40	Thermodynamic equilibrium constant values and different temperatures for CAC	103
Fig. B-41	Van't Hoff's plot for various isotherm models.	104

LIST OF TABLES

Table. No	Title of Table	Page No:
Table 1.1	Lead in periodic table	3
Table 1.2	Permissible Lead Levels from different industrial effluent	10
Table 3 .1	Comparison of Physical and Chemical Adsorption	21
Table.3.2	Various commercial adsorbents	30
Table.3.3	Typical non conventional adsorbents	31
Table A-1	Calibration curve values for lead	67
Table A-2	Effect of pH on the removal of lead using CJAC	67
Table A-3	Effect of pH on the removal of lead using CAC	68
Table A-4	Effect of Adsorbent dose on removal of lead CJAC	68
Table A-5	Effect of Adsorbent dose on removal of lead CAC	68
Table A-6	Effect of Contact time and initial concentration of lead using CJAC	69
Table A-7	Effect of Contact time and initial concentration of lead using CAC	69
Table A-8	Effect of particle size on removal of lead with CJAC	70
Table A-9	Effect of particle size on removal of lead with CAC	70
Table A-10	Lagergren Plot for removal of lead using CJAC	71
Table A-11	Lagergren Plot for removal of lead using CAC	71
Table A-12	Pseudo second order kinetic plot for removal of lead using CJAC	72
Table A-13	Pseudo second order kinetic plot for removal of lead using CAC	72
Table A-14	Weber-Morris plot for removal of lead using CJAC	73
Table A-15	Weber-Morris plot for removal of lead using CAC	73
Table A-16	Bangham's plot for removal of lead using CJAC	74
Table A-17	Bangham's plot for removal of lead using CAC	74
Table A-18	Effect of temperature on removal of lead by CJAC	75

Table A-19	Effect of temperature on removal of lead by CAC	75
Table A-20	Freundlich isotherm for removal of lead using CJAC	76
Table A-21	Freundlich isotherm for removal of lead using CAC	76
Table A-22	Langmuir isotherm for removal of lead using CJAC	77
Table A-23	Langmuir isotherm for removal of lead using CAC	77
Table A-24	Temkin isotherm for removal of lead using CJAC	78
Table A-25	Temkin isotherm for removal of lead using CAC	78
Table A-26	Redlich Peterson isotherms for removal of lead using CJAC	79
Table A-27	Redlich Peterson isotherms for removal of lead using CAC	79
Table C-1	Characteristics of coconut jute activated carbon	105
Table C-2	Characteristics of commercial activated carbon	105
Table C-3	Pseudo-first order model	106
Table C-4	Pseudo-second order model	106
Table C-5	Weber-Morris Intra-particle diffusion model	107
Table C-6	Bangham's model	107
Table C-7	Langmuir Constants (CJAC)	108
Table C-8	Langmuir Constants (CAC)	108
Table C-9	Freundlich Constants (CJAC)	108
Table C-10	Freundlich Constants (CAC)	108
Table C-11	Temkin Constants (CJAC)	109
Table C-12	Temkin Constants (CAC)	109
Table C-13	Relich-Peterson Constants (CJAC)	109
Table C-14	Relich-Peterson Constants (CAC)	109
Table C-15	Error Analysis (CJAC)	110
Table C-16	Error Analysis (CAC)	111
Table C-17	Thermodynamic parameters for adsorption of Pb(II) by CJAC and CAC	112

CHAPTER-1

INTRODUCTION

Heavy metals can be defined in variety of ways, on the basis of their physical, chemical and biological properties. Metals with specific gravity of about 5g/cm^3 or greater are generally defined as heavy metals and these include metals from group II A, III B, IV B, V B and VI B of the periodic table. Lead symbolized Pb is located in group IV of the periodic table, it has an atomic weight and number of 207.19 g and 82, respectively. It has a melting point of 327°C and a density of 11.4g/cm^3 (11.4t/m^3) and a remarkably high corrosion resistance to most acids, including sulphuric (H_2SO_4) and hydrochloric (HCl) acids with the exception of nitric acid (HNO_3). This corrosion resistance can be attributed to its ability to form a wide variety of oxides ranging from Pb_2O to PbO_2 thereby forming a protective film on the exposed surface.

Lead is a normal constituent of the earth's crust, with trace amounts found naturally in soil, plants, and water. If left undisturbed, lead is practically immobile. However, once mined and transformed into man-made products, which are dispersed throughout the environment, lead becomes highly toxic. Solely as a result of man's actions, lead has become the most widely scattered toxic metal in the world. Unfortunately for people, lead has a long environmental persistence and never loses its toxic potential, if ingested.

It is believed that mankind has used lead for over 6000 years. Lead mining probably predated the Bronze or Iron Ages, with the earliest recorded lead mine in Turkey about 6500 BC. The oldest artifact of smelted lead is a necklace found in the ancient city site in Anatolia. The estimated age of this necklace is 6,000 to 8,000 years ago. There were many reasons for lead's use other than its abundance and ease in obtaining it. Some of the properties which make it commercially attractive include: easy workability, low melting point, ability to form carbon metal compounds, hold pigments well, very easily recycled, stands up well to the outside weather elements, a high degree of corrosion resistance, it is inexpensive, etc. There are also several habits and customs of cultures that contributed to human exposure, such as using lead in medicines and cosmetics.

The Romans conducted lead mining on a massive scale and had several huge lead mine and smelter sites. Lead was in big demand and was a byproduct of refining silver and gold ore. One smelter site located in Spain required tens of thousands of slaves to operate. Another large site was in Greece and the emissions from these two sites would rise high into the atmosphere and get picked up by the world's air currents. Some lead would fall back to earth in the snow and recently, scientists measured lead particles deposited in Greenland's ice to determine the history of lead production. The massive mining and smelting of lead went on for hundreds of years and the production of Roman lead was not surpassed till the period of the Industrial Revolution.

Lead's toxicity was recognized and recorded as early as 2000 BC and the widespread use of lead has been a cause of endemic chronic plumbism in several societies throughout history. The Greek philosopher Nikander of Colophon in 250 BC reported on the colic and anemia resulting from lead poisoning. Hippocrates related gout to the food and wine, though the association between gout and lead poisoning was not recognized during this period (450-380 BC). Later during the Roman period, gout was prevalent among the upper classes of Roman society and is believed to be a result of the enormous lead intake.

Lead is not biodegradable. It persists in the soil, in the air, in drinking water, and in homes. It crosses all social, economical and geographical lines. It never disappears, it only accumulates where it is deposited and can poison generations of children and adults unless properly removed. At high levels, lead poisoning causes coma, convulsions and death. At low levels, levels far below those that present obvious symptoms, lead poisoning in childhood causes reductions in IQ and attention span, reading and learning disabilities, hyperactivity, impaired growth, behavioral problems, and hearing loss. These effects are long-term and may be irreversible.

1.1) Lead In Periodic Table:

TABLE-1.1: LEAD IN PERIODIC TABLE

Symbol	Pb
Atomic Number	82
Atomic Weight	207.2
Element Classification	Other Metal
Discovered by	Known to the ancients
Discovery Date	Unknown
Name Origin	Anglo-Saxon: lead; symbol from Latin: Plumbum
Density (g/cc)	11.35
Melting Point (°K)	600.65
Boiling Point (°K)	2013
Appearance	Very soft, highly malleable and ductile, blue-white shiny metal
Atomic Radius (pm)	175
Atomic Volume (cc/mol)	18.3
Covalent Radius (pm)	147
Ionic Radius	84 (+4e) 120 (+2e)
Specific Heat (@20°C J/g mol)	0.159
Fusion Heat (kJ/mol)	4.77
Evaporation Heat (kJ/mol)	177.8
Debye Temperature (°K)	88.00
Pauling Negativity Number	1.8
First Ionizing Energy (kJ/mol)	715.2
Oxidation States	4,2
Electronic Configuration	[Xe] 4f ¹⁴ 5d ¹⁰ 6s ² 6p ²
Lattice Structure	Face Centred Cubic(FCC) Lattice
Lattice Constant (Å)	4.950

1.2) Sources of Lead:

Lead is a naturally occurring bluish-gray metal found in small amounts in the earth's crust. It has no characteristic taste or smell. Metallic lead does not dissolve in water and does not burn. Some natural and man-made substances contain lead, but do not look like lead in its metallic form. Some of these substances can burn. It is very soft, highly malleable, ductile, and a relatively poor conductor of electricity. It is very resistant to corrosion but tarnishes upon exposure to air. Lead pipes bearing the insignia of Roman emperors, used as drains from the baths, are still in service. Alloys include pewter and solder. Lead isotopes are the end products of each of the three series of naturally occurring radioactive elements. Lead is available in several forms including foil, granules, ingots, powder, rod, shot, sheet, and wire.

Lead has many different uses. Its most important use is in the production of some types of batteries. Other uses include the production of ammunition, in some kinds of metal products (such as sheet lead, solder, and pipes) and in ceramic glazes. Some chemicals containing lead, such as tetraethyl lead and tetraethyl lead are used as gasoline additives. However, the use of these lead containing chemicals in gasoline is much less than it used to be because the last producer of these additives in the United States stopped making them in early 1991. Other chemicals containing lead are used in paint. The amount of lead added to paints and ceramic products, gasoline additives, and solder has also been reduced in recent years because of lead's harmful effects in humans and animals. However, the use of lead in ammunition and roofing has actually increased in recent years. Lead is also used for radiation shields for protection against X-rays and in a large variety of medical (electronic ceramic parts of ultrasound machines, intravenous pumps, fetal monitors, and other surgical equipment), scientific (circuit boards for computers and other electronic circuitry), and military equipment (jet turbine engine blades, military tracking systems).

Most lead used by industry comes from mined ores ("primary") or from recycled scrap metal or batteries ("secondary"). Human activities have spread lead and substances that contain lead to all parts of the environment. For example, lead is in air, drinking water, rivers, lakes, oceans, dust, and soil. Lead is also in plants and animals that humans may eat. Lead occurs naturally in the environment. However, most of the lead dispersed throughout the environment comes from human activities. Before the use of leaded gasoline was limited, most of the lead released into the U.S. environment came from car exhaust. Since the EPA has limited the use of leaded gasoline,

the amount of lead released into the air has decreased. In 1979, cars released 94.6 million kilograms (kg) of lead into the air in the United States. In contrast, in 1989 cars released only 2.2 million kg to the air. Other sources of lead released to the air include burning fuel, such as coal or oil, industrial processes, and burning solid waste.

Lead Sources in India:

Lead is a widespread constituent of the earth's crust. It has always been present in soils in rivers, lakes and seas, in the air, following the burning of wood and coal, and in plants, both edible and inedible. Throughout history, lead has been well known and extensively used by mankind and so, over a period of centuries, it has been dispersed by man into the environment. There are many reasons for the vast commercial utilization of lead. Some of the important properties include low melting points, easy workability, ability to form carbon metal compounds, favorable oxidation-reduction potential useful for electrochemical application, formation of crystal desirable in pigment, relatively low cost and easy recyclability. At present one of the major uses of lead is in the Lead Acid Storage manufacturing industries which account for about 50% of the refined lead consumption, while production of tetraethyl lead as an automobile additive to reduce engine knock accounts for almost 10% of the consumption.

India was centuries ahead of Western Europe in the industrial production of lead. This has been reaffirmed by excavation work carried out by the British Museum, Baroda University and Hindustan Zinc Limited. Zawar mines are the "earliest dated Lead-zinc mines in the world". The commercial exploitation of Zawar mines was resumed in the 20th century by Metal Corporation of India (MCI). MCI had also put up a lead smelter in Tundoo, Bihar in the year 1942 to treat lead concentrate. Hindustan Zinc Limited (HZL) was incorporated in 1966. Starting with one mine producing 500 TPD lead zinc ore and a 3600 TPA Lead Smelter in 1966, HZL has come a long way and today operates nearly six lead zinc mines. India's total identified lead ore reserves are estimated to be around 383 million tonnes (as of 1989) with Rajasthan having a major share. Andhra Pradesh, Gujarat, Orissa, Bihar and West Bengal also have some reserves. Total production of lead concentrates in India was 17,000 tonnes in 1980 and 89,000 tonnes in 1989. India has a very small share in world market for refined lead production which was only 0.5% in 1986. Production of primary lead metal follows the sinister roast, blast furnace reduction fire refining process using sulphide lead concentrates.

The sources of lead in India from the viewpoint of health hazards may be in the following order of importance:

1. Lead-battery recycling plants
2. Lead smelting as in silver refining for jewelry & articles works.
3. Lead based pigments & paints
4. Printing press
5. Ceramic pottery glazes
6. Lead containing cosmetics & folk medicines

Every country is developing recycling activities. In 1995, European industry was recycling over 10 million vehicles and 45-48 million lead-acid batteries. In 1997, Western world average lead ratio between production of refined lead & lead alloys from scrap 2,929 mt. and refined lead production 4,956 mt amounted to 59% and for USA to 76%. These activities are increasing in Asia.

Priority Areas for Investigation in India

1. Lead battery recycling activities
2. Lead smelting for silver purification for jewellery & articles
3. Childhood lead poisoning from lead based pigments & paints, soil etc. 1-6 years

1.3) Exposure of Lead:

People living near hazardous waste sites can be exposed to lead and chemicals that contain lead by breathing air, drinking water, eating foods, or swallowing or touching dust or dirt that contains lead. For people who do not live near hazardous waste sites, most exposure to lead occurs by eating foods that contain lead, occupationally in brass/bronze foundries, or in areas where leaded paints exist. Foods such as fruits, vegetables, meats grains, seafood, soft drinks, and wine may have lead in them. Cigarettes also contain small amounts of lead. In general, very little lead is in drinking water. More than 99% of all drinking water contains less than 0.005 part of lead per million parts of water (ppm). Acidic water can make the lead found in lead pipes, solder, and brass faucets enter water.

Sources of lead in drinking water include lead that can come out of lead pipes, faucets, and solder used in plumbing. Lead-containing plumbing may be found in public drinking water systems, in houses, apartment buildings, and public buildings. Sources of lead in surface water or sediment include deposits of lead-containing dust from the atmosphere, waste water from industries that handle lead (primarily iron and steel industries and lead producers), and urban runoff.

Sources of lead in food and beverages include deposition of lead-containing dust from the atmosphere on crops and during food processing and uptake of lead from soil by plants. Lead may also enter foods when foods are put into improperly glazed pottery and ceramic dishes and leaded-crystal glassware. Illegal whiskey made using stills that contain lead-soldered parts (such as truck radiators) may also contain lead. The potential for exposure to lead in canned food from lead-soldered containers is greatly reduced because the content of lead in canned foods has decreased 87% from 1980 to 1988. Lead may also be released from soldered joints in kettles used to boil water for beverages. Sources of lead in dust and soil include deposition of atmospheric lead and weathering and deterioration of lead-based paint. Lead in dust may also come from windblown soil. Disposal of lead in municipal and hazardous waste dump sites also adds lead to soil.

We may swallow a lot of lead by eating food and drinking liquids that contain it. Most of the lead that enters your body comes through swallowing, even though very little of the amount you swallow actually enters your blood and other parts of your body. The amount that gets into your body from your stomach partially depends on when you ate your last meal. It also depends on how old you are and how well the lead particles you ate dissolved in your stomach juices. Experiments in adult volunteers showed that the amount of lead that got into the body from the stomach was only about 6% in adults who had just eaten. In adults who had not eaten for a day, about 60-80% of the lead from the stomach got into their blood. On the other hand, 50% of the lead swallowed by children enters the blood and other body parts even if their stomachs are full.

Frequent skin contact with lead in the form of lead-containing dusts and soil can result in children swallowing lead through hand-to-mouth behavior. In adults, only a small portion of the lead will pass through your skin and enter your body if it is not washed off after skin contact.

More lead can pass through your skin if it is damaged. Certain types of lead compounds, however, may penetrate your skin.

1.4) Health Hazard Information:

Lead poisoning is the number one environmental disease among children in developing countries. The full impact of lead poisoning on the health of children and adults is becoming clearer to most countries, and many governments have begun to take action. Significant health and economic benefits have been realized by those countries which have developed lead prevention programs.

Exposure to lead can occur from breathing contaminated workplace air or house dust or eating lead-based paint chips or contaminated dirt. Lead is a very toxic element, causing a variety of effects at low dose levels. Brain damage, kidney damage, and gastrointestinal distress are seen from acute (short-term) exposure to high levels of lead in humans. Chronic (long-term) exposure to lead in humans results in effects on the blood, central nervous system (CNS), blood pressure, kidneys, and Vitamin D metabolism. Children are particularly sensitive to the chronic effects of lead, with slowed cognitive development, reduced growth and other effects reported.

Reproductive effects, such as decreased sperm count in men and spontaneous abortions in women, have been associated with high lead exposure. The developing fetus is at particular risk from maternal lead exposure, with low birth weight and slowed postnatal neurobehavioral development noted. Human studies are inconclusive regarding lead exposure and cancer.

Acute Effects:

1) Death from lead poisoning may occur in children who have blood lead levels greater than 125 µg/dL and brain and kidney damage have been reported at blood lead levels of approximately 100 µg/dL in adults and 80 µg/dL in children.

2) Gastrointestinal symptoms, such as colic, have also been noted in acute exposures at blood lead levels of approximately 60 µg/dL in adults and children.

Short-term (acute) animal tests in rats have shown lead to have moderate to high acute toxicity.

Chronic Effects (Noncancer):

- 1) Chronic exposure to lead in humans can affect the blood. Anemia has been reported in adults at blood lead levels of 50 to 80 µg/dL, and in children at blood lead levels of 40 to 70 µg/dL.

- 2) Lead also affects the nervous system. Neurological symptoms have been reported in workers with blood lead levels of 40 to 60 $\mu\text{g}/\text{dL}$, and slowed nerve conduction in peripheral nerves in adults occurs at blood lead levels of 30 to 40 $\mu\text{g}/\text{dL}$.
- 3) Children are particularly sensitive to the neurotoxic effects of lead. There is evidence that blood lead levels of 10 to 30 $\mu\text{g}/\text{dL}$, or lower, may affect the hearing threshold and growth in children.
- 4) Other effects from chronic lead exposure in humans include effects on blood pressure and kidney function, and interference with vitamin D metabolism.
- 5) Animal studies have reported effects similar to those found in humans, with effects on the blood, kidneys, and nervous, immune, and cardiovascular systems noted.

Reproductive/Developmental Effects:

- 1) Studies on male workers have reported severe depression of sperm count and decreased function of the prostate and/or seminal vesicles at blood lead levels of 40 to 50 $\mu\text{g}/\text{dL}$. These effects may be seen from acute as well as chronic exposures.
- 2) Occupational exposure to high levels of lead has been associated with a high likelihood of spontaneous abortion in pregnant women. However, the lowest blood lead levels at which this occurs has not been established. These effects may be seen from acute as well as chronic exposures.
- 3) Exposure to lead during pregnancy produces toxic effects on the human fetus, including increased risk of preterm delivery, low birthweight, and impaired mental development. These effects have been noted at maternal blood lead levels of 10 to 15 $\mu\text{g}/\text{dL}$, and possibly lower. Decreased IQ scores have been noted in children at blood lead levels of approximately 10 to 50 $\mu\text{g}/\text{dL}$.
- 4) Human studies are inconclusive regarding the association between lead exposure and other birth defects, while animal studies have shown a relationship between high lead exposure and birth defects.

Cancer Risk:

1) Human studies are inconclusive regarding lead exposure and an increased cancer risk. Four major human studies of workers exposed to lead have been carried out; two studies did not find an association between lead exposure and cancer, one study found an increased incidence of respiratory tract and kidney cancers, and the fourth study found excesses for lung and stomach cancers. However, all of these studies are limited in usefulness because the route(s) of exposure and levels of lead to which the workers were exposed were not reported. In addition, exposure to other chemicals probably occurred.

2) Animal studies have reported kidney tumors in rats and mice exposed to lead via the oral route.

1.5) Environmental Levels and Standards:

Environmental impacts from industries in general consist of degradation of Eco-system, pollution of air and water, and socio-economic change. Production of lead can also have similar impact. In India, permissible limit of lead in effluent discharged from industries as per standard laid down by Central and State Pollution Control Boards is 0.1 milligram/litre. Portable water having concentration about 0.1 mg/litre is considered unsafe and should be rejected for human consumption. WHO has set 0.05 mg/litre as a guideline value for lead in drinking water.

TABLE 1.2: PERMISSIBLE LEAD LEVELS FROM DIFFERENT INDUSTRIAL EFFLUENT

S.No	INDUSTRY NAME	PERMISSIBLE LEAD LEVEL(mg/l)
1	Battery Manufacturing	0.1
2	Dry Cell Manufacturing	10
3	Glass Industry	20
4	Inorganic Chemical Industry	0.1
5	Organic Chemical Industry	0.1
6	Paint Industry	0.1
7	Pharmaceuticals Industry	0.1

CHAPTER-2

GENERAL PROCESSES FOR LEAD REMOVAL

Many methods have been developed to remove lead from industrial effluents, including precipitation, co-precipitation, electro dialysis, electrocoagulation, cementation, membrane separation, solvent extraction, ionexchange, adsorption, biosorption, reverse osmosis and membrane separation.

2.1) Chemical Precipitation:

Chemical precipitation is a method of wastewater treatment. Wastewater treatment chemicals are added to form particles which settle and remove contaminants. The treated water is then decanted and appropriately disposed of or reused. The resultant sludge can be dewatered to reduce volume and must be appropriately disposed of. Chemical precipitation can be used to remove metals, fats, oils and greases (FOG), suspended solids and some organics. It can also be used to remove phosphorus, fluoride, ferrocyanide and other inorganics.

It can be used on a small or large scale. A beaker full of waste, a 50,000 tank, a 1,000,000 gallon lagoon or a lake can be batch treated with chemicals. Chemical precipitation can be used in a continuous treatment system on flows ranging from a trickle to 1 gallon/minute, 1,000 gallons/minute and more.

Chemical precipitation can be accomplished with very little equipment. For example, a 55 gallon drum and a mixing paddle can be used by a small discharger to treat wastewater with little capital investment. For larger volumes, a tank with a mixer and chemical feed pumps will suffice. For even larger volumes a continuous system with metering pumps, mixing tanks, a clarifier and control instrumentation can be employed.

2.2) Ion Exchange:

Ion exchange is a reversible chemical reaction wherein an ion (an atom or molecule that has lost or gained an electron and thus acquired an electrical charge) from solution is exchanged for a similarly charged ion attached to an immobile solid particle. These solid ion exchange particles are either naturally occurring inorganic zeolites or synthetically produced organic resins. The synthetic organic resins are the predominant type used today because their characteristics can be tailored to specific applications.

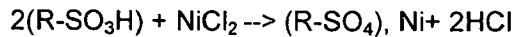
An organic ion exchange resin is composed of high-molecular-weight polyelectrolytes that can exchange their mobile ions for ions of similar charge from the surrounding medium. Each resin has a distinct number of mobile ion sites that set the maximum quantity of exchanges per unit of resin.

Most plating process water is used to cleanse the surface of the parts after each process bath. To maintain quality standards, the level of dissolved solids in the rinse water must be regulated. Fresh water added to the rinse tank accomplishes this purpose, and the overflow water is treated to remove pollutants and then discharged. As the metal salts, acids, and bases used in metal finishing are primarily inorganic compounds, they are ionized in water and could be removed by contact with ion exchange resins. In a water deionization process, the resins exchange hydrogen ions (H^+) for the positively charged ions (such as nickel, copper, and sodium) and hydroxyl ions (OH^-) for negatively charged sulfates, chromates and chlorides. Because the quantity of H^+ and OH^- ions is balanced, the result of the ion exchange treatment is relatively pure, neutral water.

Resin Types:

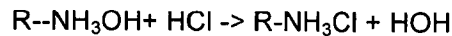
Ion exchange resins are classified as cation exchangers, which have positively charged mobile ions available for exchange, and anion exchangers, whose exchangeable ions are negatively charged. Both anion and cation resins are produced from the same basic organic polymers. They differ in the ionizable group attached to the hydrocarbon network. It is this functional group that determines the chemical behavior of the resin. Resins can be broadly classified as strong or weak acid cation exchangers or strong or weak base anion exchangers.

Strong Acid Cation Resins Strong acid resins are so named because their chemical behavior is similar to that of a strong acid. The resins are highly ionized in both the acid (R-SO₃H) and salt (R-SO₃Na) form. They can convert a metal salt to the corresponding acid by the reaction:



Weak Acid Cation Resins In a weak acid resin the ionizable group is a carboxylic acid (COOH) as opposed to the sulfonic acid group (SO₃H) used in strong acid resins. These resins behave similarly to weak organic acids that are weakly dissociated.

Strong Base Anion Resins Like strong acid resins strong base resins are highly ionized and can be used over the entire pH range. These resins are used in the hydroxide (OH) form for water deionization. They will react with anions in solution and can convert an acid solution to pure water:



Weak Base Anion Resins Weak base resins are like weak acid resins in that the degree of ionization is strongly influenced by pH. Consequently, weak base resins exhibit minimum exchange capacity above a pH of 7.0. These resins merely sorb strong acids: they cannot split salts.

Heavy-Metal-Selective Chelating Resins Chelating resins behave similarly to weak acid cation resins but exhibit a high degree of selectivity for heavy metal cations. Chelating resins are analogous to chelating compounds found in metal finishing wastewater; that is, they tend to form stable complexes with the heavy metals. In fact the functional group used in these resins is an EDTA compound. The resin structure in the sodium form is expressed as R-EDTA-Na.

For removal of lead from wastewaters we can use natural and pretreatment zeolites. The structures of zeolites consist of a three-dimensional framework of SiO₄ and AlO₄ tetrahedral. The aluminum ion is small enough to occupy the position in the center of the tetrahedron of four oxygen atoms, and the isomorphous replacement of Al⁺³ for Si⁺⁴ raises a negative charge in the lattice. The net negative charge is balanced by the exchangeable cation (sodium, potassium and calcium). These cations are exchangeable with certain cations in solutions such as lead. The fact that zeolite exchangeable ions are relatively innocuous (sodium, calcium and potassium ions)

makes them particularly suitable for removing undesirable heavy metal ions from industrial effluent waters.

2.3) Adsorption:

Adsorption, the binding of molecules or particles to a surface, must be distinguished from absorption, the filling of pores in a solid. The binding to the surface is usually weak and reversible. Just about anything including the fluid that dissolves or suspends the material of interest is bound, but compounds with color and those that have taste or odor tend to bind strongly. Compounds that contain chromogenic groups (atomic arrangements that vibrate at frequencies in the visible spectrum) very often are strongly adsorbed on activated carbon. Decolorization can be wonderfully efficient by adsorption and with negligible loss of other materials.

The most common industrial adsorbents are activated carbon, silica gel, and alumina, because they present enormous surface areas per unit weight. Activated carbon is produced by roasting organic material to decompose it to granules of carbon - coconut shell, wood, and bone are common sources. Silica gel is a matrix of hydrated silicon dioxide. Alumina is mined or precipitated aluminum oxide and hydroxide. Although activated carbon is a magnificent material for adsorption, its black color persists and adds a grey tinge if even trace amounts are left after treatment; however filter materials with fine pores remove carbon quite well.

A surface already heavily contaminated by adsorbates is not likely to have much capacity for additional binding. Freshly prepared activated carbon has a clean surface. Charcoal made from roasting wood differs from activated carbon in that its surface is contaminated by other products, but further heating will drive off these compounds to produce a surface with high adsorptive capacity. Although the carbon atoms and linked carbons are most important for adsorption, the mineral structure contributes to shape and to mechanical strength. Spent activated carbon is regenerated by roasting, but the thermal expansion and contraction eventually disintegrate the structure so some carbon is lost or oxidized. Temperature effects on adsorption are profound, and measurements are usually at a constant temperature. Graphs of the data are called *isotherms*. Most steps using adsorbents have little variation in temperature.

2.4) Electrodialysis:

Electro dialysis (ED) is a possible technique for treatment of the wastewater. The principle of ED involves removal of ionic components (like Pb^{2+}) from an aqueous solution through ion-exchange membranes using an electrical driving force. The wastewater to be treated is pumped through a membrane stack which consists of alternately placed anionic and cationic selective membranes separated by gasket frames and spacers. The membranes are fixed between two end plates that contain the electrodes producing the electric field. In order to transfer the electric current and to remove gases produced by electrode reactions, the electrode chambers are rinsed with an electrolyte solution.

2.5) Solvent Extraction:

Solvent extraction is accomplished by contacting soil with a solvent, separating the soil and solvent, and regenerating the solvent for reuse. To be successful, the extraction solvent should have a high solubility for the contaminant and low solubility in the waste matrix. Typical solvents include liquefied gas (propane or butane), supercritical carbon dioxide fluid, triethylamine, or proprietary organic fluids. The extraction solvent is well mixed with the contaminated matrix to allow contaminants to transfer to the solvent. The clean matrix and solvent are then separated by physical methods, such as gravity decanting or centrifuging. Distillation regenerates the solvent, which is then returned for reuse in the extraction process.

Extraction typically is mass transfer limited, so thorough mixing of the solvent and contaminated matrix is required. Some solvent extraction systems require the addition of water if the waste is a dry, nonflowing solid. In other systems, extraction fluid is added to make the waste flow.

The extraction solvent typically is purified by distillation. In systems that use pressurized solvents, such as liquefied gas or supercritical carbon dioxide, vaporization occurs by pressure release, which causes the solvent to boil. With higher-boiling solvents, distillation tanks or towers may be used to separate the extraction solvent from the organic contaminants.

2.6) Reverse Osmosis:

To understand "reverse osmosis," it is probably best to start with normal osmosis. According to Merriam-Webster's Collegiate Dictionary, osmosis is the "movement of a solvent through a semipermeable membrane (as of a living cell) into a solution of higher solute concentration that tends to equalize the concentrations of solute on the two sides of the membrane." That's a mouthful.

A semipermeable membrane is a membrane that will pass some atoms or molecules but not others. Saran wrap is a membrane, but it is impermeable to almost everything we commonly throw at it. The best common example of a semipermeable membrane would be the lining of your intestines, or a cell wall. Gore-tex is another common semipermeable membrane. Gore-tex fabric contains an extremely thin plastic film into which billions of small pores have been cut. The pores are big enough to let water vapor through, but small enough to prevent liquid water from passing.

The membrane allows passage of water molecules but not salt molecules. One way to understand osmotic pressure would be to think of the water molecules on both sides of the membrane. They are in constant Brownian motion. On the salty side, some of the pores get plugged with salt atoms, but on the pure-water side that does not happen. Therefore, more water passes from the pure-water side to the salty side, as there are more pores on the pure-water side for the water molecules to pass through. The water on the salty side rises until one of two things occurs:

- The salt concentration becomes the same on both sides of the membrane (which isn't going to happen in this case since there is pure water on one side and salty water on the other).
- The water pressure rises as the height of the column of salty water rises, until it is equal to the osmotic pressure. At that point, osmosis will stop.

Osmosis, by the way, is why drinking salty water (like ocean water) will kill you. When you put salty water in your stomach, osmotic pressure begins drawing water out of your body to try to dilute the salt in your stomach. Eventually, you dehydrate and die.

In reverse osmosis, the idea is to use the membrane to act like an extremely fine filter to create drinkable water from salty or metal ion (like Pb^{2+}) contaminated water. The salty or metal ion contaminated water is put on one side of the membrane and pressure is applied to stop, and then reverse, the osmotic process. It generally takes a lot of pressure and is fairly slow, but it works.

2.7) Membrane Separation:

In membrane separation, spent metal removal (like lead) fluids are pumped from a process tank at a moderate pressure (typically 30 to 50 psig) and rapid flow to a series of membranes. This flow is typically between 750 to 1,100 gallons per square foot of membrane per day and is referred to as the feed rate. Large molecules and virtually all petroleum products are blocked at the membrane surface. The compounds that do not pass through the membrane are referred to as the reject. The water-like solutions that pass through the membrane are referred to as the "permeate". The rate at which the permeate flows through the membrane is called the flux rate.

Membranes come in two basic sizes:

A) Micro filtration Membranes with a pore size of 0.1 – 10 μm perform micro filtration. Microfiltration membranes remove all bacteria. Only part of the viral contamination is caught up in the process, even though viruses are smaller than the pores of a micro filtration membrane. This is because viruses can attach themselves to bacterial biofilm. Micro filtration can be implemented in many different water treatment processes when particles with a diameter greater than 0.1mm need to be removed from a liquid.

B) Ultra filtration: For complete removal of viruses, ultra filtration is required. The pores of ultra filtration membranes can remove particles of 0.001 – 0.1 μm from fluids.

Advantages and Disadvantages of membrane separation:

Advantages:

- a) Membrane separation consistently separates a wide variety of emulsion, surfactant, and chelating chemistries and various mixtures.
- b) It requires no specific chemical knowledge.

- c) Complex instrumentation is not required.
- d) The method does not require constant attention.
- e) The basic concept is simple to understand.

Disadvantages:

- a) Membranes are expensive.
- b) Certain solvents can quickly and permanently destroy the membrane.
- c) Certain colloidal solids, especially graphite and residues from vibratory deburring operations, can permanently foul the membrane surface.
- d) The energy cost is higher than chemical treatment, although less than evaporation.
- e) Oil emulsions are not "chemically separated," so secondary oil recovery can be difficult.
- f) Synthetics are not effectively treated by this method.

2.8) Gamma Irradiation:

Removal of heavy metals ions like lead ions from waste water using gamma irradiation has been investigated. These metal ions are reduced by hydrated electrons and hydrogen atoms to lower or zero valence state and eventually precipitated out of solution. Ethanol is applied as a relatively non-toxic additive to scavenge $\cdot\text{OH}$ radicals, to enhance reduction and inhibit oxidation.

2.9) Cementation:

Cementation is the term used to describe the electrochemical precipitation of a metal (like lead), usually from an aqueous solution of its salts, by a more electropositive metal. The process has been used in industry for a long time, not only in hydrometallurgy but also in the purification of process streams and wastewater. The cementation treatment process has several advantages. These include simple control requirement, low energy consumption and recovery of valuable or toxic metals in a harmless and reusable form. The main disadvantage is electropositive metal consumption, especially when iron or zinc are used at low pH values.

2.10) Biological:

Biological treatment transforms, stabilizes and/or removes lead by means of microorganisms. Microorganisms, primarily certain specific bacteria, accomplish this by oxidation/reduction, mineralization, detoxification or methylation. Critical factors include energy and carbon source; aerobic, anoxic or anaerobic conditions; temperature; pH.

Although some of these treatment methods treatment methods can be successfully used for treating most wastewaters, others are quite limited in use. The application of chemical precipitation to dilute solutions (low concentration) can be difficult unless the addition of flocculating agents such as lime, caustic and sodium carbonate is employed. However a bulky sludge is produced and the disposal constitutes a problem. Ion exchange and activated carbon adsorption are quite expensive and require recharge of resin or spent activated carbon as well as the disposal of substantial volume of used regeneration solution. In addition to the fact that membrane technology is expensive, membranes are susceptible to attack by microorganisms, likewise other methods mentioned require elaborate and considerably high operation costs.

CHAPTER-3

ADSORPTION FUNDAMENTALS

3.1) General:

Adsorption is a surface phenomenon. The adsorption operations exploit the ability of certain solids preferentially to concentrate specific substances from solution onto their surfaces. The solute accumulated is called the adsorbate or solute and the adsorbing substance is the adsorbent. In the water purification, adsorbents are used to remove organic impurities, particularly those that are non-biodegradable or associated with taste, colour, and odour. Although adsorption is applied in low concentration, recent physical-chemical processes use adsorption as a primary technique to remove soluble organics from the wastewater. The adsorption is called physical adsorption when the bonding forces are relatively weak intermolecular forces like van der Waal's forces and, chemical when the bonding forces are strong like chemical bonding. During adsorption, the solid adsorbent becomes saturated or nearly saturated with the adsorbate. To recover the adsorbate and allow the adsorbent to be reused, it is regenerated by desorbing the adsorbed substances (i.e. the adsorbates).

3.1.1 Physical Adsorption vs. Chemisorption

Adsorption processes can be classified as physical adsorption (van der Waals adsorption) and chemisorption (activated adsorption) depending on the type of forces between the adsorbate and the adsorbent. In physical adsorption, the individuality of the adsorbate and the adsorbent are preserved. In chemisorption, there is a transfer or sharing of electron, or breakage of the adsorbate into atoms or radicals, which are bound separately.

Physical adsorption of a gas occurs when the inter-molecular attractive forces between molecules of the solid adsorbent and the gas are greater than those between molecules of the gas itself. In effect, the resulting adsorption is like condensation, which is exothermic and thus is accompanied by the release of heat, similar in magnitude to the heat of condensation. Physical adsorption occurs quickly and may be monomolecular (unimolecular) layer or monolayer, or two, three or more layers thick (multi-molecular). As physical adsorption takes place, it begins as a monolayer. It can then become multi-layer, and then, if the pores are close to the size of the molecules, more adsorption occurs until the pores are filled with adsorbate. Accordingly, the

maximum capacity of a porous adsorbent can be more related to the pore volume than to the surface area.

In contrast, chemisorption is monolayer, involves the formation of chemical bonds between the adsorbate and adsorbent, often with a release of heat much larger than the heat of condensation. Chemisorption from a gas generally takes place only at temperatures greater than 200 °C, and may be slow and irreversible.

Most commercial adsorbents rely on physical adsorption; while catalysis relies on chemisorption. A comparison between physical adsorption and chemical adsorption is given in Table 3.1.

Table 3 .1. Comparison of Physical and Chemical Adsorption

Sl. No.	Physical Adsorption	Chemical Adsorption
1.	Van der Wall's adsorption	Activated adsorption
2.	Heat of adsorption = 5 kcal/mol	Heat of adsorption = 20-100 kcal/mol
3.	Adsorption occurs only at temperature less than the boiling point of the adsorbate	Adsorption can occur even at higher temperature
4.	No activation energy is involved in the adsorption process	Activation energy may be involved
5.	Adsorption occurs in mono and multi layers	Adsorption occurs almost in mono layer
6.	Quantity adsorbed per unit mass is high i.e. entire surface is participating	Quantity adsorbed per unit mass is low i.e. only active surface sites are important
7.	Rate of adsorption controlled by mass transfer resistance	Rate of adsorption controlled by resistance reaction

3.1.2 Intra-particle Diffusion Process

The rate of adsorption is determined by the rate of transfer of the adsorbate from the bulk solution to the adsorption sites within the particles. This can be broken conceptually into a series of consecutive steps.

1. Diffusion of adsorbate across a stationary solvent film surrounding each adsorbent
2. Diffusion through the macro pore
3. Diffusion through micro pore
4. Adsorption at an appropriate site

It is assumed that the fourth step occurs very rapidly in comparison to the second step. If the system is agitated vigorously, the exterior diffusion film around the adsorbent will be very thin, offering negligible resistance to diffusion. So, it can be assumed that the main resistance to adsorption shall lie in the pore diffusion step. Weber and Morris while referring to the rate limiting step of organic materials uptake by granulated activated carbon in the rapidly mixed batch system propose the term “intra-particle transport” which comprises of surface diffusion and molecular diffusion. Several researchers have shown that surface diffusion is the dominant mechanism and is the rate-determining step. A functional relationship common to most of the treatments of intra-particle transport is that the uptake varies almost proportionally with the square root of time.

3.1.3 Stages in Adsorption Process

Adsorption is thought to occur in three stages, as the adsorbate concentration increases.

Stage I: First, a single layer of molecules builds up over the surface of the solid. This monolayer may be chemisorbed and is associated with a change in free energy that is a characteristic of the forces that hold it.

Stage II: As the fluid concentration is further increased, second, third etc., layers are formed by physical adsorption; the number of layers which can form are limited by the size of the pores.

Stage III: Finally, for adsorption from the gas phase, capillary condensation may occur in which capillaries become filled with condensed adsorbate, when its partial pressure reaches a critical value relative to the size of the pore.

3.2) Adsorption Isotherms:

When a solution is contacted with a solid adsorbent, molecules of adsorbate get transferred from the fluid to the solid until the concentration of adsorbate in solution as well as in the solid phase are in equilibrium. At equilibrium, equal amounts of solute eventually are being adsorbed and desorbed simultaneously. This is called adsorption equilibrium. The equilibrium data at a given temperature are represented by adsorption isotherm and the study of adsorption is important in a number of chemical processes ranging from the design of heterogeneous chemical reactors to purification of compounds by adsorption.

Many theoretical and empirical models have been developed to represent the various types of adsorption isotherms. Langmuir, Freundlich, Temkin, Redlich-Peterson (R-P) etc. are most commonly used adsorption isotherm models for describing the dynamic equilibrium. The isotherm equations used for the study are described follows:

3.2.1 Langmuir Isotherm

This equation based on the assumptions that:

1. Only monolayer adsorption is possible.
2. Adsorbent surface is uniform in terms of energy of adsorption.
3. Adsorbed molecules do not interact with each other.
4. Adsorbed molecules do not migrate on the adsorbent surface

The adsorption isotherm derived by Langmuir for the adsorption of a solute from a liquid solution is

$$Q_e = \frac{Q_m K_A C_e}{1 + K_A C_e} \quad (3.1)$$

where,

Q_e = Amount of adsorbate adsorbed per unit amount of adsorbent at equilibrium.

Q_m = Amount of adsorbate adsorbed per unit amount of adsorbent required for monolayer adsorption (limiting adsorbing capacity).

K_A = Constant related to enthalpy of adsorption.

C_e = Concentration of adsorbate solution at equilibrium.

The Langmuir isotherm can be rearranged to the following linear forms:

$$\frac{C_e}{Q_e} = \frac{1}{K_A Q_m} + \frac{C_e}{Q_m} \quad (3.2)$$

or

$$\frac{1}{Q_e} = \left(\frac{1}{K_A Q_m} \right) \left(\frac{1}{C_e} \right) + \left(\frac{1}{Q_m} \right) \quad (3.3)$$

3.2.2 Freundlich Isotherm

The heat of adsorption in many instances decreases in magnitude with increasing extent of adsorption. This decline in heat of adsorption is logarithmic, implying that adsorption sites are distributed exponentially with respect to adsorption energy. This isotherm does not indicate an adsorption limit when coverage is sufficient to fill a monolayer. The equation that describes such isotherm is the Freundlich Isotherm, given as

$$Q_e = K_F C_e^{\frac{1}{n}} \quad (3.4)$$

where ,

K_F and n are the constants

C_e = the concentration of adsorbate solution at equilibrium

by taking logarithm on both sides, this equation is converted into a linear form:

$$\ln Q_e = \ln K_F + \frac{1}{n} \ln C_e \quad (3.5)$$

Thus a plot between $\ln Q_e$ and $\ln C_e$ is a straight line. The Freundlich equation is most useful for dilute solutions over small concentration ranges. It is frequently applied to the adsorption of impurities from a liquid solution on to the activated carbon. A high K_F and high 'n' value is an indication of high adsorption through out the concentration range. A low K_F and high 'n' indicates a low adsorption through out the concentration range. A low 'n' value indicates high adsorption at strong solute concentration.

3.2.3 Temkin Isotherm

It is given as

$$q_e = \frac{RT}{b} \ln(K_T C_e) \quad (3.10)$$

which can be linearized as:

$$q_e = B_1 \ln K_T + B_1 \ln C_e \quad (3.11)$$

where $B_1 = \frac{RT}{b}$

Temkin isotherm contains a factor that explicitly takes into the account of adsorbing species-adsorbent interactions. This isotherm assumes that (i) the heat of adsorption of all the molecules in the layer decreases linearly with coverage due to adsorbent-adsorbate interactions, and that (ii) the adsorption is characterized by a uniform distribution of binding energies, up to some maximum binding energy. A plot of q_e versus $\ln C_e$ enables the determination of the isotherm constants B_1 and K_T from the slope and the intercept, respectively. K_T is the equilibrium binding constant (l/mol) corresponding to the maximum binding energy and constant B_1 is related to the heat of adsorption.

3.2.4 Redlich-Peterson isotherm

Redlich and Peterson (1959) model combines elements from both the Langmuir and Freundlich equation and the mechanism of adsorption is a hybrid and does not follow ideal monolayer adsorption. The Redlich-Peterson isotherm has a linear dependence on concentration in the numerator and an exponential function in the denominator. The R-P equation is a combination of the Langmuir and Freundlich models. It approaches the Freundlich model at high concentration and is in accord with the low concentration limit of the Langmuir equation. Furthermore, the R-P equation incorporates three parameters into an empirical isotherm, and therefore, can be applied either in homogenous or heterogeneous systems due to the high versatility of the equation.

It can be described as follows:

$$Q_e = \frac{K_R C_e}{1 + a_R C_e^\beta} \quad (3.12)$$

Where K_R is R–P isotherm constant (L/g), a_R is R–P isotherm constant (L/mg) and β is the exponent which lies between 1 and 0, where $\beta=1$

$$Q_e = \frac{K_R C_e}{1 + a_R C_e} \quad (3.13)$$

It becomes a Langmuir equation. Where $\beta=0$

$$Q_e = \frac{K_R C_e}{1 + a_R} \quad (3.14)$$

i.e. the Henry's Law equation

Eq. (3.12) can be converted to a linear form by taking logarithms:

$$\ln \left(K_R \frac{C_e}{Q_e} - 1 \right) = \ln a_R + \beta \ln C_e \quad (3.15)$$

Plotting the left-hand side of equation (3.15) against $\ln C_e$ to obtain the isotherm constants is not applicable because of the three unknowns, a_R , K_R and β . Therefore, a minimization procedure was adopted to solve equation (3.15) by maximizing the correlation coefficient between the theoretical data for Q_e predicted from equation (3.15) and experimental data. Therefore, the parameters of the equations were determined by minimizing the distance between the experimental data points and the theoretical model predictions with any suitable computer programme.

4. Contact time
5. Degree of agitation
6. Nature of adsorbent

3.4.1 Initial Concentration

The initial concentration of pollutant has remarkable effect on its removal by adsorption. The amount of adsorbed material increases with the increasing adsorbate concentration as the resistance to the uptake of the adsorbate from solution decreases with increasing solute concentration. Percent removal increases with decreasing concentrations.

3.4.2 Temperature

Temperature is one of the most important controlling parameter in adsorption. Adsorption is normally exothermic in nature and the extent and rate of adsorption in most cases decreases with increasing temperature of the system. Some of the adsorption studies show increased adsorption with increasing temperature. This increase in adsorption is mainly due to increase in number of adsorption sites caused by breaking of some of the internal bonds near the edge of the active surface sites of the adsorbents.

3.4.3 pH

Adsorption from solution is strongly influenced by pH of the solution. The adsorption of cations increases while that of the anions decreases with increase in pH. The hydrogen ion and hydroxyl ions are adsorbed quite strongly and therefore the adsorption of other ions is affected by pH of solution. Change in pH affects the adsorptive process through dissociation of functional groups on the adsorbent surface active sites. This subsequently leads to a shift in reaction kinetics and equilibrium characteristics of adsorption process. It is an evident observation that the surface adsorbs anions favorably at lower pH due to presence of H^+ ions, whereas the surface is active for the adsorption of cations at higher pH due to the deposition of OH^- ions.

3.4.4 Contact Time

The studies on the effect of contact time between adsorbent and adsorbate have significant importance. In physical adsorption, most of the adsorbate species are adsorbed on the adsorbent surface within short contact time. The uptake of adsorbate is fast in the initial stages of the contact period and becomes slow near equilibrium. Strong chemical binding of adsorbate with adsorbent requires a longer contact time for the attainment of equilibrium. Available adsorption results reveal that the uptake of heavy metals is fast at the initial stages of the contact period, and thereafter it becomes slow near equilibrium.

3.4.5 Degree of Agitation

Agitation in batch adsorbers is most important to ensure proper contact between the adsorbent and the solution. At lower agitation speed, the stationary fluid film around the particle is thicker and the process is mass transfer controlled. With the increase in agitation this film decreases in thickness and the resistance to mass transfer due to this film reduces and after a certain point the process becomes intra particle diffusion controlled. Whatever is the extent of agitation the solution inside the process remains unaffected and hence for intraparticle mass transfer controlled process agitation has no effect on the rate of adsorption.

3.4.6 Nature of Adsorbent

Many solids are used as adsorbents to remove the impurities from fluids. Commercial adsorbents generally have large surface area per unit mass. Most of the surface area is provided by a network of small pores inside the particles. Common industrial adsorbents for fluids include activated carbon, silica gel, activated alumina, molecular sieves etc. Adsorption capacity is directly proportional to the exposed surface. For the non-porous adsorbents, the adsorption capacity is directly proportional to the particle size diameter whereas for porous materials it is practically independent of particle size.

Activated carbon is the most widely used adsorbent for water purification. In the manufacture of activated carbon, organic materials such as coal nutshells, bagasse is first pyrolysed to a carbonaceous residue. Larger channels or pores with diameter 1000 Å are called macro pores. Most of the surface area for adsorption is provided by micropores, which are arbitrarily defined as pores with diameter from 10-1000 Å.

Table.3.2: Various commercial adsorbents

Adsorbent	Properties& method of preparation	Application
Silica gel	Hard, granular and very porous product made from gel precipitated by sodium silicate.	Drying of gases, refrigerants, organic solvents. Desiccant in packing and double glazing. Dew point control of natural gas.
Activated alumina	Hard, hydrated aluminum hydroxide which is activated by heating to drive moisture.	Drying of gases, organic solvents, transformer oils. Desiccant in packing and double glazing. Removal of HCl from hydrogen.
Carbon	Activated carbon is the residue obtained from various carbonaceous material like coal, wood, paper mills sludge, agro waste.	Nitrogen from air. Recovery of certain vapors. Purification of helium. Water purification.
Polymeric and Resin	These are hydrophobic adsorbents which are obtained from pyrolysis and activation of polymeric compounds.	Separation of fatty acids from water and toluene. Separation of aromatics from aliphatics. Removal of colour from syrups.
Fuller's Earth	These are natural clays The clay is heated and dried during which it develops a porous structure.	Treatment of edible oils. Removal of organic pigments. Refining of mineral oils.
Zeolites	It is insoluble and chemically stable aluminum silicate mineral that was formed from the glass component of volcanic ash.	Removing water from azeotropes. Sweetening sour gases and liquids. Purification of hydrogen. Separation of ammonia and hydrogen. Recovery of carbon dioxide. Separation of xylene and ethyl benzene.

Table.3.3: Typical non conventional adsorbents

Adsorbent	Application
Coal fly ash	Heavy metals, organic compounds, COD of waste water, phosphate, phenolic compounds.
Bagasse fly ash	Sugar and distillery effluents, heavy metals, chlorinated phenols.
Peat	Heavy metals, cyanide, phosphate, oil in water, color and dyes.
Lignite	Ammonia dyes.
Activated carbon from lignin sludge, bark, rice husk.	Color, heavy metals, dyes, distillery waste.
Coconut husk, peanut skin, bagasse pitch.	Heavy metals, dyes.
Hardwood, softwood, saw dust.	Heavy metals, dyes, COD.
Waste rubber.	Heavy metals.
Hematite, slag.	Heavy metals.
Tannery hair	TOC, soluble organic dyes, virus.
China clay, wollastonite.	Dyes, oxalic acid and Fluorides.

CHAPTER-4

LITERATURE REVIEW

General

Several investigations have been worked on the removal of lead by using different adsorbents. These are reported below.

The phenomena of lead, copper and cobalt adsorption by activated carbon from aqueous solution was studied in detail by **A.Netzer et.al. (1982)**. Laboratory studies were conducted to evaluate and optimize the various process variables (i.e. carbon type, solution pH, equilibrium time and carbon dose). A quantitative determination of the adsorptive capacity of activated carbon to remove these metals was also determined. Solution pH was found to be the most important parameter affecting the adsorption. Of the ten commercially available activated carbons evaluated in these experiments, Barney Cheney NL 1266 was found to adsorb the largest percentage of lead, copper and cobalt.

Waste Biogas Residual Slurry as an Adsorbent for the Removal of Pb (II) from aqueous solution and Radiator Manufacturing Industry Wastewater was studied by **C.Namasivayam et.al. (1995)**.

Waste biogas residual slurry (BRS) was used for the adsorption of Pb (II) from aqueous solution, over a range of initial metal ion concentrations, agitation times, adsorbent doses and initial pH values. The amount of Pb (II) adsorbed increased with increases in the initial concentration of Pb (II). The applicability of the Lagergren rate equation was also investigated. The process of uptake of Pb (II) by BRS followed the Langmuir isotherm model and the adsorption capacity was 28 mg/g.

The adsorption of aqueous Pb (II), EDTA, and Pb(II)-EDTA complexes onto TiO₂ were studied at both stoichiometric and non- stoichiometric Pb(II) /EDTA concentrations by **Muhammad S. Vohra et.al.(1997)**. Inner-sphere complexation was considered to occur between Pb (II), EDTA, Pb(II)-EDTA, and the TiO₂ surface sites. Surface complexes used in the modeling included Ti-O-Pb/, Ti-EDTAH₂₀, Ti-EDTA-Pb₀, and Ti-O-Pb-EDTA. The cationic-type complexation, Ti-O-Pb-EDTA, was postulated to explain and model the anomalous EDTA adsorption as noted for Pb(II) .

The sorption of lead ions from aqueous solution onto peat has been studied by **Y. S. Ho et.al.(1998)**. Kinetic studies have been carried out using an agitated batch and the effect of varying process parameters has been investigated; these include initial lead ion concentration, peat particle size, solution temperature and agitation speed. The data were analyzed using a pseudo-first order Lagergren equation and the data were correlated using a two-step first order reaction mechanism.

Removal of Cu, Zn and Pb by fly ash and fly ash/lime mixing was studied by **P.Ricou et.al.(1999)**. In the first part of the study, isotherms at different pH were carried out at room temperature. Results show increasing removal with increasing pH. In the second part, experimental design methodology was used. The objectives were to determine the influential parameters among the seven studied for adsorption of copper, zinc and lead, then to study their interactions. Results indicate greater removal by using 100 g.l⁻¹ of adsorbent with 20% mass of lime at pH 5. However, the preparation of the adsorbent must be modified to increase the role of lime in the removal mechanism.

Red mud, an aluminium industry waste, has been converted into an inexpensive and efficient adsorbent and used for the removal of lead and chromium from aqueous solutions and this investigation was done by **Vinod K. Gupta et.al.(2000)**. Effect of various factors on the removal of these metal ions from water (e.g. pH, adsorbent dose, adsorbate concentration, temperature, particle size, etc.) has been studied and discussed. The material exhibits good adsorption capacity and the data follow both Freundlich and Langmuir models. Thermodynamic parameters indicate the feasibility of the process. Kinetic studies have been performed to understand the mechanism of adsorption. Dynamic modelling of lead and chromium removal on red mud has been undertaken and found to follow first-order kinetics.

An evaluation of the application of electric furnace slag (EFS) as an adsorbent to remove Pb²⁺ and Cu²⁺ from industrial effluents was investigated by **L.Kurkovic et.al.(2000)**. In the batch experiments, parameters studied include the effect of initial concentration of lead and copper ions, temperature, and contact time. Over the temperature range studied (293–313 K) the results of adsorption experiments could be fitted by using both Langmuir and Freundlich models and thermodynamic values of corresponding to each adsorption process were calculated.

In this work, sorption of lead on sawdust (SD) has been studied by **BinYu et.al.(2001)** using batch techniques. The equilibrium sorption level for lead is a function of the solution pH, contact time, sorbent and sorbate concentration. The equilibrium adsorption capacity of sawdust for lead was measured and extrapolated using linear Freundlich and Langmuir isotherms and compared with that for copper. Metal ions which are bounded to the sawdust could be stripped by acidic solution so that the sawdust can be recycled.

This paper discusses the sorption performance of novel materials for the removal of lead(II) and copper(II) from near-neutral aqueous solutions by **D.J. Malik et.al.(2001)**. Active carbons with surface heteroatoms of oxygen and phosphorus have been prepared. The surface functional groups display weakly acidic ion exchange characteristics. The optimum solution pH for maximum metal sorption is related to the pK values of the surface functional groups. The weakly acidic carboxyl groups of structural polysaccharides present within the algal matrix display high sorption capacity for both metals. The negative surface charge of algal particles results in electrostatic interactions as well as coordination between metal species and the adsorbent surface. The surface functional groups in algae unlike those in oxidized active carbons may be represented by discrete acid-dissociation constant values.

Carbon nanotubes (CNTs) show exceptional adsorption capability and high adsorption efficiency for lead removal from water. This was studied by **Yan-Hui Li et.al.(2002)**. The adsorption is significantly influenced by the pH value of the solution and the nanotube surface status, which can be controlled by their treatment processing. The adsorption isotherms are well described by both Langmuir and Freundlich models. Our results suggest that CNTs can be good Pb^{2+} adsorbers and have great potential applications in environmental protection.

The adsorption capacity of some natural materials for lead such as animal bone powder, active carbon, Nile rose plant powder, commercial carbon and ceramics was studied by **S.H. Abdel-Halim et.al.(2002)**. The adsorption process was affected by various parameters such as contact time, pH and concentration of lead solution. The lead uptake percent reaches equilibrium state after 15, 30, 45 and 120 min for bone powder, active carbon, plant powder and commercial carbon, respectively. The uptake percent of lead increased by increasing pH value. The percent removal of lead was 100% by bone powder, 90% by active carbon, 80% by plant powder and 50% by commercial carbon. There was no removal of lead by ceramics. This may be due to the presence of high percent of lead in the constituent of ceramics (372 mg/g).

The removal of heavy metals from plating factory wastewater with economical materials was investigated by **Hideyuki Katsumata et.al.(2003)**, montmorillonite, kaolin, tobermorite, magnetite, silica gel and alumina were used as the economical adsorbents to wastewater containing Cd(II), Cr(VI), Cu(II) and Pb(II). This removal method of heavy metals proved highly effective as removal efficiency tended to increase with increasing pH and decrease with increasing metal concentration. The proposed method was successfully applied to the removal of Cd(II), Cr(VI) and Cu(II) in rinsing wastewater from plating factory in Nagoya City, Aichi Prefecture, Japan.

The adsorption of lead on a new adsorbent synthesized from natural condensed tannin has been investigated by **Xin-Min Zhan et.al.(2003)** using a series of batch adsorption experiments. The study on the adsorption mechanism indicates that the adsorbent performed in aqueous solutions as an ionic exchanger whose end group was sodium ion (Na⁺). One lead (II) ion (Pb²⁺) was adsorbed onto the adsorbent by taking the place of two Na⁺ ions. To a significant extent, pH influenced the extraction of lead from aqueous solutions. The lead removal efficiency was up to 71%, 87% and 91% with initial solution pH at 3.0, 3.6 and 4.2, respectively. The Langmuir equation fitted the adsorption isotherm data well. The maximum adsorption capacity of lead calculated was 57.5, 76.9.

Adsorption of water soluble lead on polymetallic sea nodule has been studied by **S. Bhattacharjee et.al.(2003)**. Complete decontamination of lead is possible by appropriate sea nodule dosing. Adsorption is also dependent on pH and best adsorption is achieved at pH 6. Both Freundlich and Langmuir isotherms may reasonably explain adsorption of lead on sea nodule.

Fixation of heavy metal ions (Cd(II) and Pb(II)) onto sawdust of *Pinus sylvestris* is presented in this paper. Batch experiments were conducted to study the main parameters such as adsorbent concentration, initial adsorbate concentration, contact time, kinetic, pH solution, and stirring velocity on the sorption of Cd(II) and Pb(II) by sawdust of *P. sylvestris*. Kinetic aspects are studied in order to develop a model which can describe the process of adsorption on sawdust. The capacity of the metal ions to bind onto the biomass was 96% for Cd(II), and 98% for Pb(II). The sorption followed a pseudo-second-order kinetics.

An inexpensive and effective adsorbent was developed from bagasse fly ash, obtained from a sugar industry, for the dynamic uptake of lead and chromium. This investigation was done by **V.K. Gupta et.al.(2003)**. Lead and chromium are sorbed by the developed adsorbent up to 96–98%. The removal of these two metal ions up to 95–96% was achieved by column experiments at a flow rate of 0.5 ml min⁻¹. The adsorption was found to be exothermic in nature. The adsorbent was successfully tried for the removal of lead and chromium from wastewater in our laboratory. The developed system for the removal of two ions is very useful, economic, rapid, and reproducible.

An uptake of zinc (Zn), copper (Cu), and lead (Pb) from aqueous solutions by ion exchange on natural zeolitic tuff has been studied by **J. Peri et.al.(2003)**. The Croatian zeolite clinoptilolite from the Donje Jesenje deposit has been used as a natural ion exchanger. The efficiency of removal is higher for Pb and Cu than for Zn ions. The adsorption isotherm equations; Langmuir–Freundlich, Redlich–Petersen, Toth, Dubinin–Radushkevich, modified Dubinin–Radushkevich, and Lineweaver–Burk were derived from the basic empirical equations, and used for calculation of ion exchange parameters.

In this paper, the ability of siderite to remove Pb²⁺ from aqueous solution by adsorption has been investigated by **Mehmet Erdem et.al.(2004)** through batch experiments. The Pb²⁺ adsorption property of the siderite was evaluated as a function of pH, siderite dosage, initial Pb²⁺ concentration, and temperature. Maximum Pb²⁺ adsorption yield was obtained to be 99.6% for initial Pb²⁺ concentration of 50 mg/l at 25 °C and pH 2.97 for 180 min in the presence of 10 g/l siderite. Adsorption data obtained at 25, 30 and 35 °C showed that the adsorption process fitted first-order adsorption rate expression and Langmuir and Freundlich adsorption models. Adsorption capacities of siderite at 25, 30 and 35 °C were found to be 10.32, 12.45 and 14.06 mg Pb²⁺/g siderite, respectively. Adsorption enthalpy and activation energy values were calculated to be 49.73 and 32.49 kJ/g mol from the isotherm and kinetic data, respectively.

Removal of heavy metals when present singly or in binary and ternary systems by the milling agrowaste of *Cicer arietinum* (chickpea var. black gram) as the biosorbent has been studied by **Asma Saeed et.al.(2004)**. The biosorbent removed heavy metal ions efficiently from aqueous solutions with the selectivity order of Pb > Cd > Zn > Cu > Ni. The biosorption of metal ions by black gram husk (BGH) increased as the initial metal concentration increased. Biosorption

equilibrium was established within 30 min, which was well described by the Langmuir and Freundlich adsorption isotherms.

In an attempt to reuse food waste for useful purposes, **Toshimitsu Tokimoto et.al.(2004)** investigated the possibility of using coffee grounds to remove lead ions from drinking water. They studied the lead ion adsorption characteristics of coffee beans and grounds by measuring their fat and protein content, adsorption isotherms for lead ions, and adsorption rates for lead ions. The number of lead ions adsorbed by coffee grounds did not depend on the kind of coffee beans or the temperature at which adsorption tests were performed. The rate of lead ion adsorption by coffee grounds was directly proportional to the amount of coffee grounds added to the solution. When coffee grounds were degreased or boiled, the number of lead ions decreased. When proteins contained in coffee grounds were denatured, the lead ion adsorption was considerably reduced. The lead ion adsorption capacity of coffee grounds decreased with increased concentration of perchloric acid used for treating them and disappeared with 10% perchloric acid.

Different morphologies of carbon nanotubes effect on the lead removal from aqueous solution was studied by **Yan-Hui Li et.al.(2005)**. Four kinds of CNTs with different morphologies were produced by chemical vapor deposition method. After oxidation with nitric acid, their specific surface area, particle size distribution and functional groups on the surfaces were characterized. Adsorption isothermal experiment shows that the CNTs with more defects, which can be easily, introduced more functional groups on their surfaces prepared at 650°C, have higher lead adsorption capability from aqueous solution and are promising adsorbents in wastewater treatment.

The sorption of lead ion onto palm kernel fiber was studied by **Yuh-Shan Ho et.al.(2005)** performing batch kinetic sorption experiments. The batch sorption model, based on a pseudo-second-order mechanism, was applied to predict the rate constant of sorption, the equilibrium capacity and the initial sorption rate with the effects of the initial solution pH and fiber dose. Equilibrium concentrations were evaluated with the equilibrium capacity obtained from the pseudo-second-order rate equation. In addition, pseudo-isotherms were also obtained by changing fiber doses using the equilibrium concentration and equilibrium capacity obtained based on the pseudo-second-order constants.

Maize bran is a low cost biosorbent that has been used for the removal of lead (II) from an aqueous solution and it was studied by **K.K. Singh et.al.(2005)**. The effects of various parameters such as contact time, adsorbate concentration, pH of the medium and temperature were examined. Optimum removal at 20°C was found to be 98.4% at pH 6.5, with an initial Pb (II) concentration of 100 mg /l. Dynamics of the sorption process and mass transfer of Pb (II) to maize bran were investigated and the values of rate constant of adsorption, rate constant of intraparticle diffusion and the mass transfer coefficients were calculated. Different thermodynamic parameters viz., changes in standard free energy, enthalpy and entropy were evaluated and it was found that the reaction was spontaneous and exothermic in nature. The adsorption data fitted the Langmuir isotherm. A generalized empirical model was proposed for the kinetics at different initial concentrations. The data were subjected to multiple regression analysis and a model was developed to predict the removal of Pb (II) from an aqueous solution.

The performance of a commercially available palm shell based activated carbon to remove lead ions from aqueous solutions by adsorption was evaluated by **Gulnaziya Issabayeva et.al.(2005)**. The adsorption experiments were carried out at pH 3.0 and 5.0. The effect of malonic and boric acid presence on the adsorption of lead ions was also studied. Palm shell activated carbon showed high adsorption capacity for lead ions, especially at pH 5 with an ultimate uptake of 95.2 mg/g. This high uptake showed palm shell activated carbon as amongst the best adsorbents for lead ions. Boric acid presence did not affect significantly lead uptake, whereas malonic acid decreased it. The diffuse layer surface complexation model was applied to predict the extent of adsorption. The model prediction was found to be in concordance with the experimental values.

The removal of lead ions from aqueous solution was studied by **M. Mouflih et.al.(2005)** in batch experiments using natural phosphate (NP). The effects of initial concentration of lead and initial pH of solution were investigated and the mechanism for removal of lead has been suggested. The data obtained from sorption isotherms at different temperatures conformed to the linear form of the Langmuir adsorption equation. The influence of NO₃⁻ and Cl⁻ anions has been evaluated. The effect of varying levels of Cl⁻ has significant influence on the sorption capacity of Pb²⁺, while NO₃⁻ did not. The abundance of natural phosphate, its low price and non-aggressive

nature towards the environment are advantages for its utilization in point of view of wastewater and wastes clean up.

The capacity of hydroxyapatite (HAp) to remove lead from aqueous solution was investigated by **Bailez Sandrine et.al.(2006)** under different conditions, namely initial metal ion concentration and reaction time. The sorption of lead from solutions containing initial concentrations from 0 to 8000 mg/L was studied for three different HAp powders. Soluble Pb and Ca monitoring during the experiment allows characterizing the mechanism of lead uptake. Dissolution of calcium is followed by the formation of a solid solution with a Ca/P ratio decreasing continuously. Langmuir–Freundlich classical adsorption isotherms modeled adsorption data. The adsorption capacities calculated from this equation vary from 330 to 450 mg Pb/g HAp for the different solids. Modeling of the sorption process allows to determine theoretical saturation times and residual lead concentrations at equilibrium.

In the present study, the ability of natural zeolite clinoptilolite and bentonite (clay) to remove Pb(II) from aqueous solutions has been investigated by **Vassilis J. Inglezakis et.al.(2006)** in batch reactors with a maximum contact time of 120 min. Adsorption tests of Pb(II) were carried out using a solution concentration of 1,036 ppm at initial pH = 4, and solid to liquid ratio of 2 g/100 ml. The effects of agitation speed (0, 100, 200, 500 rpm), temperature (28°C, 45°C, 60°C) and particle size (2.5–5.0 mm, dust) of the minerals were examined. The effect of acidity of the aqueous solution was also examined. Bentonite was found to be more effective for the removal of Pb(II) than clinoptilolite, under the experimental conditions used. The removal of Pb(II) using bentonite reached 100% at ambient temperature and mild agitation (100 rpm), while it was approximately 90% at 60°C without agitation.

The removal of heavy metals from wastewater using olive cake as an adsorbent was investigated by **Sabriye Doyurum et.al.(2006)**. The effect of the contact time, pH, temperature, and concentration of adsorbate on adsorption performance of olive cake for Pb(II) and Cd(II) ions were examined by batch method. Adsorption of Pb(II) and Cd(II) in aqueous solution onto olive cake was studied in single component. After establishing the optimum conditions, elution of these ions from the adsorbent surface was also examined. The optimum sorption conditions were determined for two elements. Maximum desorption of the Pb(II) and Cd(II) ions were found to be 95.92 and 53.97% by 0.5M HNO₃ and 0.2M HCl, respectively. The morphological analysis of the olive cake was performed by the scanning electron microscopy (SEM).

An indigenously prepared, steam activated and chemically modified carbon from husk and pods of *Moringa oleifera* (*M.oleifera*), an agricultural waste, was comparatively examined as an adsorbent for the removal of lead from aqueous solutions by **Muhammad Nadeem et.al.(2006)**. Studies were conducted as a function of contact time, initial metal concentration, dose of adsorbent, agitation speed, particle size, and pH. Maximum uptake capacities were found to be, 98.89, 96.58, 91.8, 88.63, 79.43% for cetyltrimethyl ammonium bromide (CTAB), phosphoric, sulfuric, hydrochloric acid treated and untreated carbon adsorbents respectively. Bangham, Pseudo-first and second order, Intra Particle Diffusion equations were implemented to express the sorption mechanism by utilized adsorbents. The results of adsorption were fitted to both the Langmuir and Freundlich models.

The biosorption of lead ions from aqueous solution by *Syzygium cumini* L. was studied by **P.King et.al.(2006)** in a batch adsorption system as a function of pH, contactn time, lead ion concentration, adsorbent concentration and adsorbent size. The biosorption capacities and rates of lead ions onto *S. cumini* L. were evaluated. The Langmuir, Freundlich, Redlich–Peterson and Temkin adsorption models were applied to describe the isotherms and isotherm constants. Biosorption isothermal data could be well interpreted by the Langmuir model followed by Temkin model with maximum adsorption capacity of 32.47 mg/g of lead ion on *S. cumini* L. leaves biomass. The kinetic experimental data were properly correlated with the second-order kinetic model.

The use of natural palygorskite clay for the removal of Pb (II) from aqueous solutions for different contact times, pHs of suspension, and amounts and particle sizes of palygorskite clay were investigated by **Hao Chen et.al.(2006)**.The variations of the pH value of Pb (II) solutions on natural palygorskite in the adsorption process were determined. Batch adsorption kinetic experiments revealed that the adsorption of Pb (II) onto palygorskite clay involved fast and slow processes. It was found that the adsorption mechanisms in the lead/palygorskite system follow pseudo-second-order kinetics with a significant contribution from film diffusion. SEM observations demonstrated that an important interaction at the lead–granule interface occurred during the adsorption process. The adsorption isotherms were described by means of the Langmuir and Freundlich isotherms and the Langmuir model represents the adsorption process better than the Freundlich model. The maximum adsorption capacity of Pb(II) onto natural palygorskite was 104.28 mg /g.

The ability of low-cost activated carbon prepared from *Ceiba pentandra* hulls, an agricultural waste material, for the removal of lead and zinc from aqueous solutions has been investigated by **M. Madhava Rao et.al.(2007)**. In the batch tests experimental parameters were studied, including solution pH, contact time, adsorbent dose and initial metal ions concentration. The adsorbent exhibited good sorption potential at pH 6.0. Maximum removal of lead (99.5%) and of zinc (99.1%) with 10 g/l of sorbent was observed at 50 mg/L sorbate concentration. Removals of about 60–70% occurred in 10 min, and equilibrium was attained at around 50 min for both metals. The desorption studies were carried out using dilute HCl, and the effect of HCl concentration on desorption was studied. Maximum desorptions of 85% for lead and 78% for zinc were attained with 0.15 M HCl.

Adsorption of copper and lead ions onto tea waste from aqueous solutions was studied by **B.M.W.P.K. Amarasinghe et.al.(2007)** to enable comparison with alternative commonly available adsorbents. Batch experiments were conducted to determine the factors affecting adsorption and kinetics of the process. Fixed bed column experiments were performed to study practical applicability and breakthrough curves were obtained. Tea waste is capable of binding appreciable amounts of Pb and Cu from aqueous solutions. The adsorption capacity was highest at solution pH range 5–6. The adsorbent to solution ratio and the metal ion concentration in the solution affect the degree of metal ion removal. The equilibrium data were satisfactorily fitted to Langmuir and Freundlich isotherms. Highest metal uptake of 48 and 65 mg/g were observed for Cu and Pb, respectively. Pb showed higher affinity and adsorption rate compared to Cu under all the experimental conditions. Kinetic studies revealed that Pb and Cu uptake was fast with 90% or more of the adsorption occurring within first 15–20 min of contact time.

The equilibrium and kinetic properties of Pb^{2+} ion adsorption by retorted shale (RS) have been investigated by P.M. Pimentel et.al.(2007) during a series of batch adsorption experiments. The effects of pH, contact time and adsorbate initial concentrations were evaluated. The pseudo-second-order model was used to predict the rate constants of adsorption system. Langmuir and Freundlich models were used to fit the equilibrium data, which showed that Langmuir best-fitted these data. Thermodynamic parameters of adsorption indicate spontaneous and endothermic nature of the process.

This paper presents the results of research on heavy metals removal from water by filtration using low cost coarse media which could be used as an alternative approach to remove heavy metals from water or selected wastewater and this was studied by **Hamidi A. Aziz et.al.(2007)**. A series of batch studies were conducted using different particle media (particle size 2.36–4.75 mm) shaken with different heavy metal solutions at various pH values to see the removal behaviour for each metal. Each solution of cadmium (Cd), lead (Pb), zinc (Zn), nickel (Ni), copper (Cu) and chromium (Cr(III)) with a concentration of 2 mg/L was shaken with the media. At a final pH of 8.5, limestone has significantly removed more than 90% of most metals followed by 80% and 65% removals using crushed bricks and gravel, respectively.

The adsorption of lead onto formaldehyde or sulphuric acid treated acorn waste was studied by **Ahmet Ornek et.al.(2007)** using a batch sorber. The aim of this study was to understand the mechanisms that govern lead removal and find a suitable equilibrium isotherm and kinetic model for the lead removal in a batch reactor. The experimental isotherm data were analyzed using the Langmuir, Freundlich and Temkin equations. The equilibrium data fit well the Langmuir isotherm. The experimental data were analyzed using four adsorption kinetic models – the pseudo first- and second-order equations, intraparticle diffusion equation and the Elovich equation – to determine the best fit equation for the adsorption of lead ions onto formaldehyde or sulphuric acid treated acorn waste. The rate constants, equilibrium capacities and related correlation coefficients for each kinetic model were calculated and discussed. Also, predicted q_t values from the kinetic equations were compared with the experimental data. Results show that the pseudo second-order equation provides the best correlation for the adsorption process, whereas the Elovich equation also fits the experimental data well.

CHAPTER-5

EXPERIMENTAL PROGRAMME

Experimental details of the study have been presented in this chapter. These details include characterization of adsorbents and batch adsorption studies.

5.1) Objective of present study:

The objective of this study is to investigate some useful information regarding the use of adsorption for the removal of lead from waste water. Here I have used Coconut Jute Activated Carbon (CJAC) and Commercial Activated Carbon (CAC) as adsorbents. The entire study deals with various parameters dealing with adsorption and adsorption kinetics.

- 1000mg/l of stock solution is to be prepared by dissolving 1.6g of lead nitrate ($\text{Pb}(\text{NO}_3)_2$) in 1000ml of distilled water, from this stock solution solutions of desired concentrations (20-100 mg/l) were prepared.
- Lead concentration is to be estimated by UV/VIS spectrophotometer (Perkin Elmer 35) using PAR reagent (2,4-pyridyl azoresorcinol) at 580 nm.
- The Physico-Chemical characteristics of adsorbents are to be found by various methods like Proximate Analysis, Density, Particle Size Analysis, Surface area measurement, Scanning Electron Micrograph (SEM) etc.,
- Study the effect of various batch parameters like optimum pH, contact time, adsorbent dose, temperature, concentration on the removal of lead.
- Study of the kinetics of adsorption.
- Studies of the isotherms are to be used to find the adsorption capacity of the adsorbent.
- Study of thermodynamic adsorption parameters, ΔG° , ΔH° and ΔS° .

5.2) Preparation of the adsorbents:

The adsorbent coconut jute activated carbon was prepared by the coconut jute. Coconut jute is a light fluffy material. India, the third largest producer of coconuts in the world, produces about 12.8 billion coconuts a year. It is estimated that the production of coconut jute in India is about 0.5 million tons per year. Coconut jute is not easily biodegradable. Preparation of activated

carbons from this cheap and abundant biomass will eliminate the costly problem of solid waste disposal while at the same time deriving economic benefits from such value-added products.

First coconut jute was washed with the distilled water and dried in sunlight. Then the dried material was washed with concentration sulfuric acid (for 1 part of material 1.8 parts of acid) and kept at atmospheric temperature for about 5 hours with occasional stirring. The product, acid-carbonized coconut jute was washed several times with distilled water and with 5% sodium bicarbonate solution for the removal of remaining amount of acid, followed by again distilled water and kept in muffle furnace at 600°C for 1 hr .It was sieved to different particle sizes, 100 to 450 µm, and finally kept in bottles. The particle size 100 µm was used in the following batch adsorption experiments.

The commercial activated carbon LR grade was supplied by S.D. Fine-Chem (Boisar, India). It was treated with acid before delivery. These were subsequently pulverized and sieved through 18 to 44 BS mesh to get the activated carbon particles of the desired size range.

5.3) Characterization of adsorbents:

The physico-chemical characteristics of the CJAC and CAC were determined using standard procedures as discussed below:

5.3.1 Proximate Analysis

Proximate analysis of the CJAC and CAC were carried out using the procedure as per IS 1350:1984.

5.3.2 Density

The Bulk density of CJAC and CAC were determined using MAC bulk density meter.

5.3.3 Energy dispersive spectrum (EDS)

Energy dispersive x-ray spectroscopy (EDS) is a chemical microanalysis technique performed in conjunction with a Scanning Electron Micrograph (SEM) for analysis of CJAC and CAC.

5.3.4 Scanning Electron Micrograph (SEM)

SEM analysis of CJAC and CAC were carried out before and after the adsorption of lead from waste water by using LEO 435 VP Scanning electron microscope.

5.4) Adsorbate:

Synthetic wastewater solutions of Lead of desired concentrations (20–100 mg/l) were prepared by dissolving accurately weighed quantity of lead nitrate ($\text{Pb}(\text{NO}_3)_2$) of AR grade in distilled water.

5.4.1 Analytical measurement

Concentration of lead was estimated spectrophotometrically by using PAR reagent (2,4-pyridyl azoresorcinol) monitoring the absorbance characteristic wavelength using UV/VIS spectrophotometer (Perkin Elmer 35). To the sample add PAR reagent drop wise which is acting as complexing agent and it turns the sample to pink colour. The intensity of the colour is proportional to the lead concentration in the solution. A standard solution of Lead was taken and the absorbance was determined at different wavelengths to obtain a plot of absorbance versus wavelength. The wavelength corresponding to maximum absorbance (λ_{max}) was determined from this plot. The λ_{max} for Lead was found to be 580 nm. Calibration curve was plotted between the absorbance and the concentration of Lead solution. The linearity of calibration curve (Fig. 5.1) indicated the applicability of the Lambert-Beer's Law.

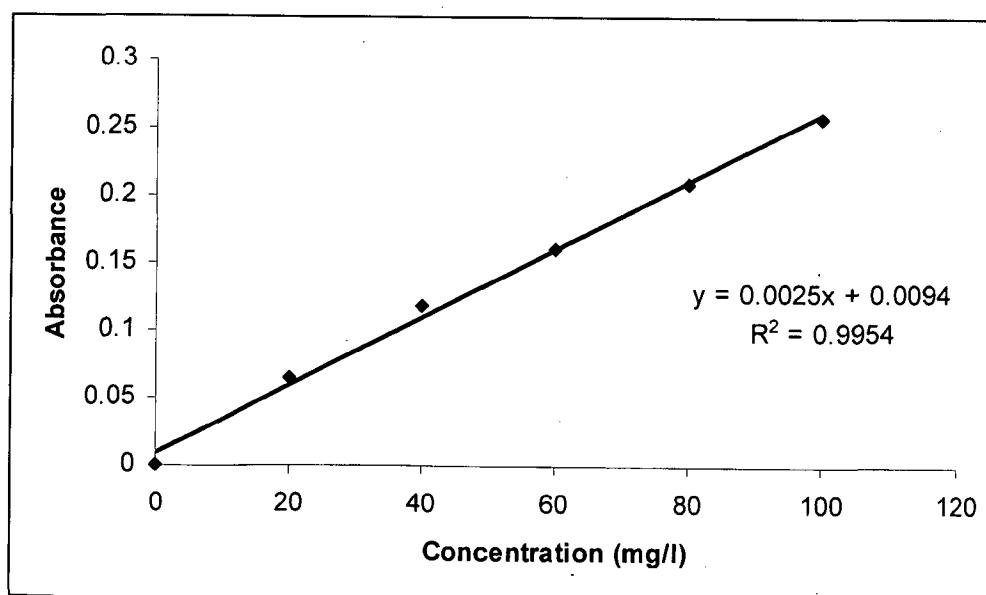


Fig. 5.1: Calibration Graph of Lead (II)

5.5) Experimental Programme:

The experimental programme was performed by Batch adsorption studies.

5.5.1 Batch Adsorption Experiments

To study the effect of important parameters like initial pH (pH_0), adsorbent dose (m), initial concentration (C_0), contact time (t), adsorbent size(s) and temperature (T) on the adsorptive removal of lead by CJAC and CAC, batch experiments were conducted at 30 ± 1 °C. For each experimental run, 100 ml of lead solution of known C_0 , pH_0 , known adsorbent size and known amount of the adsorbent were taken in a 250 ml stoppered conical flask. This mixture was agitated in a temperature-controlled shaking water bath at a constant speed at 30 ± 1 °C. Samples were withdrawn at appropriate time intervals. After filtration Pb(II) remaining in solution was analyzed spectrophotometrically using UV/VIS spectrophotometer at 580 nm, using PAR reagent (2,4-pyridyl azoresorcinol). The effect of pH_0 on lead removal was studied over a pH_0 range of 2 to 8. pH_0 was adjusted by the addition of dilute aqueous solutions of HNO₃ or NaOH (0.10 M). For the optimum amount of m , a 100 ml dye solution was contacted with different amounts of CJAC and CAC till equilibrium was attained. To see the effect of temperature for the adsorption of lead from solution by CJAC and CAC, experiments were also conducted at 35°C, 50°C and 60°C. The kinetics of adsorption was determined by analyzing adsorptive uptake of the Lead from the aqueous solution at different time intervals. For adsorption isotherms, lead solutions of different concentrations were agitated with the known amount of adsorbent till the equilibrium was achieved. The residual lead concentration of the solution was then determined. Blank experimental runs, with only the adsorbent in 100 ml of distilled water, were conducted simultaneously at similar conditions to account for any colour leached by the adsorbents and adsorbed by glass containers. Batch tests were carried out to compare the adsorptive capacity and intensity of CJAC and CAC.

The percentage removal of lead and equilibrium adsorption uptake in solid phase, q_e (mg/g), was calculated using the following relationships:

$$\text{Percentage metal ions removal} = 100(C_0 - C_e) / C_0 \quad (4.1)$$

$$\text{Amount of adsorbed metal ions per g of solid, } q_e = (C_0 - C_e)V/w \quad (4.2)$$

where, C_0 is the initial metal ion concentration (mg/l), C_e is the equilibrium phosphate concentration (mg/l), V is the volume of the solution (l) and w is the mass of the adsorbent (g).

CHAPTER-6

RESULTS AND DISCUSSION

6.1) General:

The detailed discussion on the results of the experiments conducted is given in this chapter. These results include

- Characterization of Coconut Jute Activated Carbon (CJAC) and Commercial Activated Carbon (CAC).
- Batch adsorption studies.

6.2) Characterization of Coconut Jute Activated Carbon (CJAC) and Commercial Activated Carbon (CAC):

Characteristics of CJAC and CAC included proximate analysis was carried out for the physico-chemical characteristics. The physico-chemical characteristics of CJAC and CAC are given in Table C-1 and C-2 respectively. Due to presence of high carbon content, CJAC and CAC may be treated as organic in nature. The organic nature of AC imparts porosity to it. Compared to CJAC CAC has more carbon content.

For structural and morphological characteristics, scanning electron micrograph (SEM) analysis and Energy dispersive spectrum were carried out. Scanning electron micrograph photographs of CJAC and CAC before and after adsorption are shown in Figs. B-1, B-2 and Figs. B-3, B-4 respectively. These photographs reveal their surface texture and porosity. This photomicrograph shows fibrous structure of CJAC and CAC. However, the surface of the CJAC and CAC becomes smooth after adsorption of lead as shown in Fig. B-2 and B-4 respectively.

The EDS x-ray detector measures the number of emitted x-rays versus their energy. The energy of the x-ray is characteristic of the element from which the x-ray was emitted. A spectrum of the energy versus relative counts of the detected x-rays is obtained and evaluated for

qualitative and quantitative determinations of the elements present in the sampled volume. Figs.B-5, B-6 and B-7, B-8 shows the energy dispersive spectrum for the CJAC and CAC before and after adsorption respectively. Fig.B-5 , B-7 reveals that the CJAC and CAC contains high carbon besides silica, sodium, sulphur etc., In Fig.B-6,B-8 there was peak of lead due to adsorption of lead on CJAC and CAC.

6.3) Batch adsorption study:

Batch operations were performed to study the effect of different parameters. Batch adsorption experiments were carried out in 250 ml Stoppard conical flask for removal of lead from synthetic solutions of known concentrations by using CJAC and CAC. The effect of various operating parameters, viz. pH, adsorbent dose, initial concentration, contact time, adsorbent size and temperature are studied and presented here.

6.3.1. Effect of initial pH (pH_0)

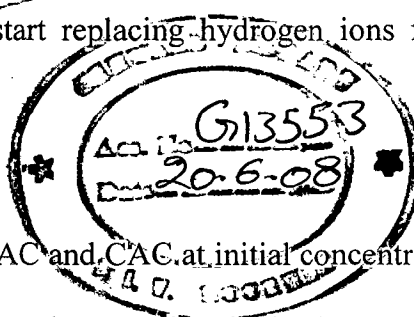
pH is one of the most important environmental factors influencing not only site dissociation, but also the solution chemistry of the heavy metals: hydrolysis, complexation by organic and/or inorganic ligands, redox reactions, and precipitation are strongly influenced by pH and, on the other hand, strongly influence the speciation and adsorption availability of heavy metals.

Adsorption of lead on CJAC and CAC was studied at varying pH values to optimize the removal and shown in Fig. B-9 and Fig.B-10, respectively. It is apparent that uptake is quite low at low pH, however with an increase in pH, a significant enhancement in adsorption was recorded. The optimum pH for CJAC-Pb and CAC-Pb systems was found to be 5 and 4.2 with removal about 68% and 79% metal from solution with initial lead concentration of 20 mg/l respectively. At lower pH values the electrostatic forces of repulsion between adsorbents (CJAC

and CAC) and adsorbate (Pb^{2+}) is prominent. So the efficiency of metal removal is low at lower pH. At pH above 6.0 (for CJAC), 5 (for CAC), there is a possibility of Pb^{2+} precipitation as $Pb(OH)_2$ on the surface of the adsorbents by nucleation. So the lead removal efficiency is low. Between pH 2 and 5 (for CJAC), 2.0 and 4.2 (for CAC) the percentage removal increases sharp. This might be due to the fact that metal ions start replacing hydrogen ions from adsorbent surface.

6.3.2. Effect of adsorbent dosage (m)

The effect of m on the removal of lead by CJAC and CAC at initial concentration = 20 mg/l is shown in Figs. B-11 and B-12, respectively. It can be seen that the lead removal increases up to a certain limit and then it remains almost constant. Optimum m was found to be 1g/l for CJAC and 1g/l for CAC. An increase in the adsorption with the adsorbent dose can be attributed to greater surface area and the availability of more adsorption sites.



6.3.3 Effect of initial lead concentration (C_0)

The effect of C_0 on the removal of lead by CJAC and CAC is shown in Figs. B-13, B-14 and B-15, B-16 respectively. It is evident from the Figures, that the amount of lead adsorbed per unit mass of adsorbent (q_e) increased with the increase in C_0 (Figs. B-13 and B-15), although percentage lead removal decreased with the increase in C_0 (Figs. B-14 and B-16). q_e increased with the increase in C_0 as the resistance to the uptake of lead from the solution decreases with the increase in lead concentration. The rate of adsorption also increases with the increase in C_0 due to increase in the driving force.

6.3.4 Effect of contact time (t)

The effect of contact time on the removal of lead by CJAC and CAC at $C_0 = 20, 40, 60, 80$ and 100 mg/l is given in Figs. B-14 and B-16, respectively. The contact time curves show rapid adsorption of lead in the first 30 min, thereafter, the adsorption rate decreases gradually and the adsorption reaches equilibrium in 4 h for CJAC and CAC (optimum contact time). Aggregation of lead molecules with the increase in contact time makes it almost impossible to diffuse deeper into

the adsorbent structure at highest energy sites. This aggregation negates the influence of contact time as the mesopores get filled up and start offering resistance to diffusion of aggregated lead molecules in the adsorbents. This is the reason why an insignificant enhancement in adsorption after optimum time. Hence further experiments were conducted for optimum contact time only. The curves are single, smooth and continuous leading to saturation. The adsorption curves of contact time indicate the possible mono-layer coverage of lead ions on the surface of CJAC and CAC.

6.3.5 Effect of particle size(s)

The effect of particle size on uptake of lead was studied with different adsorbent sizes from 100 to 300 μm . Fig.B-17 (for CJAC) and Fig.B-18 (for CAC) shows that the percent removal of lead increases from 38 to 69% (for CJAC) and 43 to 79% (for CAC) as the particle size decreases from 300 to 100 μm for an initial concentration of 20 mg/l lead solution. The extent of the adsorption process increases with increased specific surface area. The specific surface available for adsorption will be greater for smaller particles and hence percent removal increases as particle size decreases. For larger particles the diffusional resistance to mass transport is higher and most of the internal surface of the particle may not be utilized for adsorption. Consequently the amount of lead adsorbed is small.

6.3.6 Effect of temperature (T)

Temperature has a pronounced effect on the adsorption capacity of the adsorbents. Figs. B-19-B-20 and B-21-B-22 show the plots of adsorption isotherms, for Pb-CJAC and Pb-CAC systems at 303, 323 and 343 K, respectively. It shows that the adsorptivity of lead increases with the increase in temperature. This increase shows that the adsorption process may be by chemisorption. Since sorption is an exothermic process, it would be expected that an increase in temperature of the adsorbate-adsorbent system would result in decreased sorption capacity. However, if the adsorption process is controlled by the diffusion process (intraparticle transport-pore diffusion), the sorption capacity will show an increase with an increase in temperatures. This is basically due to the fact that the diffusion process is an endothermic process. With an increase in temperature, the mobility of the lead ions increases and the retarding forces acting on the diffusing ions decrease, thereby increasing the sorptive capacity of adsorbent.

6.4) Adsorption Kinetics Study:

There are various models available to explain the kinetics of adsorption. In order to investigate the adsorption process of Pb (II) on CJAC and CAC, four kinetics models viz. pseudo- first-order model, pseudo-second-order model, intraparticle diffusion model and Bangham's model were used.

6.4.1 Pseudo-first-order model:

Lagergren rate equation is one of the most widely used sorption rate equations for the adsorption.

The pseudo-first-order equation is

$$\frac{dQ}{dt} = k_f(Q_e - Q_t) \quad (6.1)$$

where Q_t is the amount of adsorbate adsorbed at time t (mg/g), Q_e is the adsorption capacity in equilibrium (mg/g), k_f is the rate constant of pseudo-first-order model (min^{-1}), and t is the time (minute). After definite integration by applying initial conditions at $t=0$, $Q_t=0$ and at $t=t$, $Q_t=Q_t$, the equation becomes:

$$\log(Q_e - Q_t) = \log Q_e - \frac{k_f}{2.303} t \quad (6.2)$$

The values of adsorption rate constant (k_f) for lead ions adsorption on CJAC and CAC at $C_0=20, 40, 60, 80$ and 100 mg/l were determined from the plot of $\log(Q_e - Q_t)$ against t (Figs. B-23 and B-24). The k_f values are given in Table C-3.

6.4.2 Pseudo-second-order model:

The pseudo-second-order model is represented as:

$$\frac{dq_t}{dt} = k_s(q_e - q_t)^2 \quad (6.3)$$

Where, k_s is the pseudo-second-order rate constant (g/mg/min). Integrating Eq (6.3) and noting that $q_t=0$ at $t=0$, the following equation is obtained:

$$\frac{t}{q_t} = \frac{1}{k_s q_e^2} + \frac{1}{q_e} t \quad (6.4)$$

The initial sorption rate, h (mg/g/min), at $t \rightarrow 0$ is defined as

$$h = k_s q_e^2$$

Figs. B-25 and B-26 shows the plot of t/q_t versus t for CJAC and CAC, respectively, at $C_0 = 20, 40, 60, 80$ and 100 mg/l. The q_e is obtained from the slope of the plot and the h value is obtained from the intercept. Since q_e is known from the slope, k_s can be determined from the h value. The k_s and h values as calculated from the Figures are listed in Table C-4 for both the adsorbents. The calculated correlation coefficients are also closer to unity and also $q_{e, \text{calc}}$ and $q_{e, \text{expt}}$ values are almost same for pseudo-second-order kinetics than that for the pseudo first-order kinetic model. Therefore the sorption can be approximated more appropriately by the pseudo-second-order kinetic model. It can be seen that the CAC has higher h and q_e values for lead ions adsorption.

6.4.3 Weber-Morris intra-particle diffusion model:

The adsorbate transport from the solution phase to the surface of the adsorbent particles occurs in several steps. The overall adsorption process may be controlled either by one or more steps, e.g. film or external diffusion, pore diffusion, surface diffusion and adsorption on the pore surface, or a combination of more than one step. In a rapidly stirred batch adsorption, the diffusive mass transfer can be related by an apparent diffusion coefficient, which will fit the experimental sorption-rate data. Generally, a process is diffusion controlled if its rate is dependent upon the rate at which components diffuse towards one another. The possibility of intra-particle diffusion was explored by using the intra-particle diffusion model.

$$q_t = k_{id}t^{1/2} + I \quad (6.5)$$

Where, k_{id} is the intra-particle diffusion rate constant (mg/g min^{1/2}) and I is the intercept (mg/g). Plot of q_t versus $t^{1/2}$ should be a straight line with a slope k_{id} and intercept I when adsorption mechanism follows the intra-particle diffusion process. If the Weber-Morris plot of q_t versus $t^{1/2}$ satisfies the linear relationship with the experimental data, then the sorption process is found to be controlled by intra-particle diffusion only. However, if the data exhibit multi-linear plots, then two or more steps influence the sorption process. Fig. B-27 and Fig. B-28 represents plot of q_t versus $t^{1/2}$ at $C_0 = 20, 40, 60, 80$ and 100 mg/l for lead adsorption on CJAC and CAC, respectively. In Fig. B-27, B-28 the data points are related by two straight lines—the first straight portion depicting macropore diffusion and the second representing meso-pore diffusion. These show only the pore diffusion data. The deviation of straight lines from the origin may be due to difference in rate of mass transfer in the initial and final stages of adsorption. Further, such

deviation of straight line from the origin indicates that the pore diffusion is not the sole rate-controlling step. The adsorption data for q_t versus $t^{1/2}$ for the initial period show curvature, usually attributed to boundary layer diffusion effects or external mass transfer effects. The values of rate parameters ($k_{id,I}$ and $k_{id,II}$) are given in Table C-5. The values of the correlation coefficients are also given in Table C-5.

6.4.4. Bangham's model:

The rate constants, K_r for the sorption of lead were calculated using the simplest form of Bangham equation :

$$dQ/dt = Q_t / (mt) \quad (6.6)$$

The integral form of the equation can be written as:

$$Q_t = K_r t^{1/m} \quad (6.7)$$

Assessment of the rate constants is possible by simple linear transformation of the equation:

$$\log Q_t = \log K_r + (1/m) \log t \quad (6.8)$$

As can be observed from the Fig.B-29, B-30, the linearity of the obtained plots indicate the applicability of the of the $1/m$ th order kinetics for the system under observation. The adsorption rate constants were calculated from the intercepts and slopes of the straight lines and are reported in Table C-6.

6.5) Adsorption Equilibrium Study:

To optimize the design of an adsorption system for the adsorption of adsorbates, it is important to establish the most appropriate correlation for the equilibrium curves. Various isotherm equations have been used to describe the equilibrium characteristics of adsorption. Some of these equations are Freundlich, Langmuir, Temkin and Redlich Peterson equations.

6.5.1 Freundlich and Langmuir Isotherms

Linearised form of Freundlich and Langmuir isotherm equations are given as

$$\ln Q_e = \ln K_F + \frac{1}{n} \ln C_e \quad (\text{Linear form}) \quad (6.9)$$

$$\frac{C_e}{Q_e} = \frac{1}{K_A Q_m} + \frac{C_e}{Q_m} \quad (\text{Linear form}) \quad (6.10)$$

Fig.B-31, B-32 shows the Freundlich isotherm plots ($\ln Q_e$ versus $\ln C_e$) for adsorption of lead on CJAC, CAC at 303, 323 and 343 K, respectively. Langmuir isotherm plot (C_e/Q_e versus C_e)

shown in Fig.B-33,B-34 for adsorption onto CJAC,CAC respectively. Freundlich and Langmuir isotherm parameters for both adsorbents along with linear and non-linear correlation coefficients are given in Table C-7, C-8, C-9 and C-10. At all temperatures, Langmuir isotherm represents a better fit of the experimental data than Freundlich isotherm. This suggests adsorption of lead ions by CJAC and CAC are apparently with monolayer coverage of adsorbed molecules. The essential characteristics of a Langmuir isotherm can be expressed in terms of a dimensionless factor, R_L , which describes the type of pattern and is defined as $R_L=1/(1+K_A C_0)$ indicates the nature of adsorption as

If	$R_L > 1$	Unfavorable
	$R_L = 1$	Linear
	$0 < R_L < 1$	Favorable
	$R_L = 0$	Irreversible

The value of R_L is found to be less than 1 for adsorption of lead ions on CJAC and CAC, so adsorption using CJAC and CAC is favorable.

6.5.2 Temkin Isotherm

It is given as

$$q_e = \frac{RT}{b} \ln(K_T C_e) \quad (6.11)$$

which can be linearized as:

$$q_e = B_1 \ln K_T + B_1 \ln C_e \quad (6.12)$$

where $B_1 = \frac{RT}{b}$

Temkin isotherm contains a factor that explicitly takes into the account adsorbing species-adsorbent interactions. This isotherm assumes that (i) the heat of adsorption of all the molecules in the layer decreases linearly with coverage due to adsorbent-adsorbate interactions, and that (ii) the adsorption is characterized by a uniform distribution of binding energies, up to some maximum binding energy. A plot of q_e versus $\ln C_e$ enables the determination of the isotherm constants B_1 and K_T from the slope and the intercept, respectively. K_T is the equilibrium binding constant (l/mol) corresponding to the maximum binding energy, constant B_1 is related to the heat of adsorption and R is gas constant (8.314 J/mol K). Fig.B-35,B-36 shows the Temkin isotherm

plots for both adsorbents. The Temkin isotherm parameters listed in Table C-11,C-12. It shows better fit than Langmuir isotherm.

6.5.3 Redlich-Peterson Isotherm

Redlich and Peterson (1959) model combines elements from both the Langmuir and Freundlich equation and the mechanism of adsorption is a hybrid and does not follow ideal monolayer adsorption. The Redlich Peterson isotherm has a linear dependence on concentration in the numerator and an exponential function in the denominator. The R-P equation is the combination of Langmuir and Freundlich models. It approaches Freundlich model at high concentration and is accord with the low concentration limit of Langmuir equation. Furthermore, the R-P equation incorporates three parameters into an empirical isotherm, and therefore can be applied either in homogeneous or heterogeneous system due to high versatility of the equation.

It can be described as follows:

$$Q_e = \frac{K_R C_e}{1 + a_R C_e^\beta} \quad (6.13)$$

where K_R is R-P isotherm constant (l/g), a_R is R-P isotherm constant (l/mg) and β is the exponent which lies between 1 and 0, where $\beta=1$

$$Q_e = \frac{K_R C_e}{1 + a_R C_e} \quad (6.14)$$

It becomes Langmuir equation. Where $\beta=0$

$$Q_e = \frac{K_R C_e}{1 + a_R} \quad (6.15)$$

i.e. the Henry's law equation.

Above Eq. can be converted into al linear form by taking logarithms:

$$\ln\left(K_R \frac{C_e}{Q_e} - 1\right) = \ln a_R + \beta \ln C_e \quad (6.16)$$

Plotting the left hand side of above eq. against $\ln C_e$ to obtain isotherm constant is not applicable because of three unknowns, a_R , K_R and β . Therefore a minimization procedure was adopted to solve the equation by maximizing the correlation coefficient between theoretical data for Q_e predicted from equation and experimental data. Therefore, the parameters of equations were determined by minimizing the distance between the experimental data points and the theoretical model predictions with solver add-in function of Microsoft excel. The Fig.B-37, B-38

shows the R-P isotherm plots for both adsorbents. The R-P isotherm parameters listed in Table C-13,C-14. The R-P isotherm parameters and the correlation coefficients are significantly higher than both the Langmuir and Freundlich values for Pb (II) adsorption on CJAC and CAC. The Redlich-Peterson is the certainly best fit isotherm equation of the four isotherm studied so far.

6.6 Error Analysis:

The use of R^2 is limited to solving linear forms of isotherm equation, which measure the difference between experimental data and theoretical data in linear plots only, but not the errors in isotherm curves. Purely, from a comparison of the correlation coefficients (R^2 values) for the linearized models, it can be seen that higher weightage is given to the higher C_e value data points, thus giving a better fit correlation to the higher C_e value data points. Due to the inherent bias resulting from linearization, error functions of non-linear regression basin are employed to evaluate the isotherm constants and compare them with the less accurate linearized analysis values. Five different error functions of non-linear regression basin were employed in this study to find out the best-fit isotherm model to the experimental equilibrium data.

6.6.1 The Sum of the Squares of the Errors (SSE)

This error function, SSE is given as

$$SSE = \sum_{i=1}^n (q_{e,calc} - q_{e,exp})_i^2 \quad (6.17)$$

Here, $q_{e,cal}$ and $q_{e,exp}$ are, respectively, the calculated and the experimental value of the equilibrium adsorbate solid concentration in the solid phase (mg/g) and n is the number of data points. This most commonly used error function, SSE has one major drawback in that it will result in the calculated isotherm parameters providing a better fit at the higher end of the liquid phase concentration range. This is because of the magnitude of the errors, which increase as the concentration increases. The values of SSE are given in Tables C-15 and C-16, both for CJAC and CAC, respectively.

6.6.2 The Average Relative Error (ARE)

ARE is given as

$$ARE = \frac{100}{n} \sum_{i=1}^n \left| \frac{(q_{e,exp} - q_{e,calc})}{q_{e,exp}} \right|_i \quad (6.18)$$

This error function attempts to minimize the fractional error distribution across the entire concentration range. The values of ARE are given in Tables C-15 and C-16, both for CJAC and CAC, respectively.

6.6.3 The Hybrid Fractional Error Function (HYBRID)

HYBRID is given as

$$HYBRID = \frac{100}{n-p} \sum_{i=1}^n \left[\frac{(q_{e,exp} - q_{e,calc})}{q_{e,exp}} \right]_i \quad (6.19)$$

This error function was developed to improve the fit of the ARE method at low concentration values. Instead of n as used in ARE, the sum of the fractional errors is divided by $(n-p)$ where p is the number of parameters in the isotherm equation. The values of HYBRID error functions are given in Tables C-15 and C-16, both for CJAC and CAC, respectively.

6.6.4 Marquardt's Percent Standard Deviation (MPSD)

MPSD has been used by a number of researchers in the field to test the adequacy and accuracy of the model fit with the experimental data. It has some similarity to the geometric mean error distribution, but was modified by incorporating the number of degrees of freedom. This error function is given as

$$100 \sqrt{\frac{1}{n-p} \sum_{i=1}^n \left(\frac{(q_{e,meas} - q_{e,calc})}{q_{e,meas}} \right)^2}_i \quad (6.19)$$

The values of MPSD error functions are given in Tables C-15 and C-16, both for CJAC and CAC, respectively.

6.6.5 The Sum of the Absolute Errors (SAE)

SAE is given as

$$SAE = \sum_{i=1}^n |q_{e,calc} - q_{e,exp}|_i \quad (6.20)$$

The isotherm parameters determined by this method provide a better fit as the magnitude of the errors increase, biasing the fit towards the high concentration data. The values of SAE are given in Tables C-15 and C-16, both for CJAC and CAC, respectively.

6.6.6 Choosing best-fit isotherm based on error analysis

The values of the five error functions are presented in Tables C-15 and C-16. By comparing the results of the values of the error functions, it is found that Temkin and Langmuir isotherms are best-fitted the isotherm data for Pb(II) adsorption on CJAC at almost all temperatures and Langmuir, Temkin and Redlich-Peterson isotherms are best-fitted for Pb(II) on CAC at almost all temperatures .

6.7) Thermodynamic study:

The Gibbs free energy change of the adsorption process is related to the equilibrium constant by the classic Van't Hoff equation

$$\Delta G^0 = -RT \ln K \quad (6.21)$$

According to thermodynamics, the Gibbs free energy change is also related to the entropy change and heat of adsorption at constant temperature by the following equation:

$$\Delta G^0 = \Delta H^0 - T\Delta S^0 \quad (6.22)$$

Combining above two equations, we get

$$\ln K = \frac{-\Delta G^0}{RT} = \frac{\Delta S^0}{R} - \frac{\Delta H^0}{R} \frac{1}{T} \quad (6.23)$$

where ΔG^0 is the free energy change (kJ/mol), ΔH^0 is the change in enthalpy (kJ/mol), ΔS^0 is the entropy change (J/mol K), T is the absolute temperature (K) and R is the universal gas constant (8.314 J/mol K) and K is the thermodynamic equilibrium constant.

Thermodynamic parameters are calculated from the variation of the thermodynamic equilibrium constant K (or the thermodynamic distribution coefficient) with changes in temperature. K for the adsorption reaction can be defined:

$$K = \frac{a_s}{a_e} = \frac{v_s C_s}{v_e C_e} \quad (6.24)$$

where a_s is the activity of the adsorbed solute, a_e the activity of the solute in the equilibrium solution, C_s , the surface concentration of adsorbate and C_e is the concentration of adsorbate in

equilibrium suspension v_s , the activity coefficient of the adsorbed solute, and v_e the activity coefficient of the solute in the equilibrium solution. As the concentration of the solute in the solution approaches zero, the activity coefficient v approaches unity. Equation (6.24) may then be written as:

$$\lim_{C_e \rightarrow 0} \frac{C_s}{C_e} = \frac{a_s}{a_e} = K \quad (6.25)$$

Values of K are obtained by plotting $\ln(C_s/C_e)$ versus C_e , and extrapolating to zero C_e . From Fig.B-39 (for CJAC), B-40(CAC) K values are obtained at different temperatures. The increase in K with increase in temperature indicates the endothermic nature of the process.

The ΔG^0 is calculate from the equation 6.21 for different temperatures. The negative values of ΔG^0 indicate the process to be feasible and adsorption to be spontaneous. And ΔH^0 and ΔS^0 were calculated using the equation 6.23. A plot of $\ln K$ vs $1/T$ was found to be linear in Fig.B-41. ΔH^0 and ΔS^0 are determined from the slope and intercept of the plot.

The positive ΔH^0 value confirms the endothermic nature of the overall-sorption process. The adsorption process in the solid-liquid system is a combination of two processes: (a) the desorption of the molecules of solvent (water) previously adsorbed and (b) the adsorption of adsorbate species. Basically adsorption process is exothermic in nature, in this study it is endothermic may be due to the desolvation of the adsorbing species(lead ions), the changes in the size of pores, and the enhanced rate of intraparticle diffusion of adsorbate. The value of ΔH^0 was less than 20 KJ/mol, so the adsorption is physical adsorption.

The positive value of ΔS^0 suggests increased randomness at the solid/solution interface with some structural changes in the adsorbate and adsorbent and an affinity of CJAC and CAC towards lead ions. Also, positive ΔS^0 value corresponds to an increase in the degree of freedom of the adsorbed species. All the thermodynamic parameters are given in the Table C-17.

CHAPTER-7

CONCLUSION AND RECOMMENDATIONS

7.1 Conclusions:

The following major conclusions can be drawn from the present work .

1. Bulk density of coconut jute activated carbon was found to be 318.90 Kg/m^3 , fixed carbon percentage is 0.571 and bulk density of commercial activated carbon was found to be 268.70, fixed carbon is 0.711, which shows excellent adsorptive characteristics of activated carbon for the removal of Pb (II) from waste water.
2. SEM of CAC shows fibrous structure with large pore size with strands in each fibre. Number of pores in CJAC is lesser than that in CAC. Surface of the CJAC and CAC becomes smooth after adsorption of Pb(II).
3. Percent removal of Pb(II) increases with the increase in adsorbent dose for both CJAC and CAC up to a certain limit and then remains almost constant. However, Percent removal decreases with increase in Pb(II) concentration for both the adsorbents.
4. Adsorption of Pb(II) on CJAC and CAC is maximum in acidic pH range. Adsorption of Pb (II) increases with increase in pH and reaches to maximum value at 5 (for CJAC), 4.2 (for CAC) and then percent removal slightly decreases after this pH region.
5. Effect of initial Pb(II) concentration on removal by CJAC and CAC shows that for any contact time the percent removal decreases with increase in initial concentration of Pb(II). Amount adsorbed per amount of adsorbent (q_t) increased with the increase in initial Pb(II) concentration .
6. Increase in temperature slightly increases the amount adsorbed for both adsorbents indicating endothermic in nature.
7. The percent removal of Pb (II) increases (for both adsorbents) as the particle size decreases because of specific surface available for adsorption will be greater for smaller particles.

8. Kinetic study shows that adsorption of Pb(II) on CJAC and CAC follows the second order kinetics for both adsorbents.
9. Weber-Morris plot reveals that the intraparticle transport (pore diffusion) is not the only rate-controlling step.
10. Langmuir isotherm best-fitted the isotherm data for Pb(II) adsorption on CJAC and CAC at almost all temperatures, However, the non-linear correlation coefficients, R^2 and the error analysis values are nearly similar for the Temkin and Langmuir isotherms(for CJAC) and Langmuir, Temkin and Redlich-Peterson(for CAC). Hence we can use Temkin or Langmuir for Pb(II) adsorption on CJAC and Temkin, Langmuir or Redlich-Peterson on CAC.
11. Adsorption capacity of CJAC and CAC for Pb(II) removal increases with increase in temperature for both the adsorbents, showing the endothermic nature of adsorption. The energy of adsorption reveals that it is a transitional state adsorption.
12. The increase in K with increase in temperature indicates the endothermic nature of the process. The negative values of ΔG^0 indicate the process to be feasible and adsorption to be spontaneous. And ΔH^0 and ΔS^0 are 2.5441 KJ/mol and 17.6350 J/K mol (for CJAC), 3.4611 KJ/mol and 23.7780 J/ K mol (for CAC) respectively.
13. Lead removal efficiency for CJAC is less than CAC (the difference is not very high). But CJCA was prepared by cheap coconut jute which is abundantly available in India . So the low cost coconut jute can be used as a potential adsorbent for the removal of Pb(II) from wastewater in developing countries like India.

7.2 Recommendations :

- 1) Coconut Jute Activated Carbon should be characterized for physical-chemical parameters and surface characteristics to arrive at average values for use in design.
- 2) Costing of the adsorption based on industrial scale treatment system should be carried out to popularize the adsorption technique with coconut jute activated carbon.
- 3) Further pilot scale studies are required to evaluate the suitability of coconut jute activated carbon for the adsorptive removal on plant scale.

- 4) To further improve adsorption properties of coconut jute activated carbon, it should be gone through some treatment processes which improves adsorption property.
- 5) Under continuous study, fixed bed column study should be carried out to get effect of different parameters on removal of metal ion from waste water.
- 6) Equilibrium adsorption data should be obtained for mixed metal ions concentrations encountered in industries.
- 7) Many more combination of different adsorbents could be tried to get much better result.
- 8) It could also be tested for removal of other heavy metals.

REFERENCES

1. Activated carbon from an agricultural by-product , for the treatment of dyeing industry waste water by K.Kadirvelu, M.Palanvival, R.Kalpana, S.Rajeswari, *Bioresource Technology* 74(2000)263-265.
2. Adsorption of malachite green on groundnut shell waste based powdered activated carbon by R.Malik, D.S. Ramteke , S.R. Wate, *Waste Management* (2006).
3. Adsorptive removal of malachite green dye from aqueous solution by bagasse fly ash and activated carbon-kinetic study and equilibrium isotherm analyses by Indra Deo Mall , Vimal Chandra Srivastava, Nitin Kumar Agarwal, Indra Mani Mishra, *Colloids and Surfaces A: Physicochemical Engineering Aspects* 264 (2005) 17–28.
4. Adsorption Thermodynamics of Carbofuran on Sn (IV) Arsenosilicate in H⁺, Na⁺ and Ca²⁺ Forms by Asif A. Khan and R.P. Singh, *Colloids and Surfaces*, 24 (1987) 33-42.
5. Adsorptive Removal of Auramine-O: Kinetic and equilibrium study by Indra Deo Mall, Vimal Chandra Srivastava, Nitin Kumar Aggarwal, *Journal of Hazardous Materials* 143(2007) 386-395.
6. Central Pollution Control Board, Ministry of Environment and Forests, Govt. of India, Delhi.
7. Characterization of mesoporous rice husk ash (RHA) and adsorption kinetics of metal ions from aqueous solution onto RHA by Vimal Chandra Srivastava, Indra Deo Mall and Indra Mani Mishra, *Journal of Hazardous Materials* B134 (2006) 257–267.
8. Combined ultrafiltration and suspended pellets for lead removal by Chi-Wang Li, Yang-Min Liang, Yi-Ming Chen, *Separation and Purification Technology* 45 (2005) 213–219.
9. *Hand Book of Drinking Water Quality* by John DeZuane, 80-85, second edition, 1996.
10. Influence of pH, ionic strength and temperature on lead biosorption by *Gelidium* and agar extraction algal waste by Vitor J.P. Vilar, Cida'lia M.S. Botelho, Rui A.R. Boaventura , *Process Biochemistry* 40 (2005) 3267–3275.
11. Kinetics and equilibrium adsorption study of lead (II) onto activated carbon prepared from coconut shell by M. Sekar, V. Sakthi, S. Rengaraj, *Journal of Colloid and Interface Science* 279 (2004) 307–313.

12. Kinetic and isothermal studies of lead ion adsorption onto palygorskite clay by Hao Chen ,Aiqin Wang , Journal of Colloid and Interface Science 307 (2007) 309–316
13. Kinetics of adsorption on carbon from solution by W.J. Weber Jr., J.C. Morris, J. Sanitary Engineering. Div. ASCE 89 (SA2) (1963) 31–59.
14. Lead removal from foundry waste by solvent extraction by Shah DB, Phadke AV, Kocher WM., Journal of Air Waste Manag Assoc. 1995 Mar;45(3):150-5.
15. Lead removal in fixed-bed columns by zeolite and sepiolite by Mustafa Turan , Ugur Mart , Baris Yuksel , Mehmet S. C, elik , Chemosphere 60 (2005) 1487–1492..
16. Mass-transfer operations by Robert E.Treybal,3rd edition, McGraw-Hill Book Company.
17. Molecular approach to remove lead from drinking water by B Francois Cuenot, Michel Meyer, Arnaud Bucaille, Roger Guilard,Journal of Molecular Liquids 118 (2005) 89– 99.
18. Pseudo-second-order model for lead ion sorption from aqueous solutions onto palm kernel fiber by Yuh-Shan Ho,, Augustine E. Ofomaja , Journal of Hazardous Materials B129 (2006) 137–142.
19. Pseudo-second order model for sorption processes by Y.S., McKay G., Process Biochemistry, 34 (1999), 451-465.
20. Recycling Fe(III)/Cr(III) hydroxide, an industrial solid waste for the removal of phosphate from water by C. Namasivayam, K. Prathap ,Journal of Hazardous Materials B123 (2005) 127–134.
21. Recovery of heavy metals from metal industry waste waters by chemical precipitation and nanofiltration by María Jesús González-Muñoz, María Amparo Rodríguez, Susana Luquea, José Ramón Álvarez,Desalination 200 (2006) 742–744.
22. Removal and recovery of lead (II) from single and multimetal (Cd, Cu, Ni, Zn) solutions by crop milling waste (black gram husk) by Asma Saeeda, Muhammed Iqbal, M. Waheed Akhtar,Journal of Hazardous Materials B117 (2005) 65–73.
23. Removal of aqueous lead ions by hydroxyapatites: Equilibria and kinetic processes by Baille Sandrine , Nzihou Angea,, Bernache-Assolant Didier b, Champion Eric , Sharrock Patrick , Journal of Hazardous Materials A139 (2007) 443–446
24. Removal of lead(II) and cadmium(II) from aqueous solutions using grape stalk waste by Mar'ia Mart'inez , N'uria Miralles , Soraya Hidalgo , N'uria Fiol , Isabel Villaescusa , Jordi Poch , Journal of Hazardous Materials B133 (2006) 203–2

25. Removal of lead from aqueous solutions by precipitation with sodium di-(n-octyl) phosphinate by Jamaledin O. Esalah, Martin E. Weber, Juan H. Vera , Separation and Purification Technology 18 (2000) 25–36.
26. Removal of lead ions from industrial waste water by different types of natural materials by S.H. Abdel-Halim, A.M.A. Shehata, M.F. El-Shahat, Water Research 37 (2003) 1678–1683.
27. Removal of Pyridine from Aqueous Solution by Adsorption on Bagasse Fly Ash by Dilip H. Lataye, Indra M. Mishra, Indra D. Mall, Ind. Eng. Chem. Res. 45 (2006) 3934-3943.
28. Roles of physical and chemical properties of activated carbon in the adsorption of lead ions by K. Zhang, W.H. Cheung 1, M. Valix , Chemosphere 60 (2005) 1129–1140.
29. Sorption of Pb(II), Ni(II), Cu(II) and Cd(II) from aqueous solution by olive stone waste by N'uria Fiol , Isabel Villaescusa , Mar'ia Mart'inez , N'uria Miralles , Jordi Poch , Joan Serarols , Separation and Purification Technology 50 (2006) 132–140.
30. Sorption of Lead from Aqueous Solution by Chemically Modified Carbon Adsorbents by Muhammad Nadeem, A. Mahmood, S.A. Shahid, S.S. Shah, A.M. Khalid, G. McKay, Journal of Hazardous Materials (2006).
31. Standard Methods for the Examination of Water and Waste Water, 18 th ed., American Public Health Association, Washington.DC.1992.
32. Waste Biogas Residual Slurry as an adsorbent for the removal of Pb (II) from aqueous solution and radiator manufacturing industry waste by C. Namasivayam& R. T. Yamuna, Bioresource Technology 52 (1995) 125-131.
33. Waste water engineering, treatment disposal reuse by Metcalf and Eddy, 3rd edition. Tata McGraw-Hill Publishing Company Limited.

APPENDIX – A

Table A-1: Calibration curve for lead

Concentration of lead (mg/l)	Absorbance
0	0
20	0.0652
40	0.1183
60	0.1610
80	0.2090
100	0.2570

Table A-2: Effect of pH on the removal of lead using CJAC
(T=303 K, Dose=1g/l, t=4 hr, C_o=20 mg/l)

pH	% Removal
2	34.85
3	55.76
4	60.83
5	68.275
6	56.865
7	52.16
8	47.34

Table A-3: Effect of pH on the removal of lead using CAC
(T=303 K, Dose=1g/l, t=4 hr, C₀=20 mg/l)

pH	% Removal
2	42.56
3	59.34
4	78.33
5	72.33
6	58.89
7	52.54
8	35.55

Table A-4: Effect of Adsorbent dose on removal of lead using CJAC
(T=303 K, t=4 hr, C₀=20 mg/l, pH=5)

Adsorbent Dose (mg)	% Removal
10	16.41
20	27.34
30	42.95
60	65.14
80	66.67
100	68.83
150	69.01

Table A-5: Effect of Adsorbent dose on removal of lead using CAC
(T=303 K, t=4 hr, C₀=20 mg/l, pH=4.2)

Adsorbent Dose (mg)	% Removal
10	27.52
20	40.07
30	55.32
60	61.67
80	78.49
100	79.17
150	79.54

Table A-6: Effect of Contact time and initial concentration of lead removal of using CJAC (T=303 K, pH=5, Dose= 1 g/l)

Time(min)	% Removal (20 mg/l)	% Removal (40 mg/l)	% Removal (60 mg/l)	% Removal (80 mg/l)	% Removal (100 mg/l)
10	31.875	18.750	15.000	13.750	9.500
20	37.250	25.875	20.830	17.250	17.250
30	53.625	51.875	46.500	36.250	29.450
60	58.750	54.750	46.670	38.750	32.250
120	65.500	56.250	48.170	39.657	33.250
180	67.750	58.125	49.160	41.250	36.250
240	68.125	58.625	49.830	42.250	37.250

Table A-7: Effect of Contact time and initial concentration of lead removal of using CAC (T=303 K, pH=4.2, Dose= 1 g/l)

Time(min)	% Removal (20 mg/l)	% Removal (40 mg/l)	% Removal (60 mg/l)	% Removal (80 mg/l)	% Removal (100 mg/l)
10	32.540	28.75	24.250	23.750	19.000
20	46.620	36.875	30.560	27.350	21.880
30	55.470	60.875	58.460	46.250	37.000
60	59.160	64.920	60.061	48.750	39.000
120	67.530	65.750	61.750	49.550	39.640
180	78.330	68.125	62.150	51.650	41.321
240	79.160	68.575	62.750	51.950	41.560

Table A-8: Effect of particle size on removal of lead using CJAC
(T=303 K, pH=5, Dose=1 g/l, t=4 hr, C₀=20 mg/l)

Particle Size (μm)	% Removal
100	69.14
125	66.57
150	61.05
250	55.09
300	38.17

Table A-9: Effect of particle size on removal of lead using CAC
(T=303 K, pH=4.2, Dose=1 g/l, t=4 hr, C₀=20 mg/l)

Particle Size (μm)	% Removal
100	79.53
125	69.82
150	63.79
250	49.07
300	43.14

Table A-10: Lagergren plot for the removal of lead for different initial concentrations using CJAC
(pH=5, T=303 K, Dose=1g/l)

Time(min)	log (q _e -q _t) (20 mg/l)	log (q _e -q _t) (40 mg/l)	log (q _e -q _t) (60 mg/l)	log (q _e -q _t) (80 mg/l)	log (q _e -q _t) (100 mg/l)
10	0.8603	1.2028	1.3201	1.3579	1.4433
20	0.7906	1.1173	1.2405	1.3010	1.3010
30	0.4624	0.4314	0.3010	0.6812	0.8948
60	0.2730	0.1903	0.2787	0.4472	0.6989
120	-0.2798	-0.0223	0.0000	0.3010	0.6020
180	-1.1249	-0.6989	-0.3979	-0.0969	0.0000
240	-	-	-	-	-

Table A-11: Lagergren plot for the removal of lead for different initial concentrations using CAC
(pH=4.2, T=303 K, Dose=1g/l)

Time(min)	log (q _e -q _t) (20 mg/l)	log (q _e -q _t) (40 mg/l)	log (q _e -q _t) (60 mg/l)	log (q _e -q _t) (80 mg/l)	log (q _e -q _t) (100 mg/l)
10	0.9696	1.2022	1.3636	1.3533	1.4425
20	0.8134	1.1031	1.2859	1.2940	1.2576
30	0.6756	0.4885	0.4106	0.6589	0.8261
60	0.6020	0.1649	0.2079	0.4082	0.6608
120	0.3666	0.0531	-0.2218	0.2833	0.4624
180	-0.7799	-0.7447	-0.4437	-0.6198	-0.2218
240	-	-	-	-	-

Table A-12: Pseudo second order kinetic plot for the removal of lead for different initial concentrations using CJAC (pH=5, T=303 K, Dose=1 g/l)

Time(min)	$t/q_t(\text{min.g/mg})$ (20 mg/l)	$t/q_t(\text{min.g/mg})$ (40 mg/l)	$t/q_t(\text{min.g/mg})$ (60 mg/l)	$t/q_t(\text{min.g/mg})$ (80 mg/l)	$t/q_t(\text{min.g/mg})$ (100 mg/l)
10	1.5686	1.3333	1.1111	0.9091	1.0526
20	2.6846	1.9324	1.6000	1.4493	1.1594
30	2.7972	1.4458	1.0753	1.0345	1.0204
60	5.1064	2.7397	2.1428	1.9355	1.8605
120	9.1603	5.3333	4.1522	3.7736	3.6090
180	13.2841	7.7419	6.1017	5.4545	4.9655
240	17.6147	10.2345	8.0267	7.1006	6.4429

Table A-13: Pseudo second order kinetic plot for the removal of lead for different initial concentrations using CAC (pH=4.2, T=303 K, Dose=1 g/l)

Time(min)	$t/q_t(\text{min.g/mg})$ (20 mg/l)	$t/q_t(\text{min.g/mg})$ (40 mg/l)	$t/q_t(\text{min.g/mg})$ (60 mg/l)	$t/q_t(\text{min.g/mg})$ (80 mg/l)	$t/q_t(\text{min.g/mg})$ (100 mg/l)
10	1.5366	0.8696	0.6873	0.5263	0.5333
20	2.1450	1.3559	1.0907	0.9141	0.7055
30	2.7042	1.2320	0.8553	0.8108	0.7547
60	5.0710	2.3105	1.6650	1.5385	1.4330
120	8.8849	4.5627	3.2389	3.0272	2.7554
180	4.4898	6.6055	4.8270	4.3562	3.9258
240	15.1592	8.7495	6.3745	5.7748	5.1668

Table A-14: Weber Morris plot for the removal of lead for different initial concentrations using CJAC
(pH=5, T=303 K, Dose=1 g/l).

$t^{1/2}(\text{min}^{1/2})$	$q_t(\text{mg/g})$ (20 mg/l)	$q_t(\text{mg/g})$ (40 mg/l)	$q_t(\text{mg/g})$ (60 mg/l)	$q_t(\text{mg/g})$ (80 mg/l)	$q_t(\text{mg/g})$ (100 mg/l)
3.1623	6.3750	7.5000	9.0000	11.0000	9.5000
4.4721	7.4500	10.3500	12.5000	13.8000	17.2500
5.4772	10.7250	20.7500	27.9000	29.0000	29.4000
7.7460	11.7500	21.9000	28.0000	31.0000	32.2500
10.9544	13.1000	22.5000	28.9000	31.8000	33.2500
13.4164	13.5500	23.2500	29.5000	33.0000	36.2500
15.4919	13.6250	23.4500	29.9000	33.8000	37.2500

Table A-15: Weber Morris plot for the removal of lead for different initial concentrations using CAC
(pH=4.2, T=303 K, Dose=1 g/l).

$t^{1/2}(\text{min}^{1/2})$	$q_t(\text{mg/g})$ (20 mg/l)	$q_t(\text{mg/g})$ (40 mg/l)	$q_t(\text{mg/g})$ (60 mg/l)	$q_t(\text{mg/g})$ (80 mg/l)	$q_t(\text{mg/g})$ (100 mg/l)
3.1623	6.5080	11.5000	14.4500	19.0000	18.7500
4.4721	9.3240	14.7500	18.3360	21.8800	28.3500
5.4772	11.0940	24.3500	35.0760	37.0000	39.7500
7.7460	11.8320	25.9680	36.0360	39.0000	41.8700
10.9544	13.5060	26.3000	37.0500	39.6400	43.5500
13.4164	15.6660	27.2500	37.2900	41.3200	45.8500
15.4919	15.8320	27.4300	37.6500	41.5600	46.4500

Table A-16: Bangham's plot for the removal of lead for different initial concentrations using CJAC
(pH=5, T=303 K, Dose=1 g/l).

log t	log q _t (20 mg/l)	log q _t (40 mg/l)	log q _t (60 mg/l)	log q _t (80 mg/l)	log q _t (100 mg/l)
1	0.8045	0.8751	0.9542	1.0414	0.9777
1.3010	0.8721	1.0149	1.0969	1.1399	1.2368
1.4771	1.0304	1.3170	1.4456	1.4624	1.4683
1.7782	1.0700	1.3404	1.4471	1.4914	1.5088
2.0792	1.1173	1.3522	1.4609	1.5024	1.5218
2.2553	1.1319	1.3664	1.4698	1.5185	1.5593
2.3802	1.1343	1.3701	1.4757	1.5289	1.5711

Table A-17: Bangham's plot for the removal of lead for different initial concentrations using CAC
(pH=4.2, T=303 K, Dose=1 g/l).

log t	log q _t (20 mg/l)	log q _t (40 mg/l)	log q _t (60 mg/l)	log q _t (80 mg/l)	log q _t (100 mg/l)
1	0.8134	1.0607	1.1598	1.2787	1.2730
1.3010	0.9696	1.1688	1.2633	1.3400	1.4525
1.4771	1.0451	1.3865	1.5450	1.5682	1.5993
1.7782	1.0730	1.4144	1.5567	1.5911	1.6219
2.0792	1.1305	1.4199	1.5688	1.5981	1.6389
2.2553	1.1949	1.4354	1.5716	1.6162	1.6613
2.3802	1.1995	1.4382	1.5758	1.6187	1.6669

Table A-18: Effect of temperature on removal of lead by CJAC
(pH=5, Dose=1 g/l, t=4 hr, C_o=20 mg/l)

Time (min)	303 K	323 K	343 K
	Q _t (mg/g)	Q _t (mg/g)	Q _t (mg/g)
10	6.3750	6.5750	6.7750
20	7.4500	7.7850	7.9850
30	10.7250	10.3728	10.5728
60	11.7500	12.0500	12.2500
120	13.1000	13.4300	13.8300
180	13.5000	13.9500	14.3500
240	13.6250	14.0250	14.4250

Table A-19: Effect of temperature on removal of lead by CAC
(pH= 4.2, Dose=1 g/l, t=4 hr, C_o=20 mg/l)

Time (min)	303 K	323 K	343 K
	Q _t (mg/g)	Q _t (mg/g)	Q _t (mg/g)
10	6.5080	6.3080	6.5080
20	9.3240	9.5920	9.7920
30	11.0940	11.4500	11.6500
60	11.8320	12.0320	12.2320
120	13.5060	13.9060	14.3060
180	15.6660	16.0660	16.4660
240	15.8320	16.2320	16.6320

Table A-20: Freundlich isotherm for the removal of lead at different temperatures using CJAC
(pH=5, t= 4 hr, Dose=1 gm/l).

Initial Concentration (mg/l)	303 K		323 K		343 K	
	ln Q _e	ln C _e	ln Q _e	ln C _e	ln Q _e	ln C _e
20	2.6119	1.8524	2.6408	1.7876	2.6690	1.7183
40	3.1549	2.8064	3.1884	2.7568	3.2209	2.7047
60	3.3978	3.4045	3.4371	3.3639	3.4750	3.3215
80	3.5205	3.8329	3.5667	3.7977	3.6109	3.7612
100	3.6176	4.1391	3.6699	4.1068	3.7196	4.0733

Table A-21: Freundlich isotherm for the removal of lead at different temperatures using CAC
(pH=4.2, t= 4 hr, Dose=1 gm/l).

Initial Concentration (mg/l)	303 K		323 K		343 K	
	ln Q _e	ln C _e	ln Q _e	ln C _e	ln Q _e	ln C _e
20	2.7620	1.4274	2.7870	1.3265	2.8113	1.2143
40	3.3116	2.5313	3.3439	2.4655	3.3683	2.3952
60	3.6283	3.1068	3.6597	3.0516	3.6901	2.9930
80	3.7271	3.6491	3.7655	3.6059	3.8013	3.5622
100	3.8384	3.9806	3.8805	3.9425	3.9210	3.9030

Table A-22: Langmuir isotherm for the removal of lead at different temperatures using CJAC
(pH=5, t= 4 hr, Dose=1 gm/l).

Initial Concentration (mg/l)	303 K		323 K		343 K	
	C_e	C_e/Q_e	C_e	C_e/Q_e	C_e	C_e/Q_e
20	6.3750	0.4679	5.9750	0.4260	5.5750	0.3865
40	16.5500	0.7057	15.7500	0.6495	14.9500	0.5968
60	30.1000	1.0067	28.9020	0.9294	27.7020	0.8577
80	46.2000	1.3669	44.6000	1.2599	43.0000	1.1622
100	62.7500	1.6846	60.7500	1.5478	58.7500	1.4242

Table A-23: Langmuir isotherm for the removal of lead at different temperatures using CAC
(pH=4.2, t= 4 hr, Dose=1 gm/l).

Initial Concentration (mg/l)	303 K		323 K		343 K	
	C_e	C_e/Q_e	C_e	C_e/Q_e	C_e	C_e/Q_e
20	4.1680	0.2633	3.7680	0.2321	3.3680	0.2025
40	12.5700	0.4583	11.7700	0.4155	10.9700	0.3779
60	22.3500	0.5936	21.1500	0.5444	19.9500	0.4981
80	38.4400	0.9249	36.8160	0.8525	35.2400	0.7873
100	53.5500	1.1528	51.5500	1.0640	49.5500	0.9822

Table A-24: Temkin isotherm for the removal of lead at different temperatures using CJAC
(pH=5, t= 4 hr, Dose=1 gm/l).

Initial Concentration (mg/l)	303 K		323 K		343 K	
	Qe	ln Ce	Qe	ln Ce	Qe	ln Ce
20	13.6250	1.8524	14.0250	1.7876	14.4250	1.7183
40	23.4500	2.5064	24.2500	2.7568	25.0500	2.7047
60	29.9000	3.4045	31.0980	3.3639	32.2980	3.3215
80	33.8000	3.8329	35.4000	3.7977	37.0000	3.7612
100	37.2500	4.1391	39.2500	4.1068	41.2500	4.0733

Table A-25: Temkin isotherm for the removal of lead at different temperatures using CAC
(pH=4.2, t= 4 hr, Dose=1 gm/l).

Initial Concentration (mg/l)	303 K		323 K		343 K	
	Qe	ln Ce	Qe	ln Ce	Qe	ln Ce
20	15.8320	1.4274	16.2320	1.3265	16.6320	1.2143
40	27.4300	2.5313	28.3300	2.4655	29.0300	2.3952
60	37.6500	3.1068	38.5500	3.0516	40.0500	2.9930
80	41.5600	3.6491	43.1840	3.6059	44.7600	3.5622
100	46.4500	3.9806	48.4500	3.9425	50.4500	3.9030

Table A-26: Redlich -Peterson isotherm for the removal of lead at different temperatures using CJAC

(pH=5, t= 4 hr, Dose=1 gm/l).

Here, $W = \ln((KR*(Ce/Qe)-1))$

Initial Concentration (mg/l)	303 K		323 K		343 K	
	ln Ce	W	ln Ce	W	ln Ce	W
20	1.8524	0.3299	1.7876	0.4003	1.7183	0.5450
40	2.5064	0.9579	2.7568	1.0294	2.7047	1.1655
60	3.4045	1.4217	3.3639	1.4899	3.3215	1.6187
80	3.8329	1.7892	3.7977	1.8516	3.7612	1.9731
100	4.1391	2.0292	4.1068	2.0862	4.0733	2.2017

Table A-27: Redlich -Peterson isotherm for the removal of lead at different temperatures using CAC

(pH=4.2, t= 4 hr, Dose=1 gm/l).

Here, $W = \ln((KR*(Ce/Qe)-1))$

Initial Concentration (mg/l)	303 K		323 K		343 K	
	ln Ce	W	ln Ce	W	ln Ce	W
20	1.4274	-0.2625	1.3265	-0.1381	1.2143	0.0249
40	2.5313	0.7321	2.4655	0.8589	2.3952	1.0222
60	3.1068	1.0950	3.0516	1.2202	2.9930	1.3817
80	3.6491	1.6516	3.6059	1.7701	3.5622	1.9277
100	3.9806	1.9091	3.9425	2.0249	3.9030	2.1773

APPENDIX – B

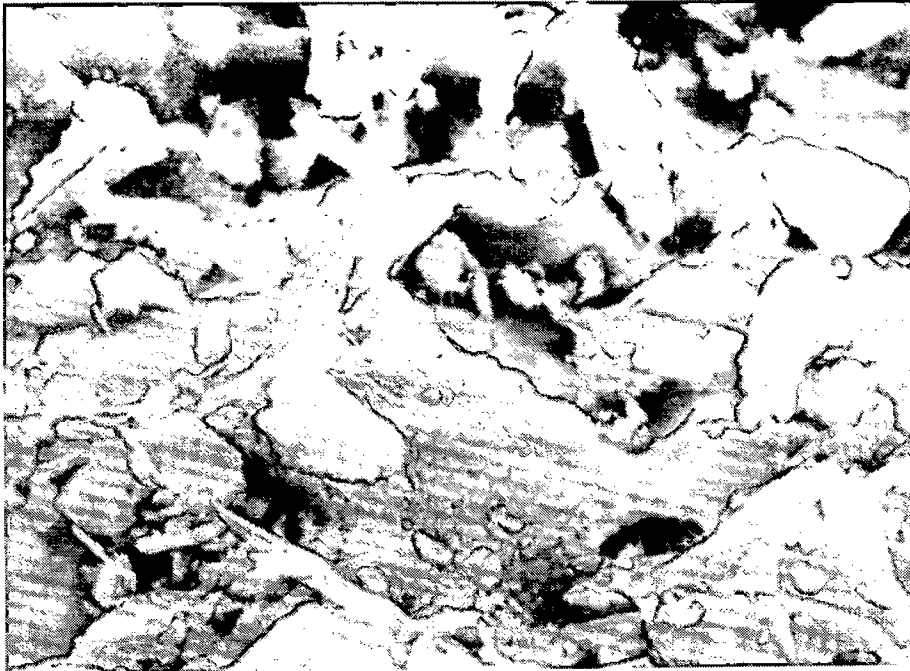


Fig B -1: Scanning electron micrograph of CJAC before adsorption at 1000 X magnification

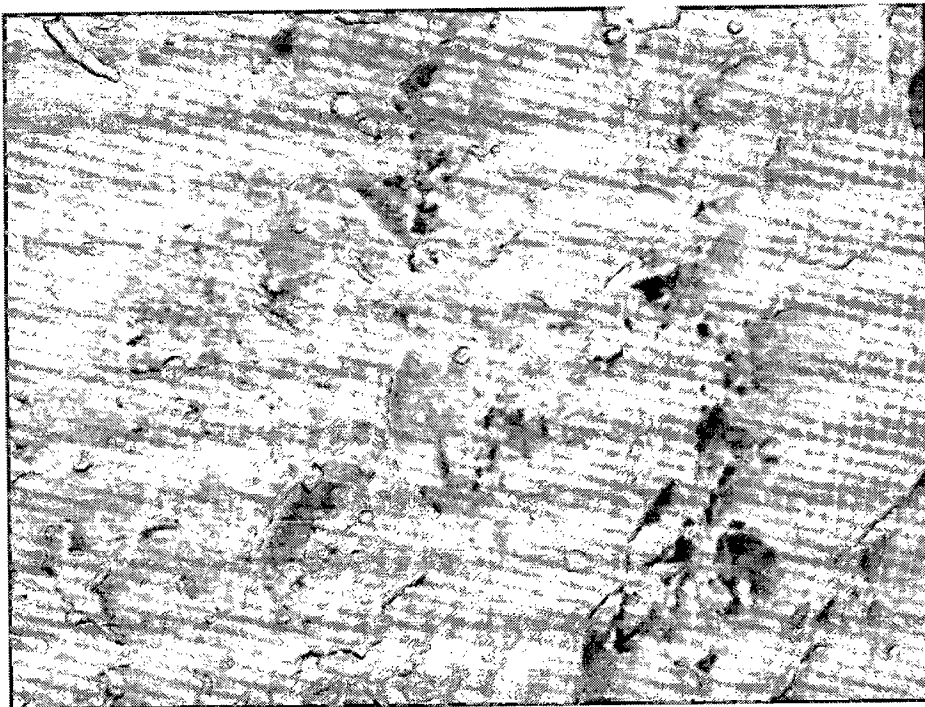


Fig B -2: Scanning electron micrograph of CJAC after adsorption at 1000 X magnification

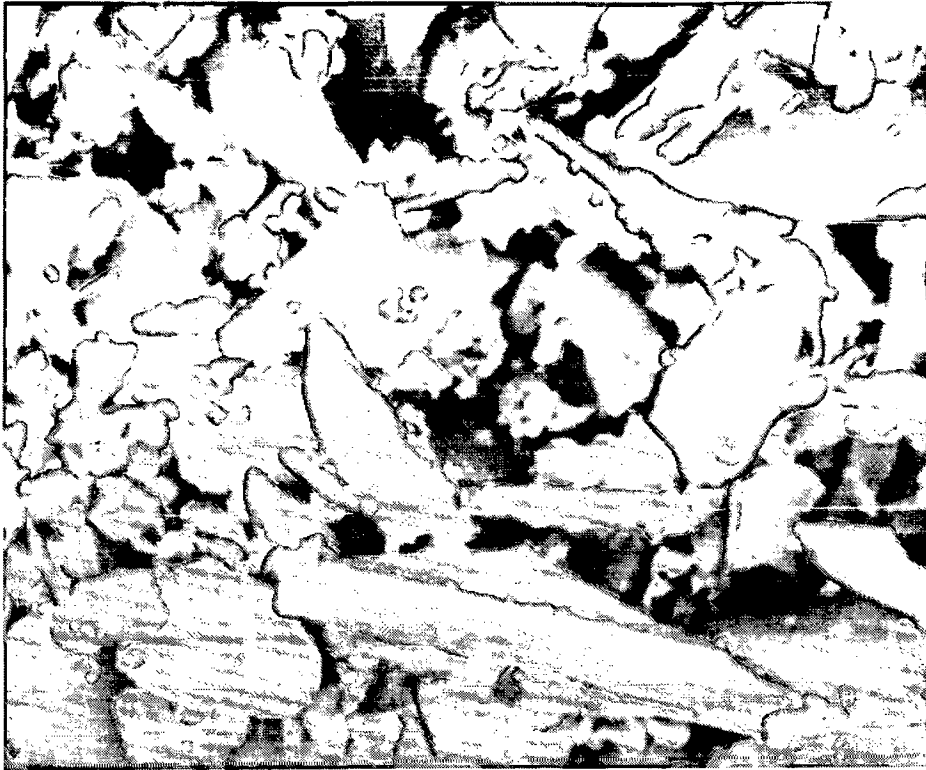


Fig B-3: Scanning electron micrograph of CAC before adsorption at 1000 X magnification

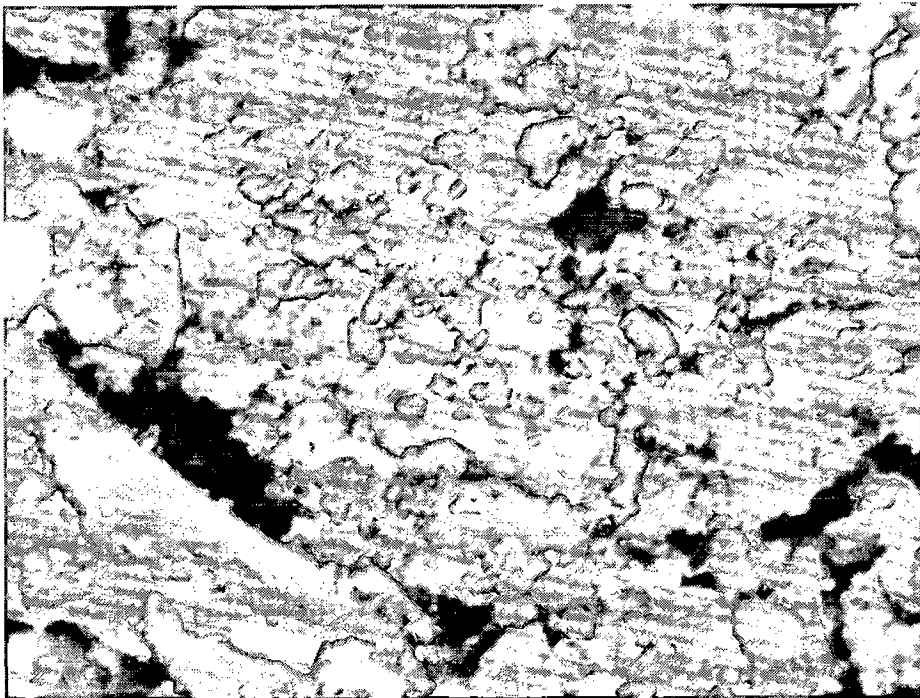


Fig B - 4: Scanning electron micrograph of CAC after adsorption at 1000 X magnification

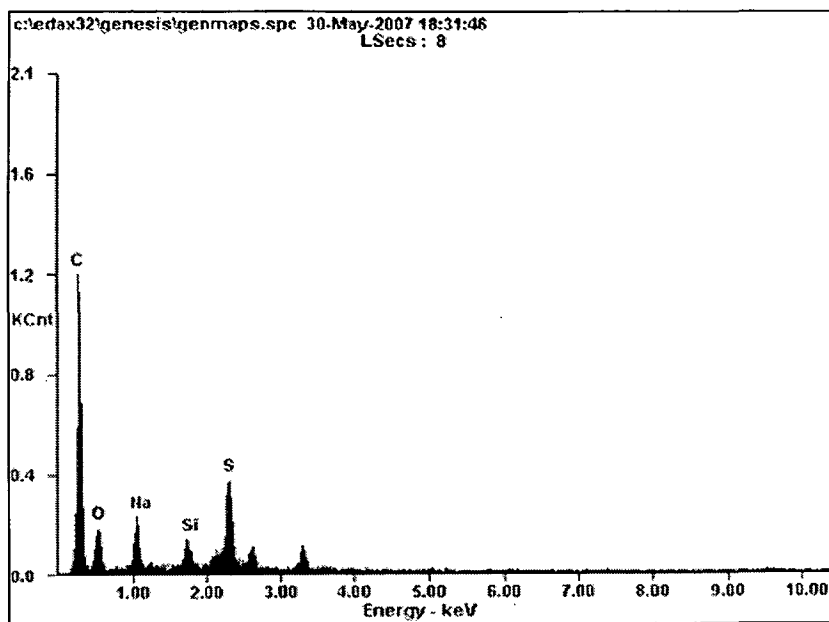


Fig.B - 5: EDS pattern for CJAC before adsorption

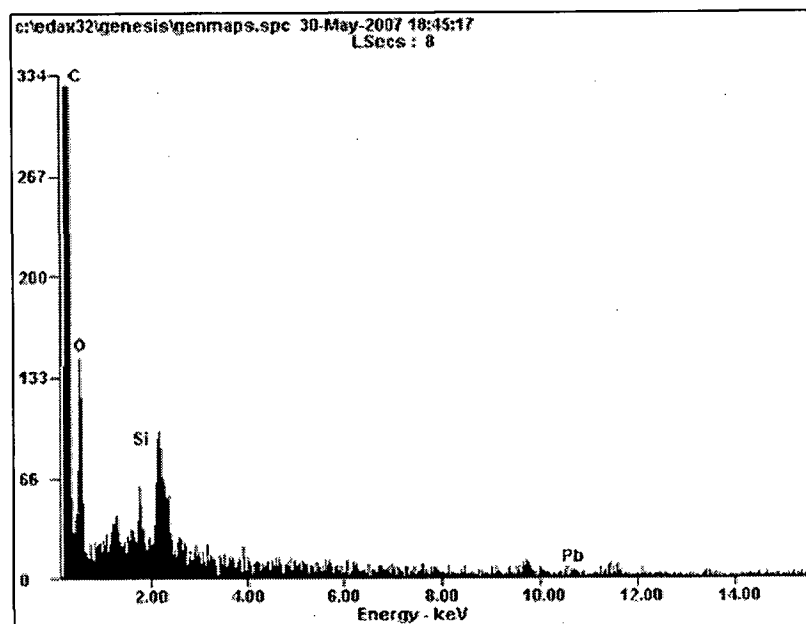


Fig.B - 6: EDS pattern for CJAC after adsorption

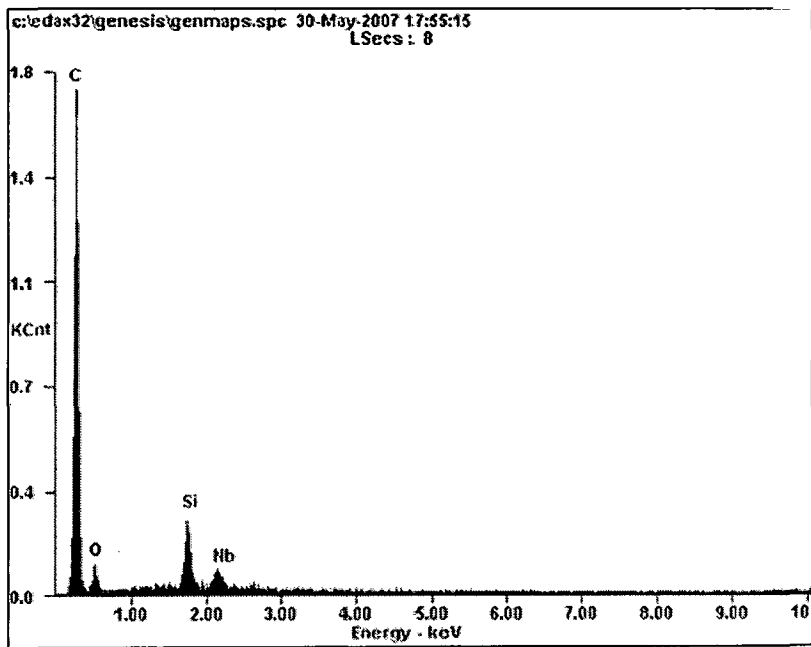


Fig.B - 7: EDS pattern for CAC before adsorption

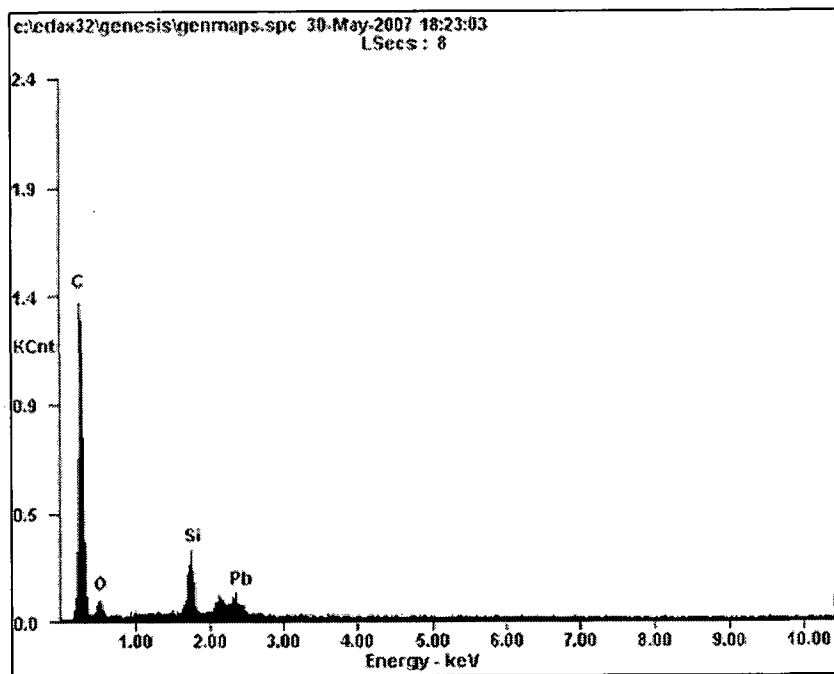


Fig.B- 8: EDS pattern for CAC after adsorption

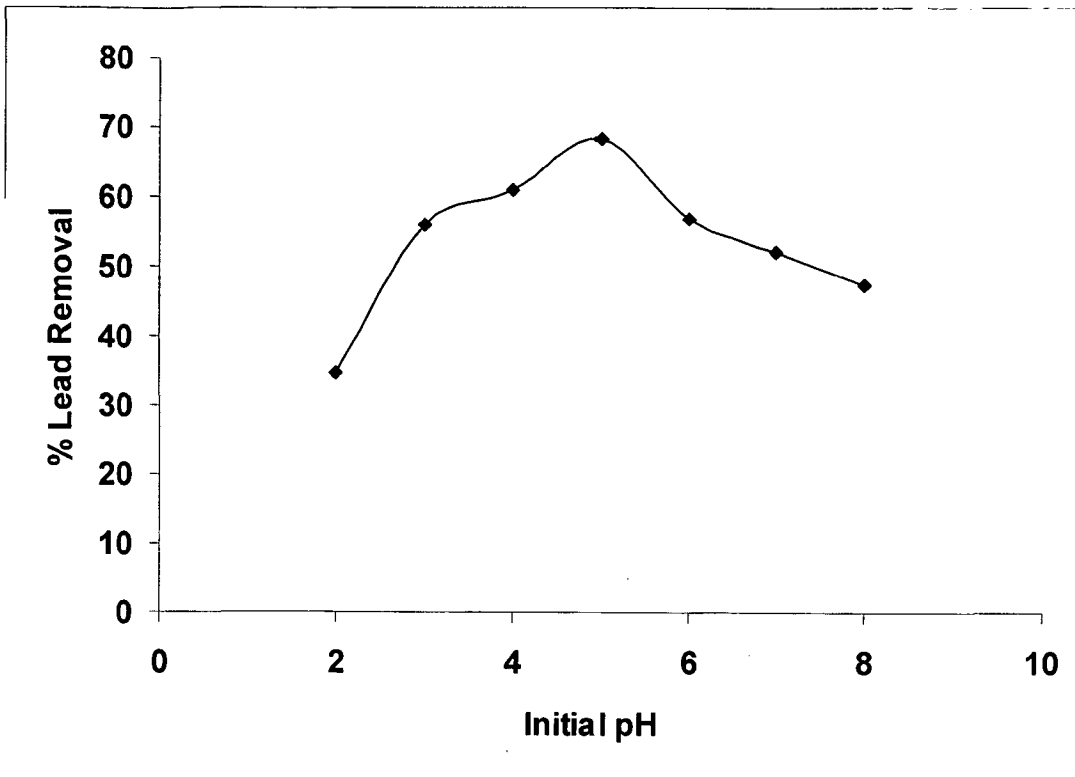


Fig. B - 9: Effect of pH_0 on the adsorption of Pb(II) using CJAC as an adsorbent
 ($T = 303K$, $t = 4$ h, $C_0 = 20$ mg /l, CJAC dose =1 g /l).

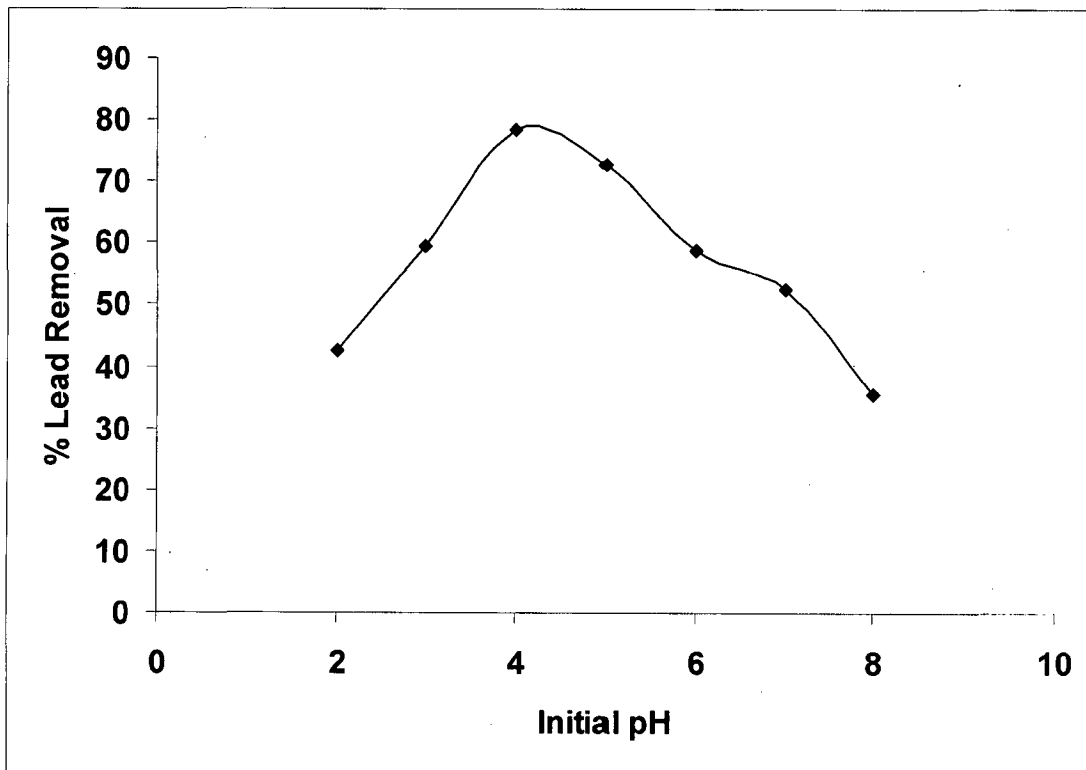


Fig. B - 10: Effect of pH_0 on the adsorption of Pb(II) using CAC as an adsorbent
 ($T = 303K$, $t = 4$ h, $C_0 = 20$ mg /l, CAC dose =1 g /l).

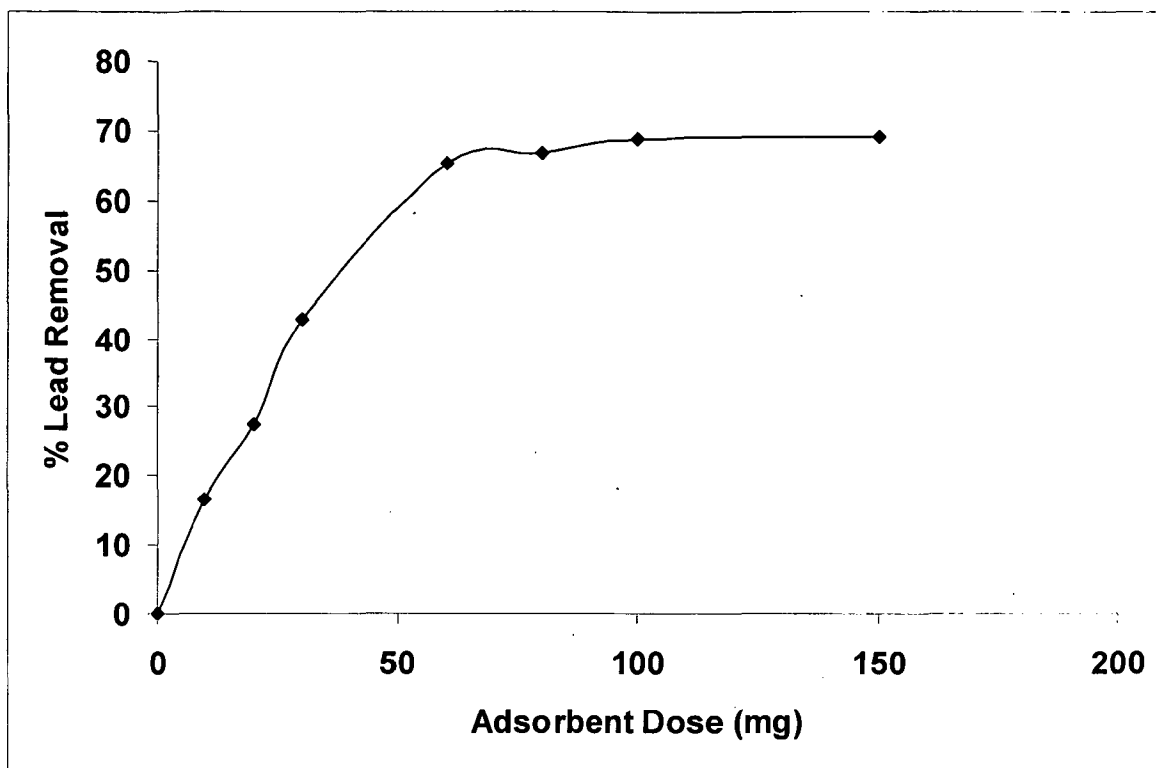


Fig. B - 11: Effect of adsorbent dose on the adsorption of Pb(II) using CJAC as an adsorbent

($T = 303\text{K}$, $t = 4\text{ h}$, $C_0 = 20\text{ mg/l}$, $\text{pH} = 5$, CJAC dose = 1 g/l).

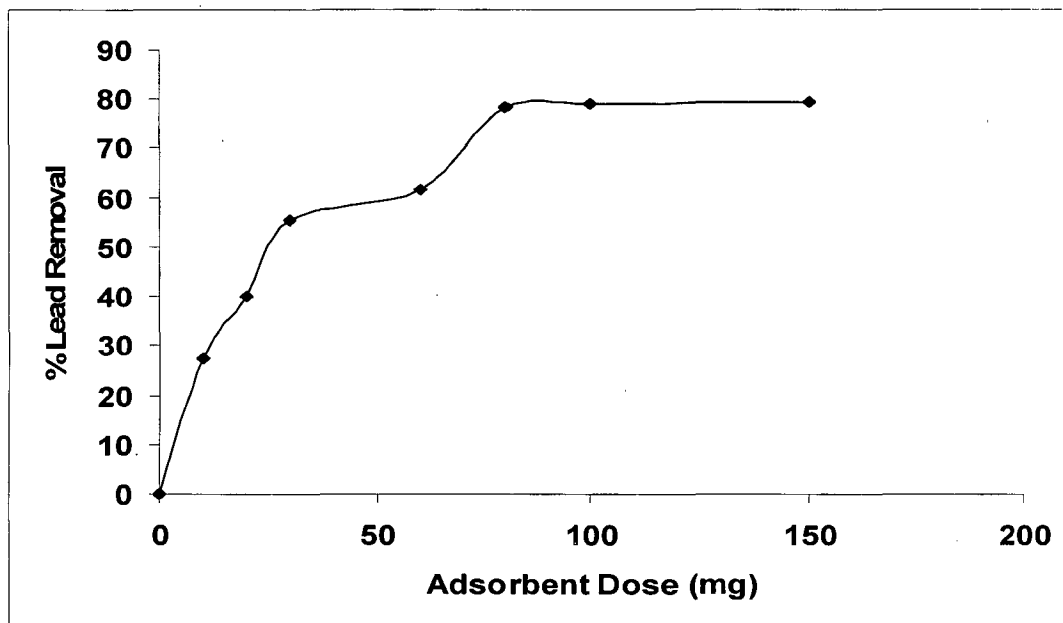


Fig. B - 12: Effect of adsorbent dose on the adsorption of Pb(II) using CAC as an adsorbent

($T = 303\text{K}$, $t = 4\text{ h}$, $C_0 = 20\text{ mg/l}$, $\text{pH} = 4.2$, CAC dose = 1 g/l).

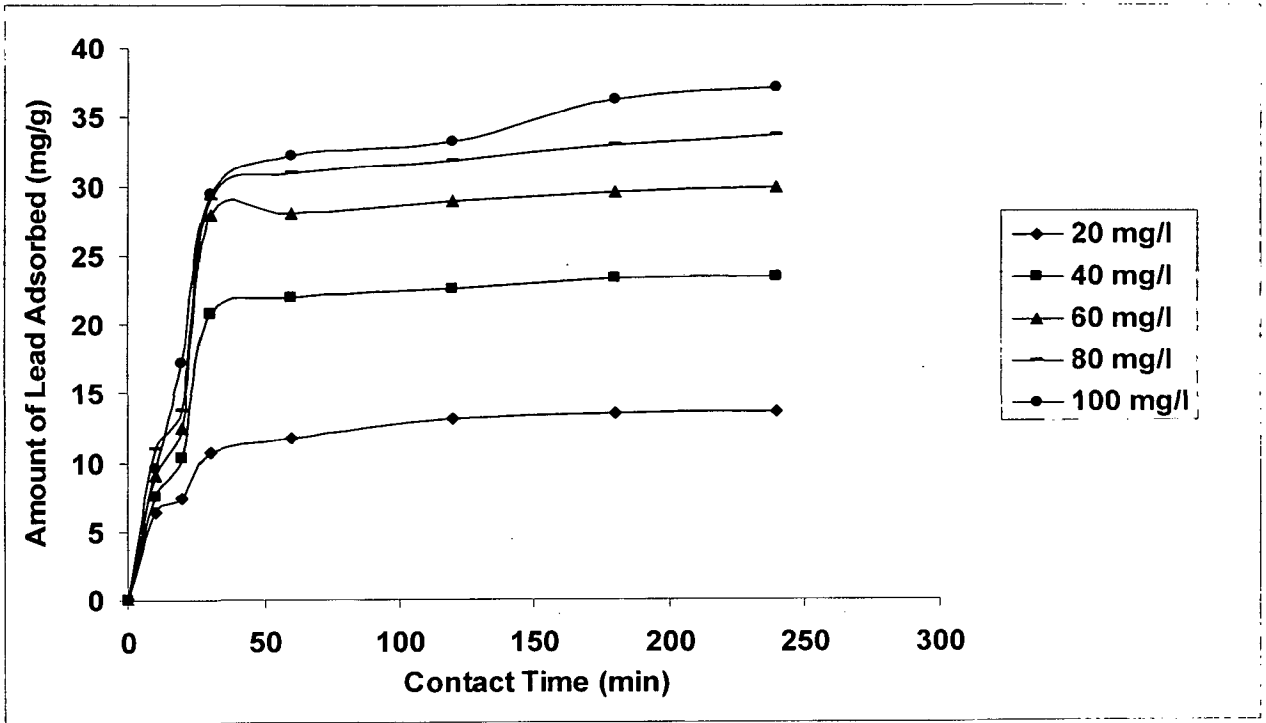


Fig. B - 13: Effect of contact time and initial concentration on the adsorption of Pb(II) using CJAC as an adsorbent
 (T = 303K, t = 4 h, C₀ = 20 mg /l, pH=5, CJAC dose = 1 g /l).

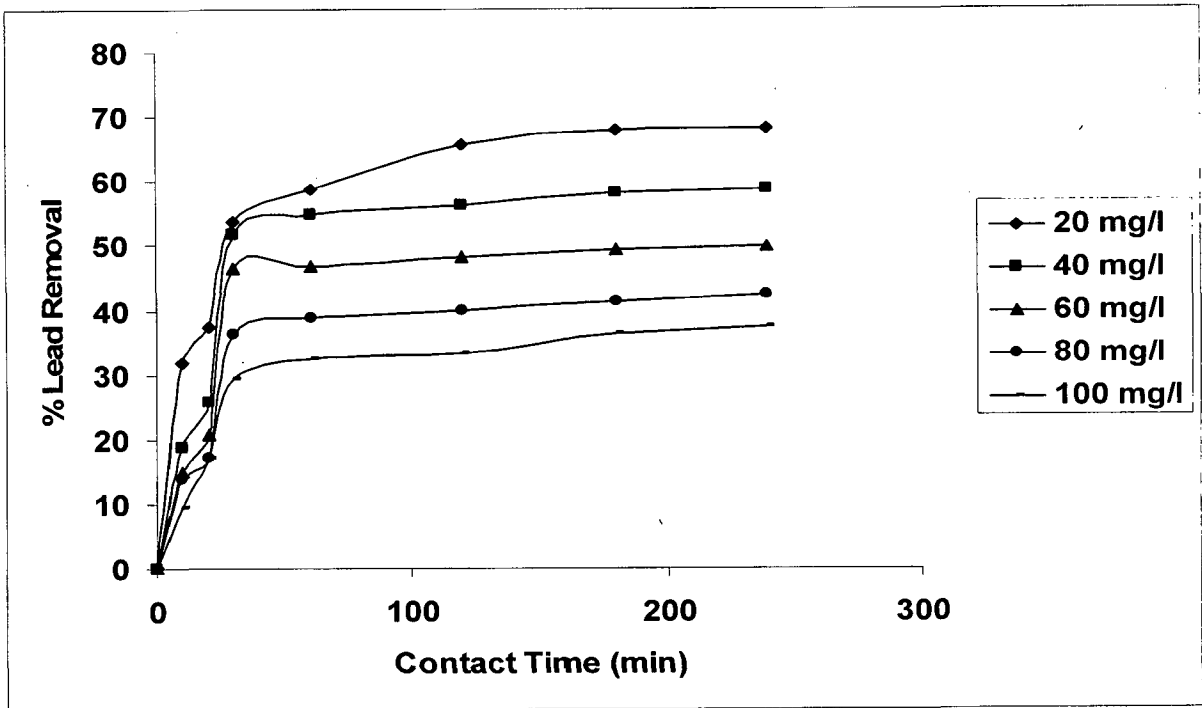


Fig. B - 14: Effect of contact time and initial concentration on the adsorption of Pb(II) using CJAC as an adsorbent
 (T = 303K, t = 4 h, C₀ = 20 mg /l, pH=5, CJAC dose = 1 g /l).

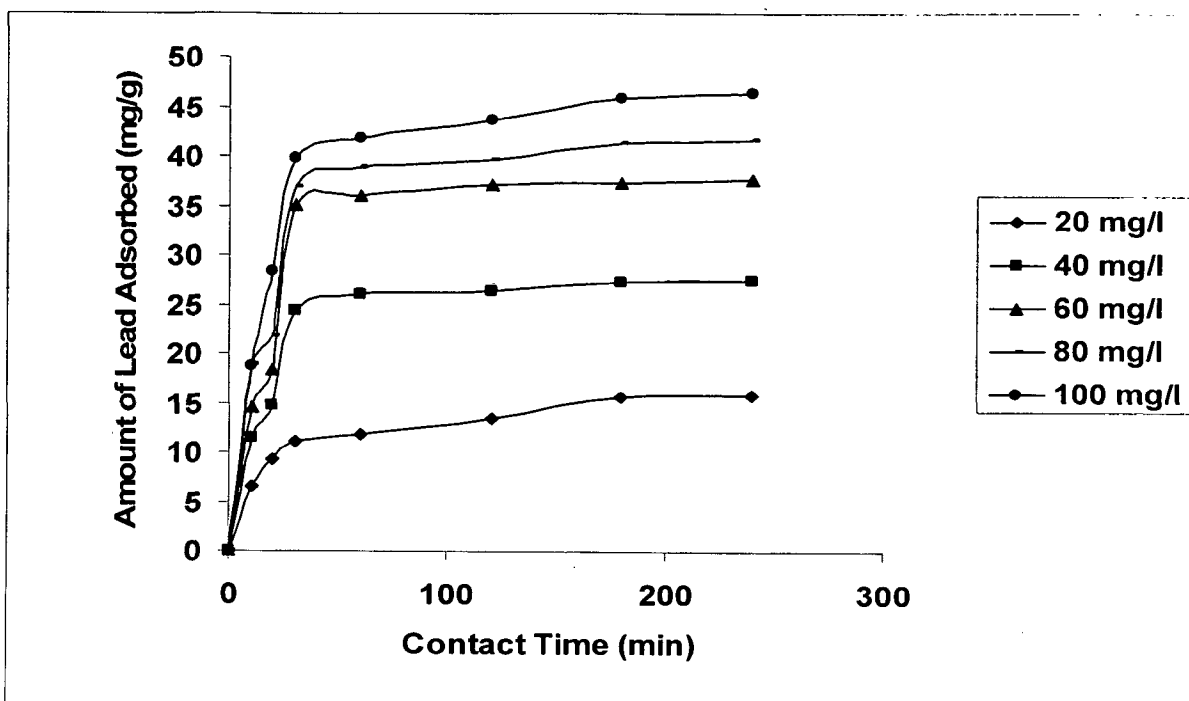


Fig. B - 15: Effect of contact time and initial concentration on the adsorption of Pb(II) using CAC as an adsorbent

($T = 303\text{K}$, $t = 4\text{ h}$, $C_0 = 20\text{ mg/l}$, $\text{pH} = 4.2$, CAC dose = 1 g/l).

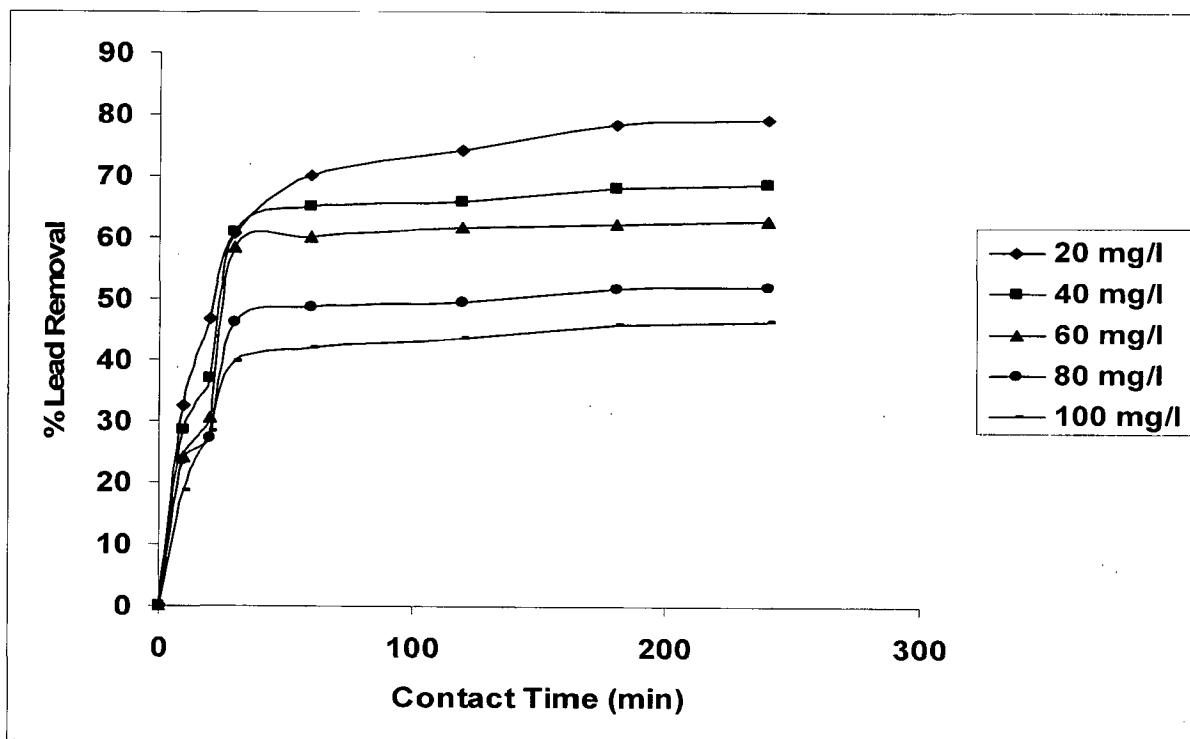


Fig. B - 16: Effect of contact time and initial concentration on the adsorption of Pb(II) using CAC as an adsorbent

($T = 303\text{K}$, $t = 4\text{ h}$, $C_0 = 20\text{ mg/l}$, $\text{pH} = 4.2$, CAC dose = 1 g/l).

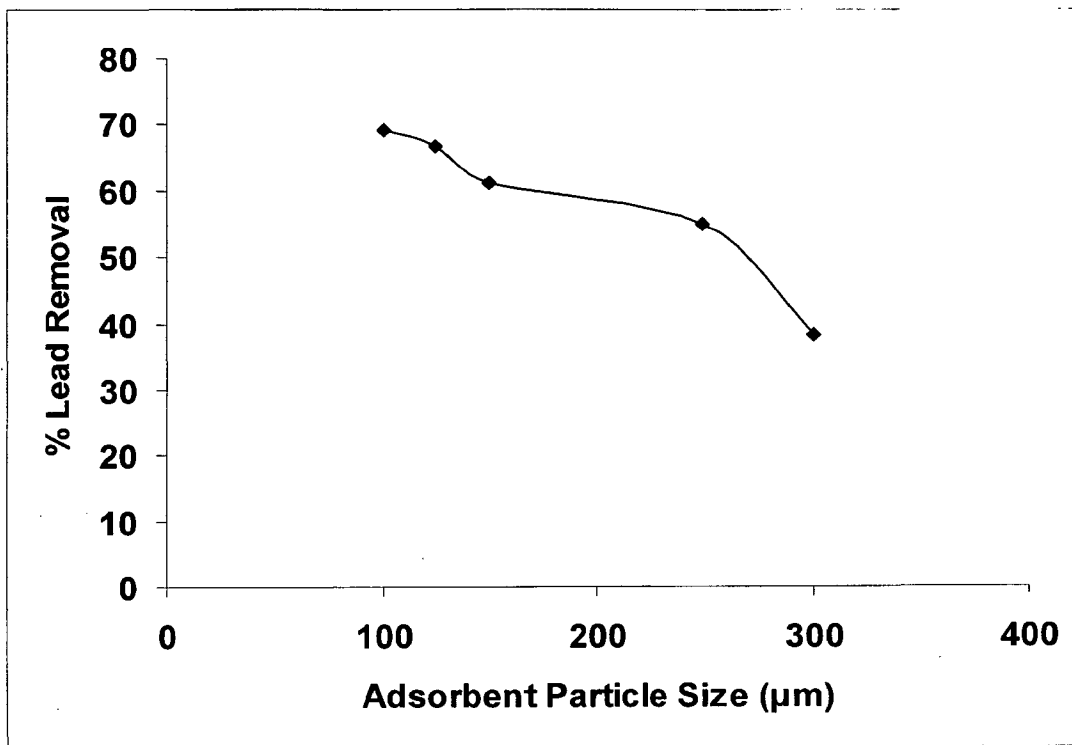


Fig. B - 17: Effect of particle size on the adsorption of Pb(II) using CJAC as an adsorbent (T = 303K, t = 4 h, C₀ = 20 mg /l, pH=5,CJAC dose =1 g /l).

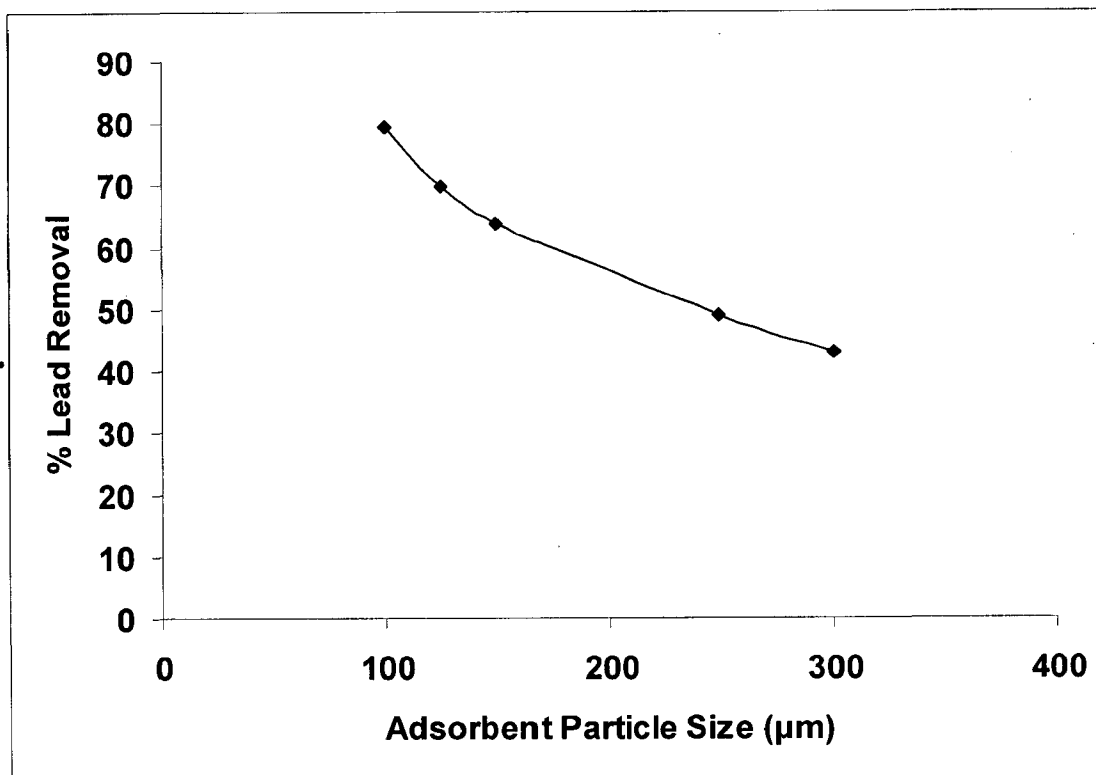


Fig. B - 18: Effect of particle size on the adsorption of Pb(II) using CAC as an adsorbent (T = 303K, t = 4 h, C₀ = 20 mg /l, pH=4.2,CAC dose =1 g /l).

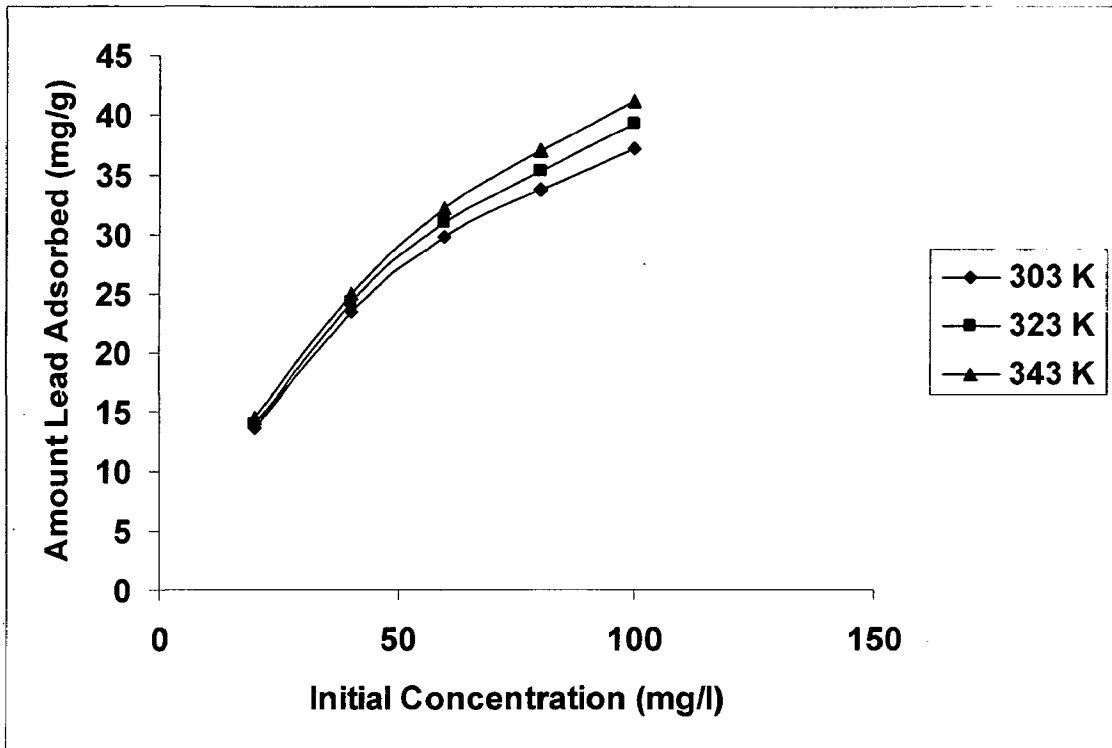


Fig. B - 19: Effect of temperature on removal of Pb(II) by using CJAC
($t = 4$ h, pH=5, dose=1 g/l).

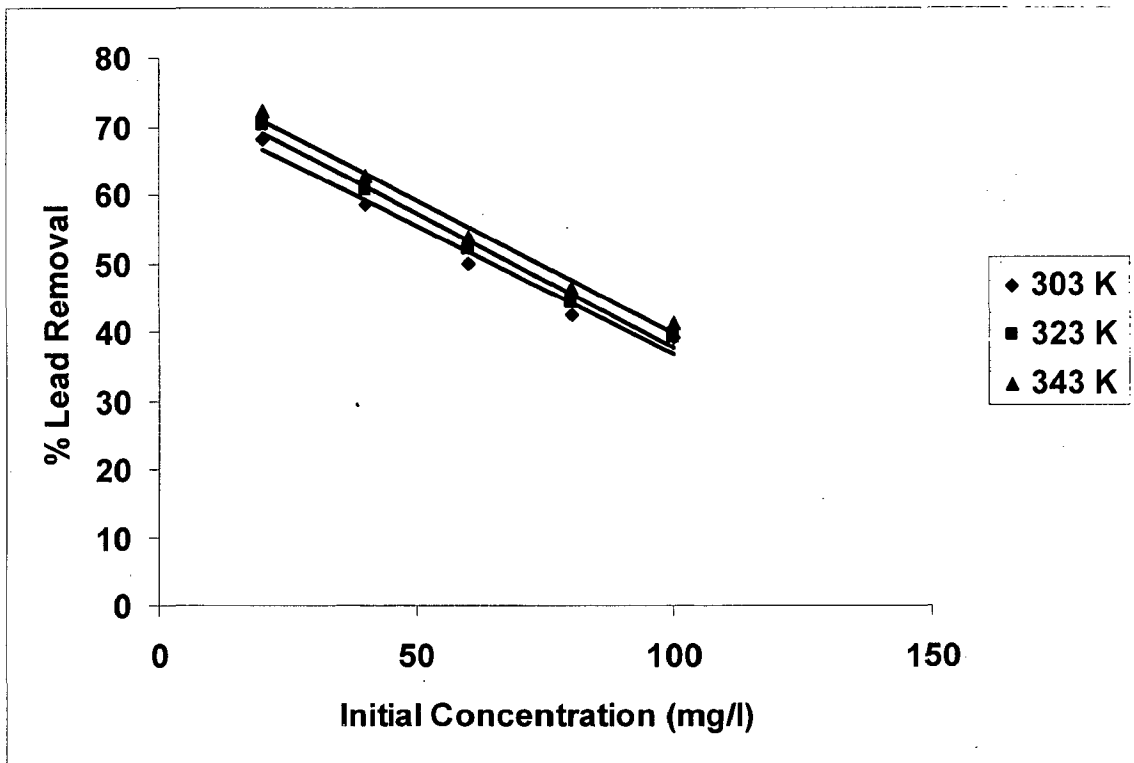


Fig. B - 20: Effect of temperature on removal of Pb(II) by using CJAC
($t = 4$ h, pH=5, dose=1 g/l).

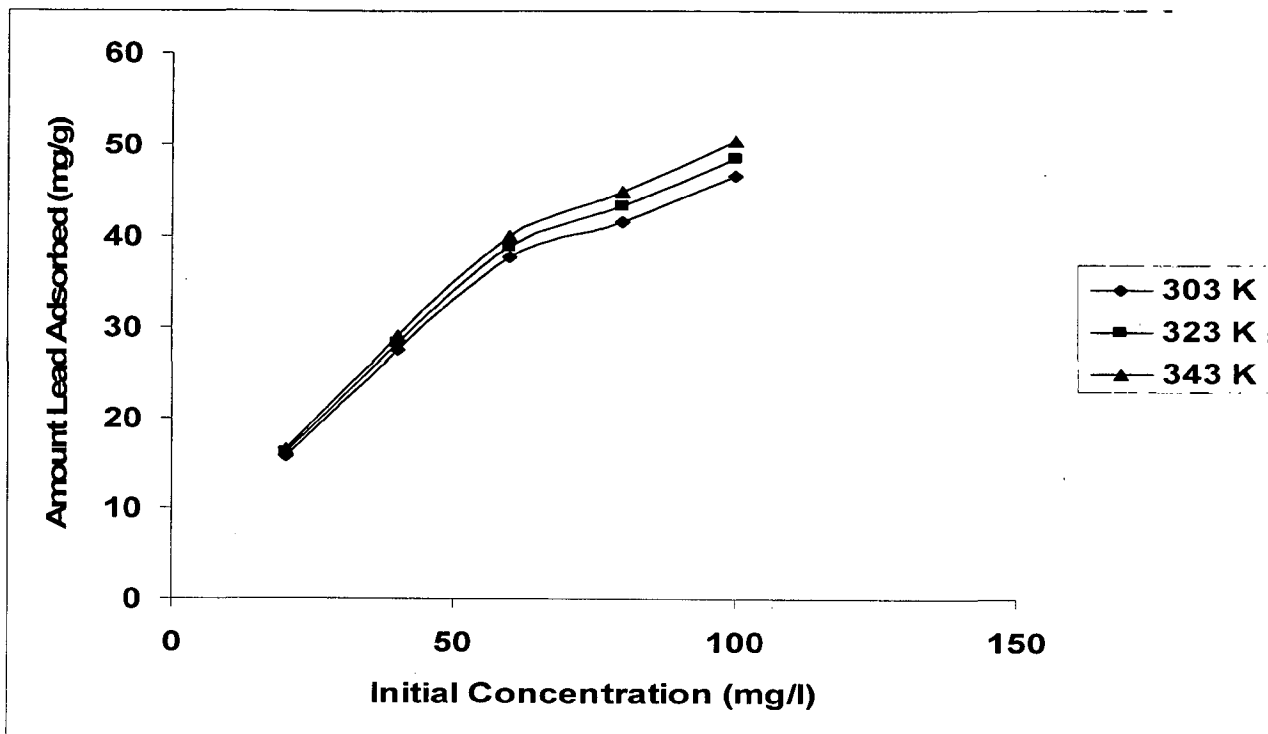


Fig. B - 21: Effect of temperature on removal of Pb(II) by using CAC
 ($t = 4$ h, $\text{pH}=4.2$, $\text{dose}=1$ g/l).

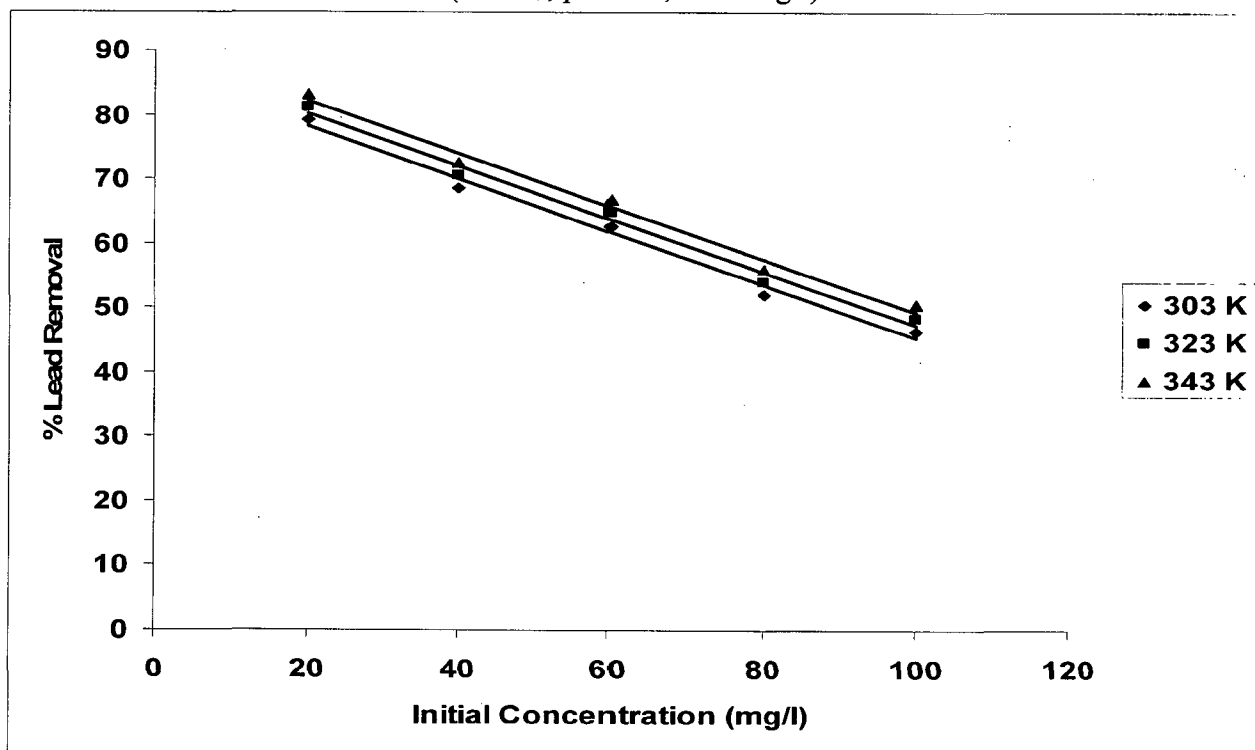


Fig. B - 22: Effect of temperature on removal of Pb(II) by using CAC
 ($t = 4$ h, $\text{pH}=4.2$, $\text{dose}=1$ g/l).

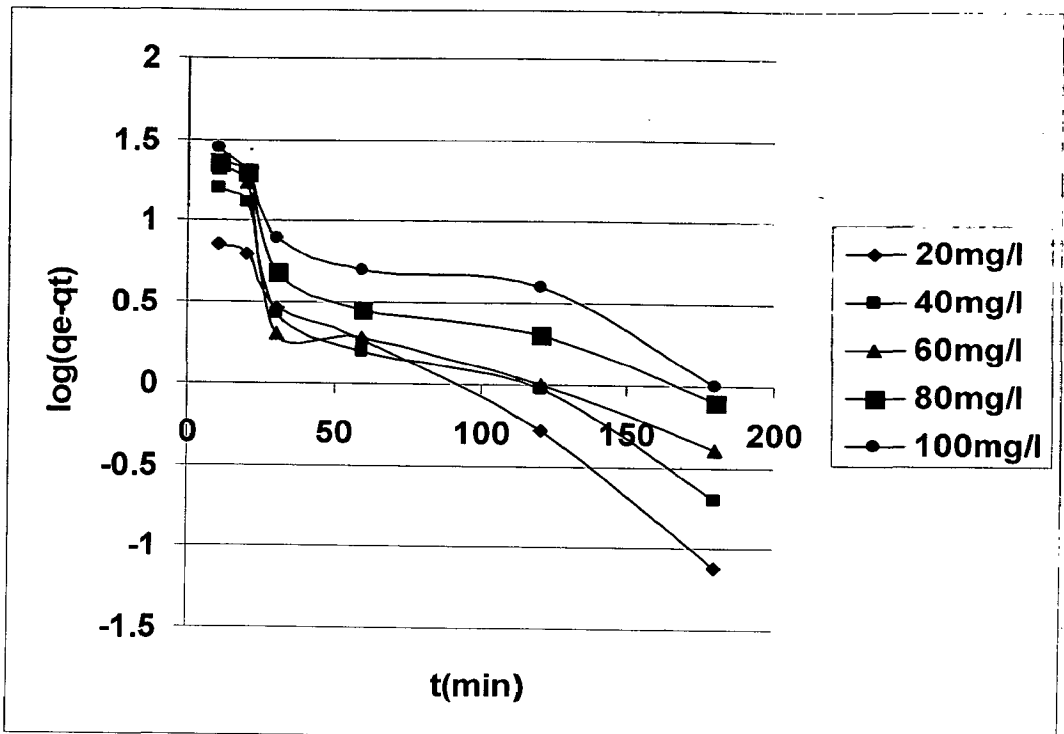


Fig. B - 23: Pseudo - First Order Kinetics for the removal of Pb(II) for CJAC (T= 303 K, dose =1 g/l, pH=5, t=4h).

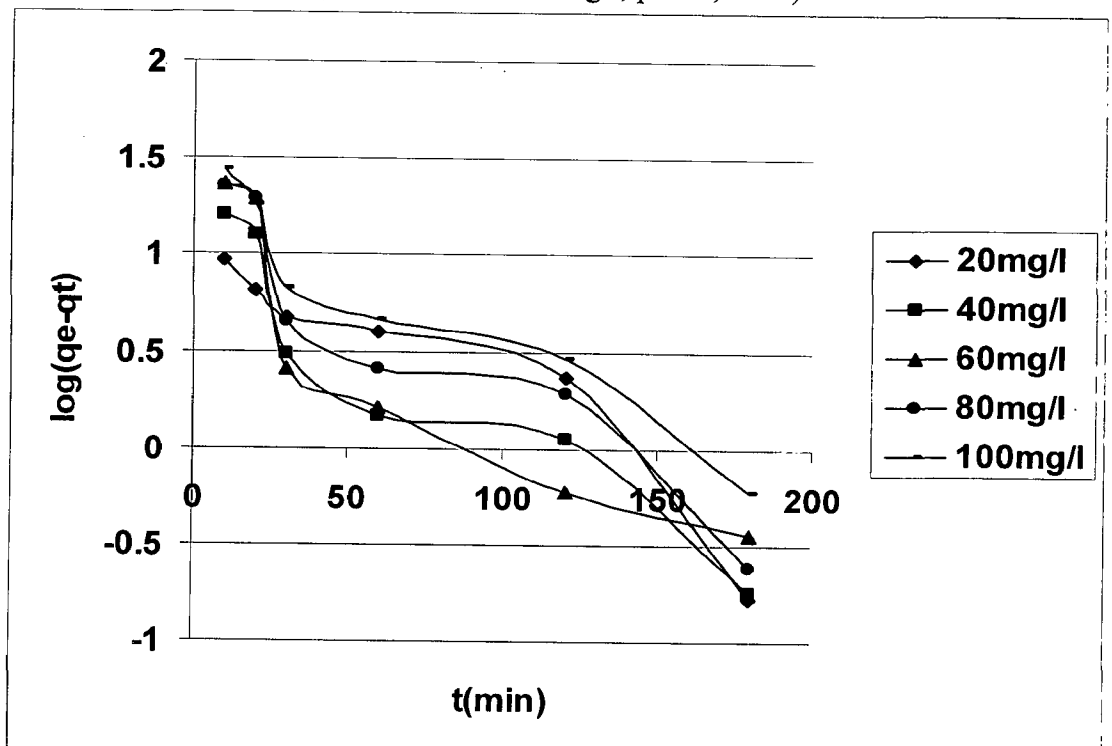


Fig. B - 24: Pseudo - First Order Kinetics for the removal of Pb(II) for CAC (T= 303 K, dose =1 g/l, pH=4.2, t=4h).

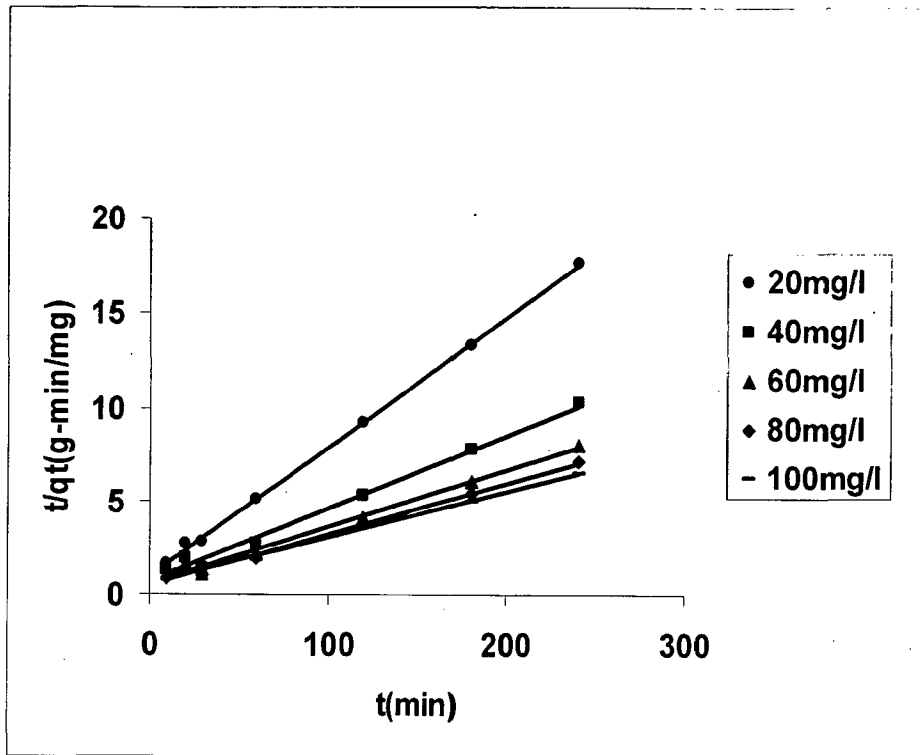


Fig. B - 25: Pseudo - Second Order Kinetics for the removal of Pb(II) for CJAC (T= 303 K, dose =1 g/l, pH=5, t=4h).

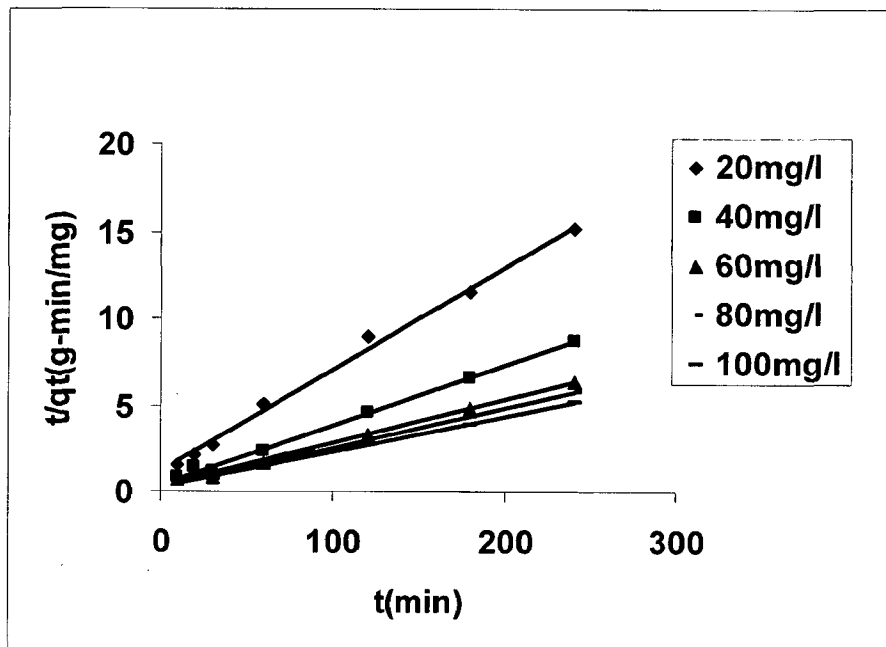


Fig. B - 26: Pseudo - Second Order Kinetics for the removal of Pb(II) for CAC (T= 303 K, dose =1 g/l, pH=4.2, t=4h).

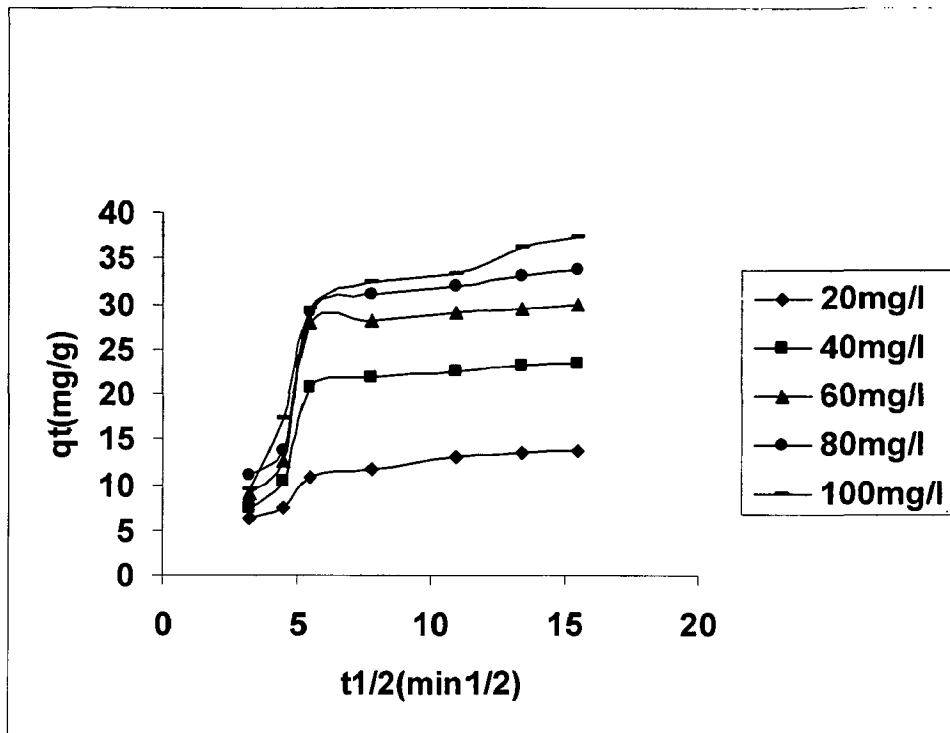


Fig. B - 27: Intra-particle diffusion model for the removal of Pb(II) for CJAC (T= 303 K, dose =1 g/l, pH=5, t=4h).

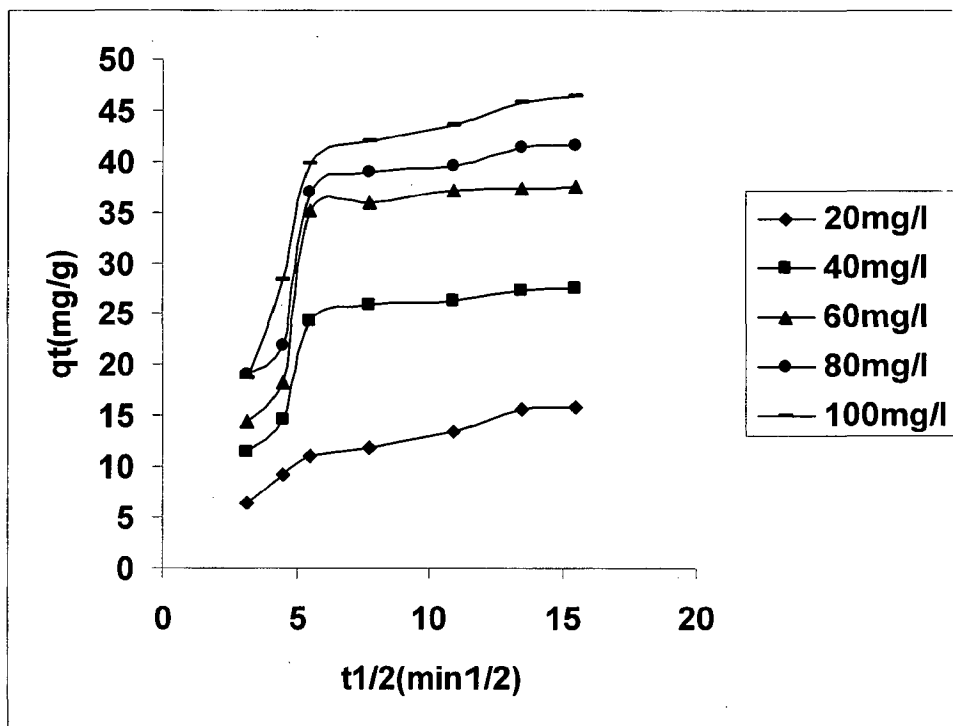


Fig. B - 28: Intra-particle diffusion model for the removal of Pb(II) for CAC (T= 303 K, dose =1 g/l, pH=4.2, t=4h).

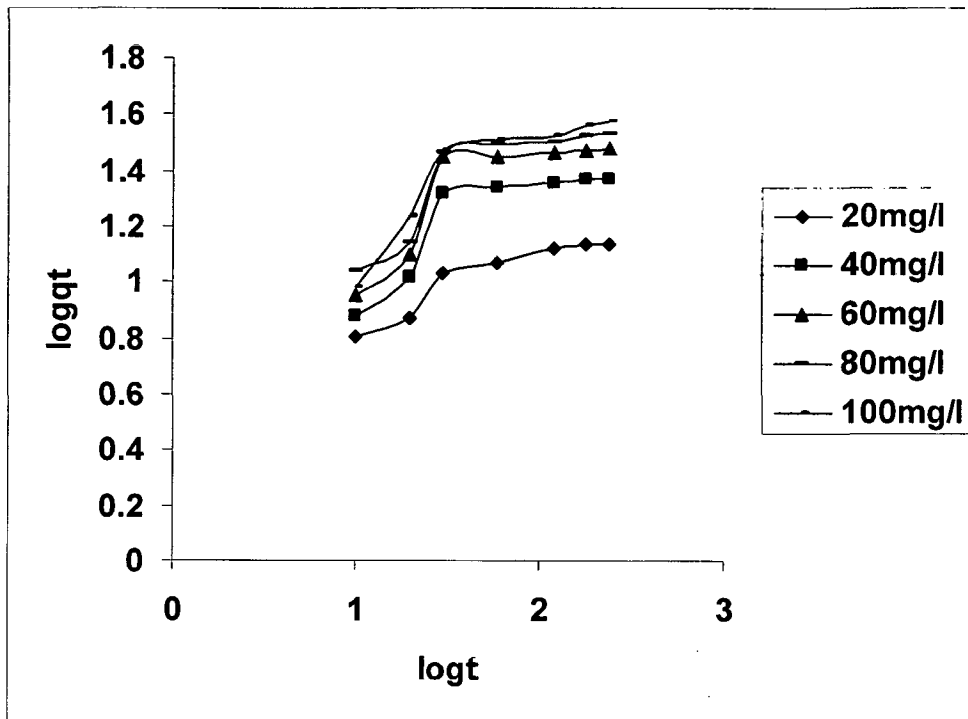


Fig. B - 29: Bangham's model for the removal of Pb(II) for CJAC (T= 303 K, dose =1 g/l, pH=5, t=4h).

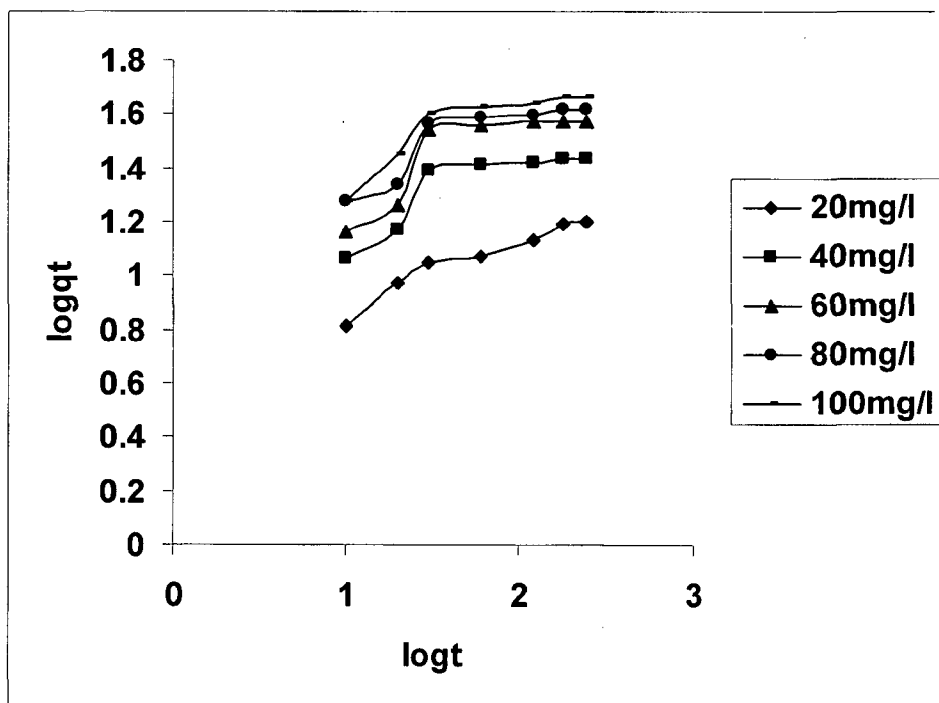


Fig. B - 30: Bangham's model for the removal of Pb(II) for CAC (T= 303 K, dose =1 g/l, pH=4.2, t=4h).

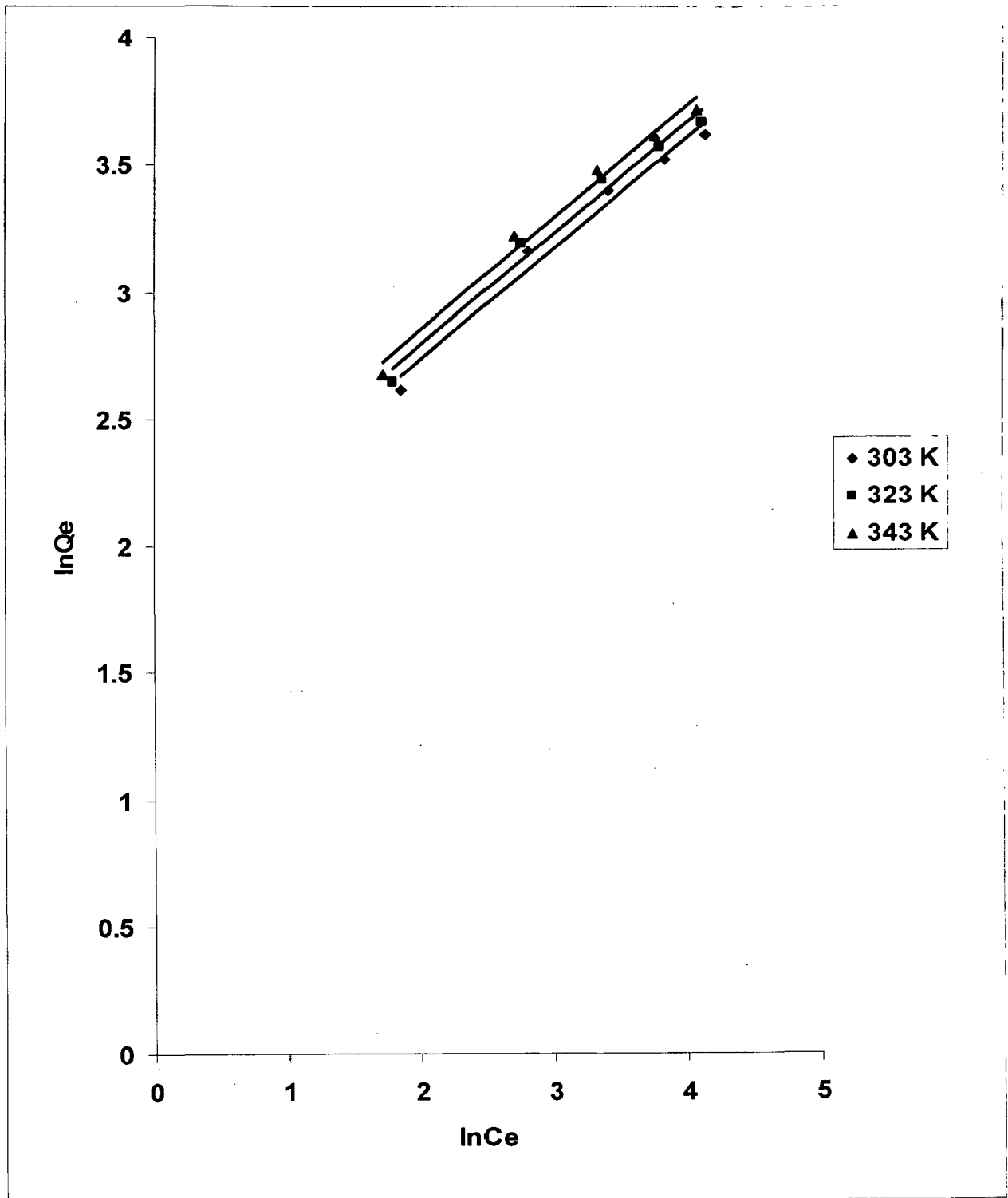


Fig. B - 31: Freundlich isotherm plots for the removal of Pb(II) for CJAC

($t=4$ h, dose = 1 g/l, pH=5, $C_0 = 20, 40, 60, 80$ and 100 mg/l).

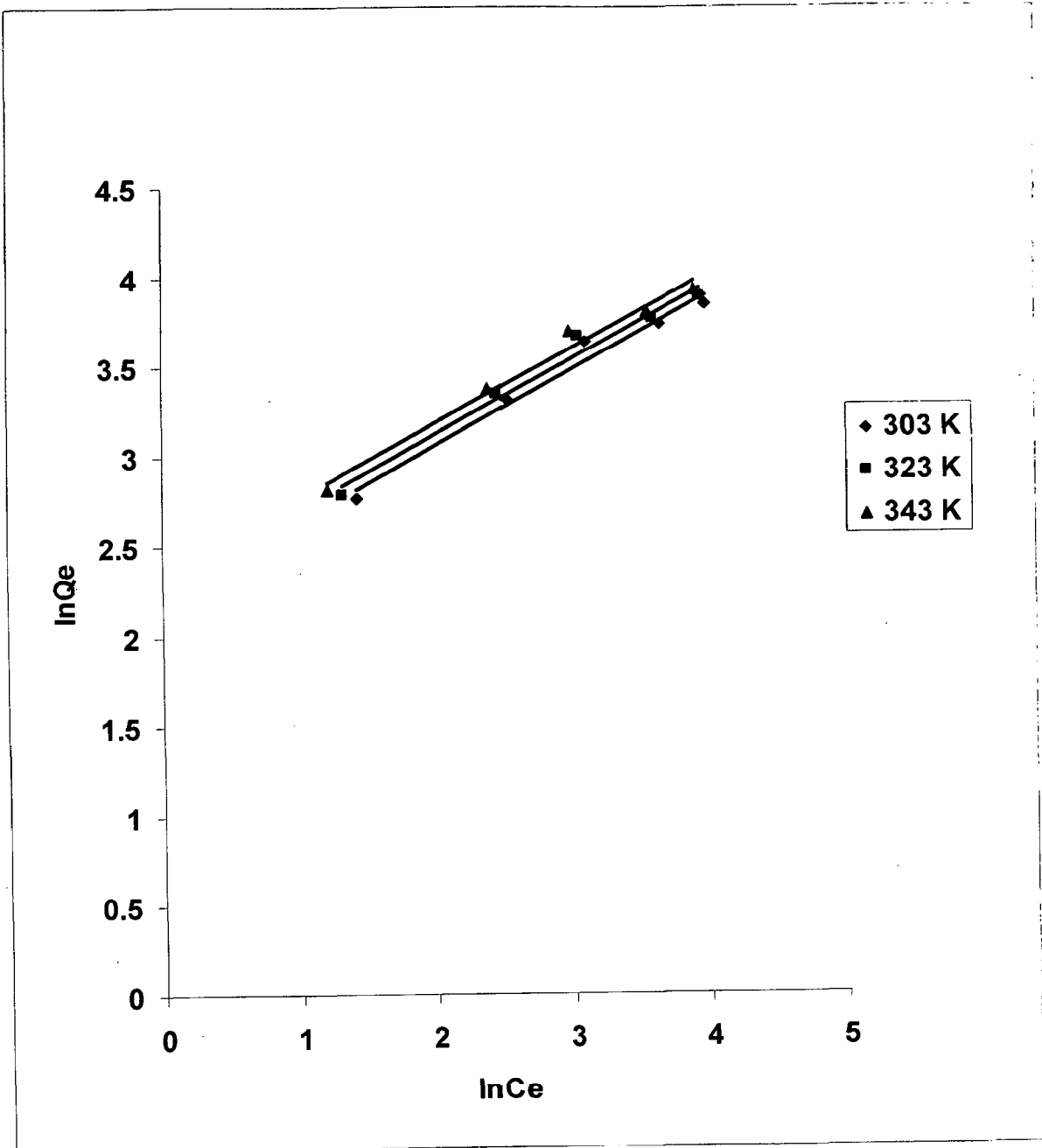


Fig. B - 32: Freundlich isotherm plots for the removal of Pb(II) for CAC

($t=4$ h, dose = 1 g/l, pH=4.2, $C_0 = 20, 40, 60, 80$ and 100 mg/l).

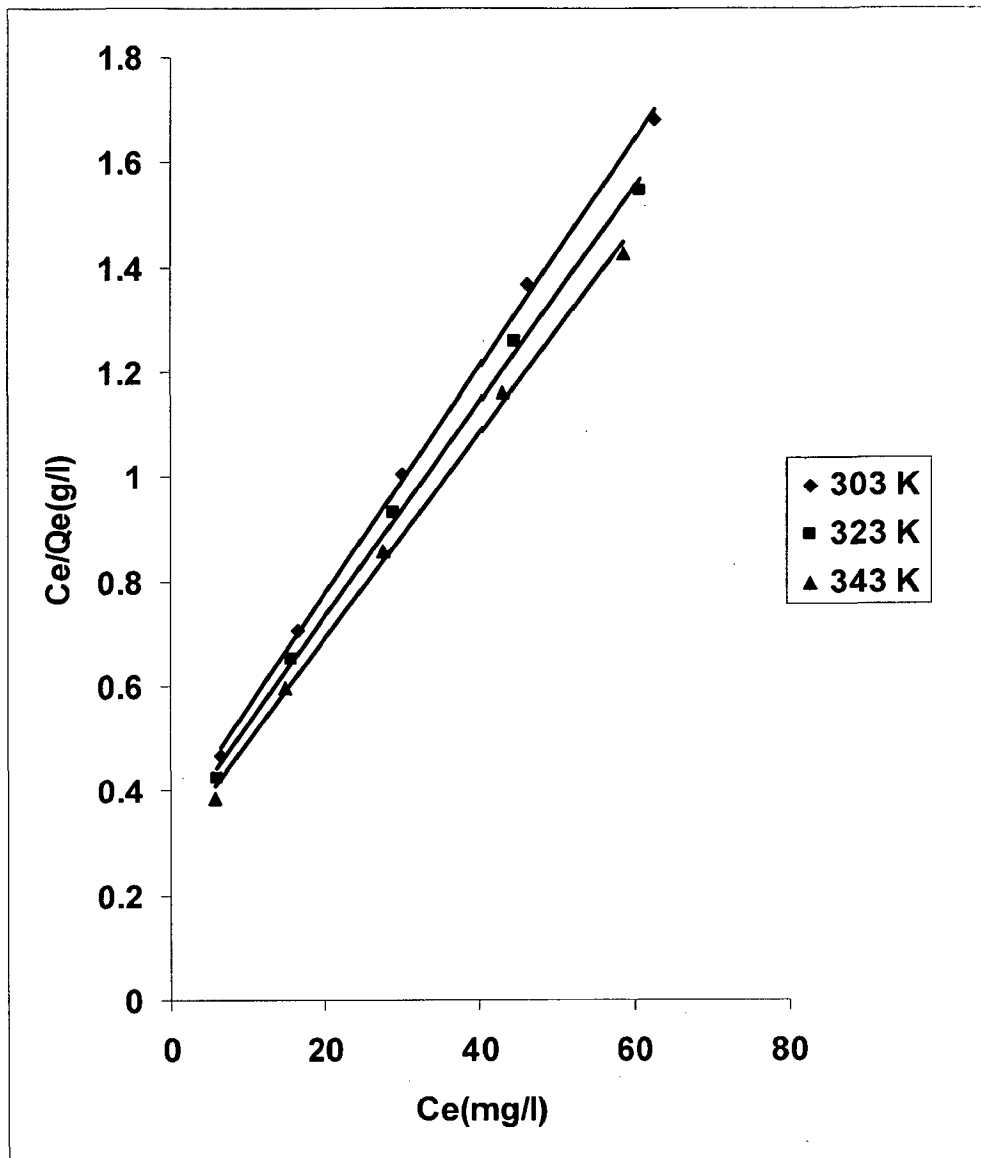


Fig. B - 33: Langmuir isotherm plots for the removal of Pb(II) for CJAC

($t=4$ h, dose = 1 g/l, pH=5, $C_0 = 20, 40, 60, 80$ and 100 mg/l).

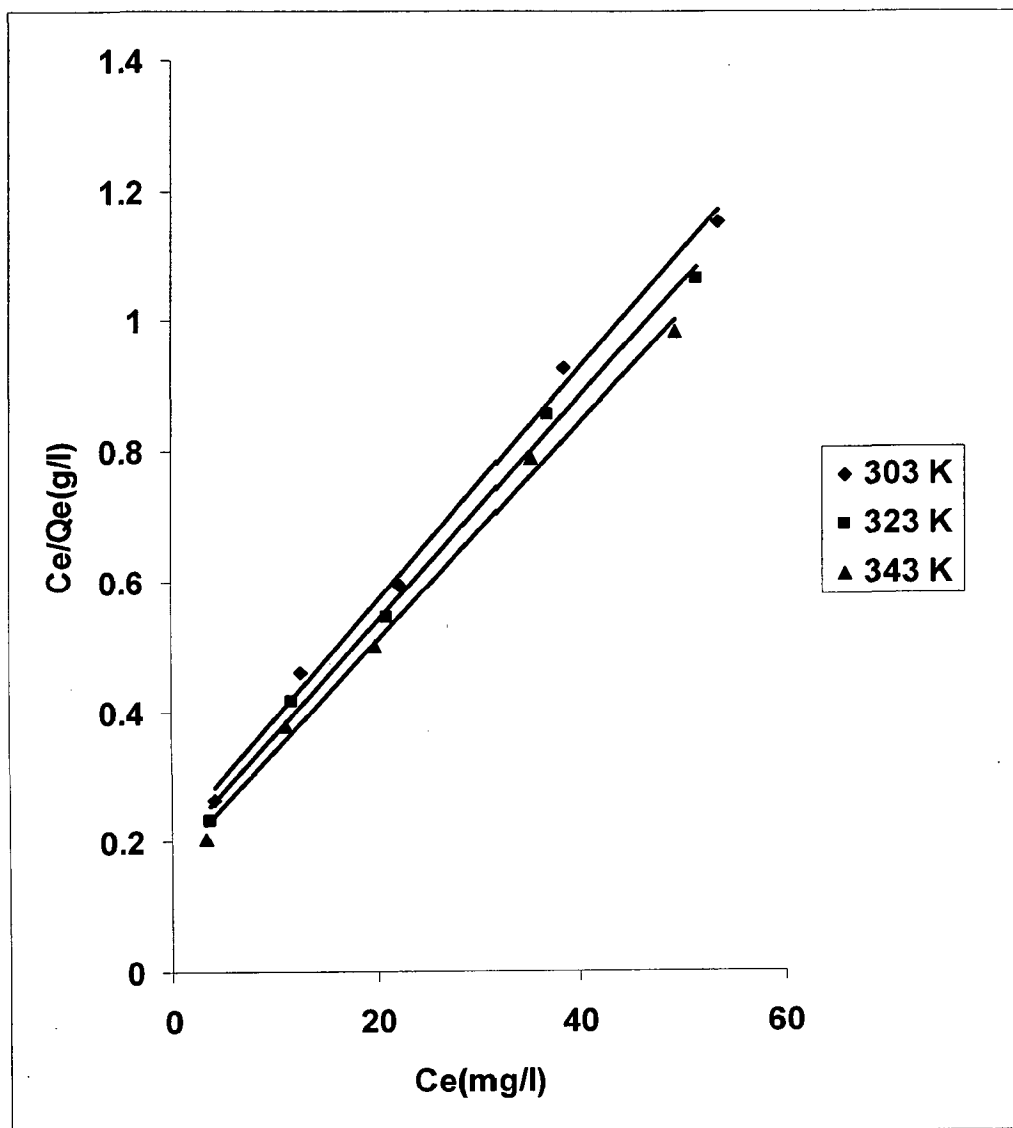


Fig. B - 34: Langmuir isotherm plots for the removal of Pb(II) for CAC

($t=4$ h, dose = 1 g/l, pH=4.2, $C_0 = 20, 40, 60, 80$ and 100 mg/l).

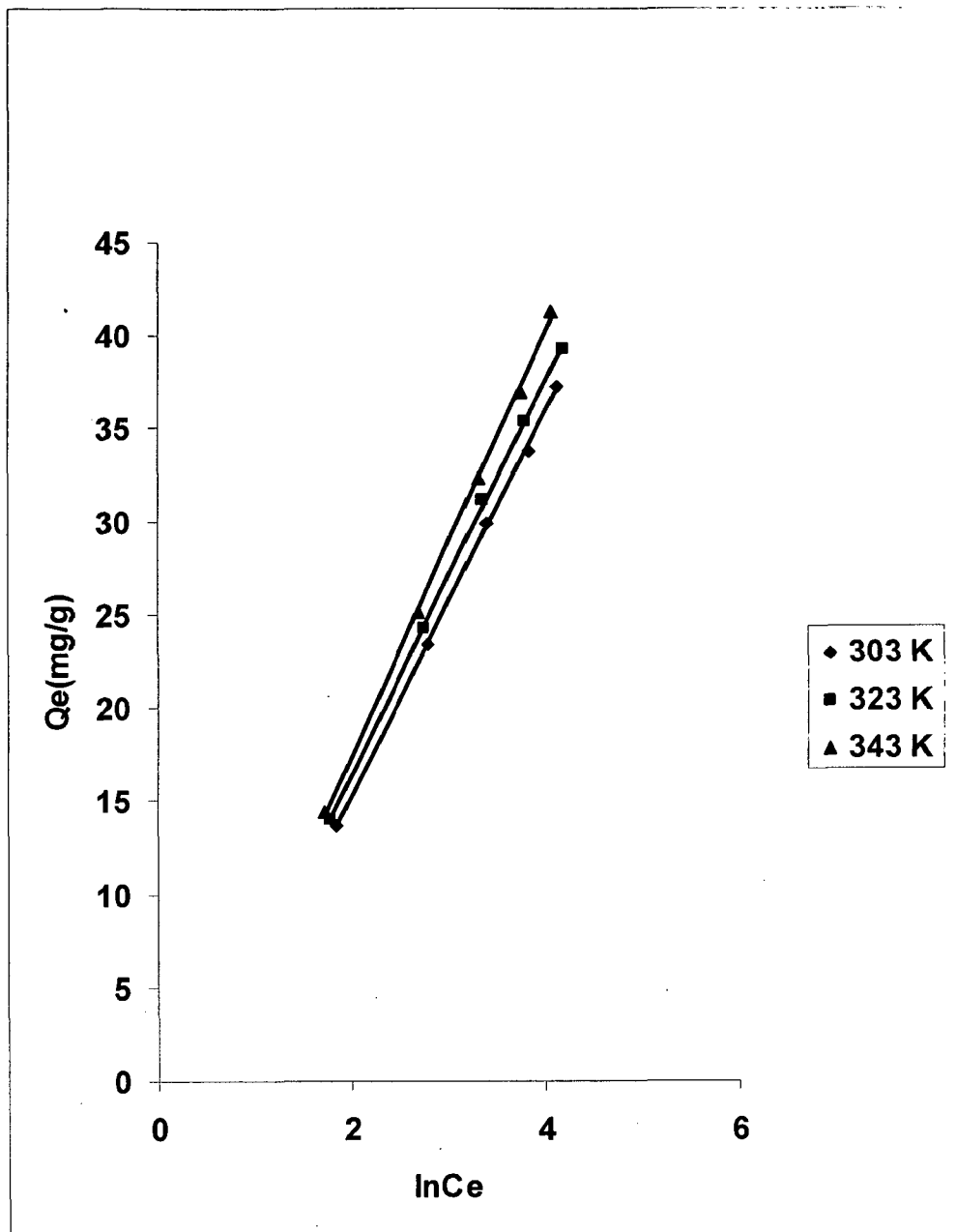


Fig. B - 35: Temkin isotherm plots for the removal of Pb(II) for CJAC

($t=4$ h, dose = 1 g/l, pH=5, $C_0 = 20, 40, 60, 80$ and 100 mg/l).

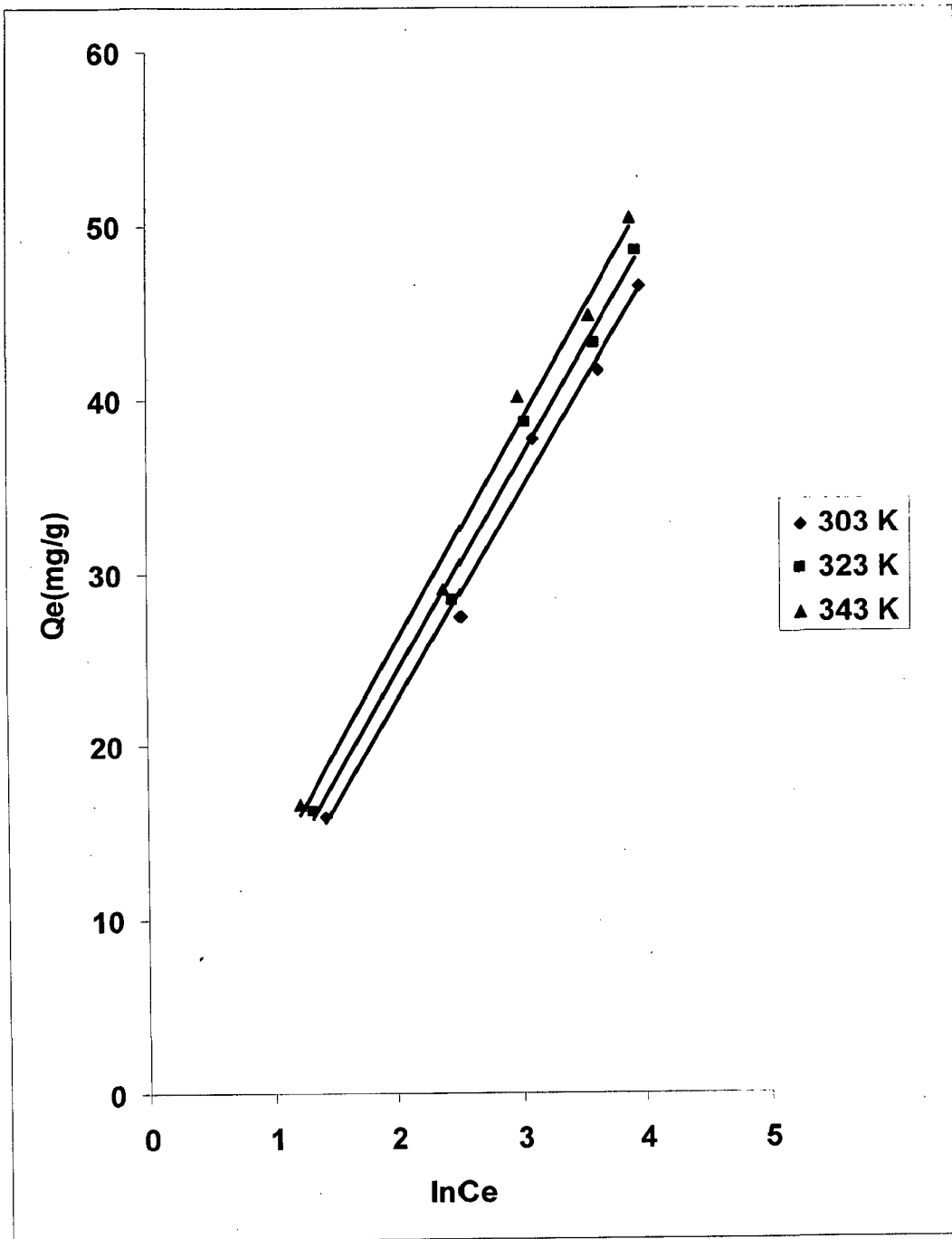


Fig. B - 36: Temkin isotherm plots for the removal of Pb(II) for CAC

($t=4$ h, dose = 1 g/l, pH=4.2, $C_0 = 20, 40, 60, 80$ and 100 mg/l).

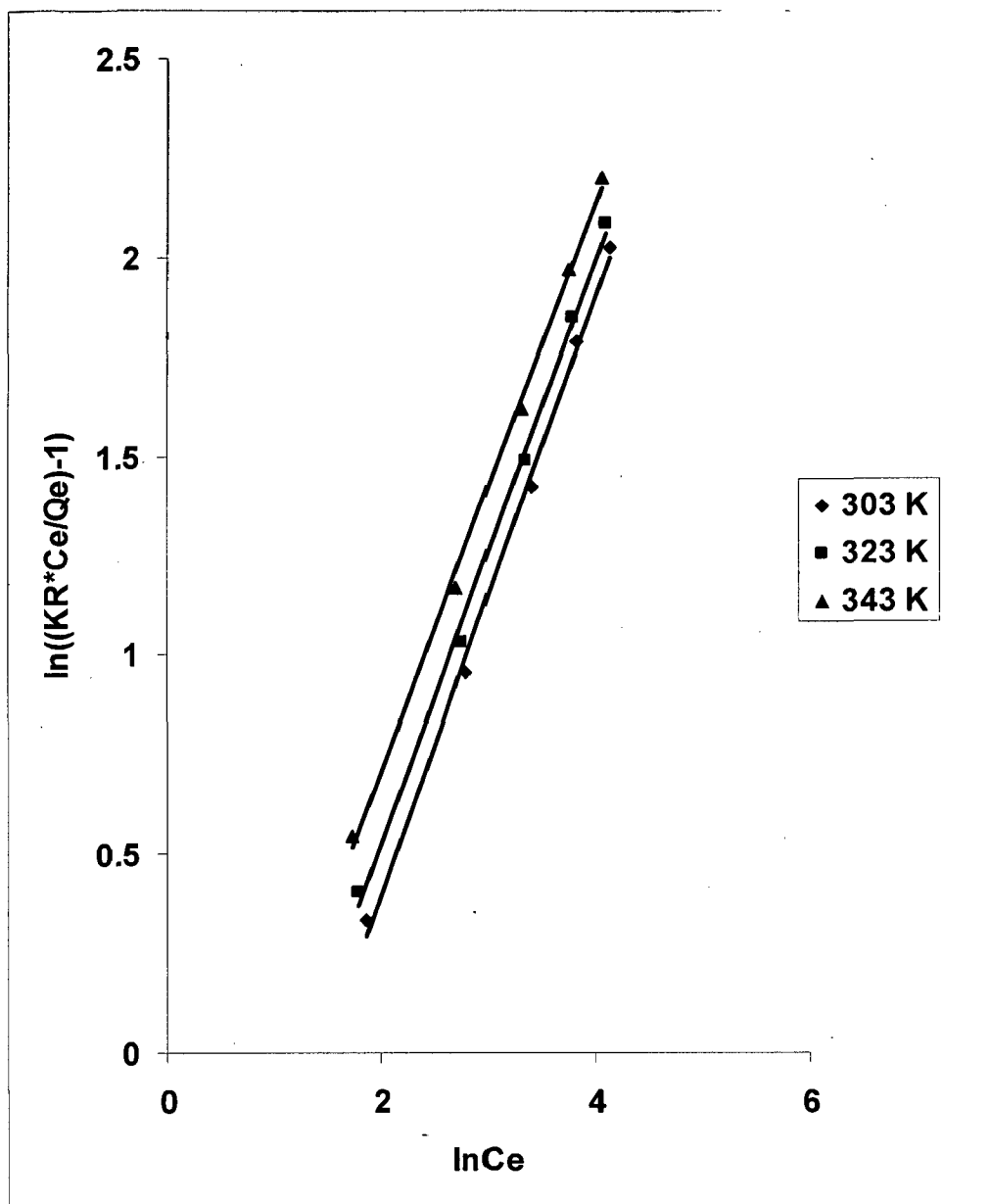


Fig. B - 37: Redlich-Peterson isotherm plots for the removal of Pb(II) for CJAC

($t=4$ h, dose = 1 g/l, pH=5, $C_0 = 20, 40, 60, 80$ and 100 mg/l).

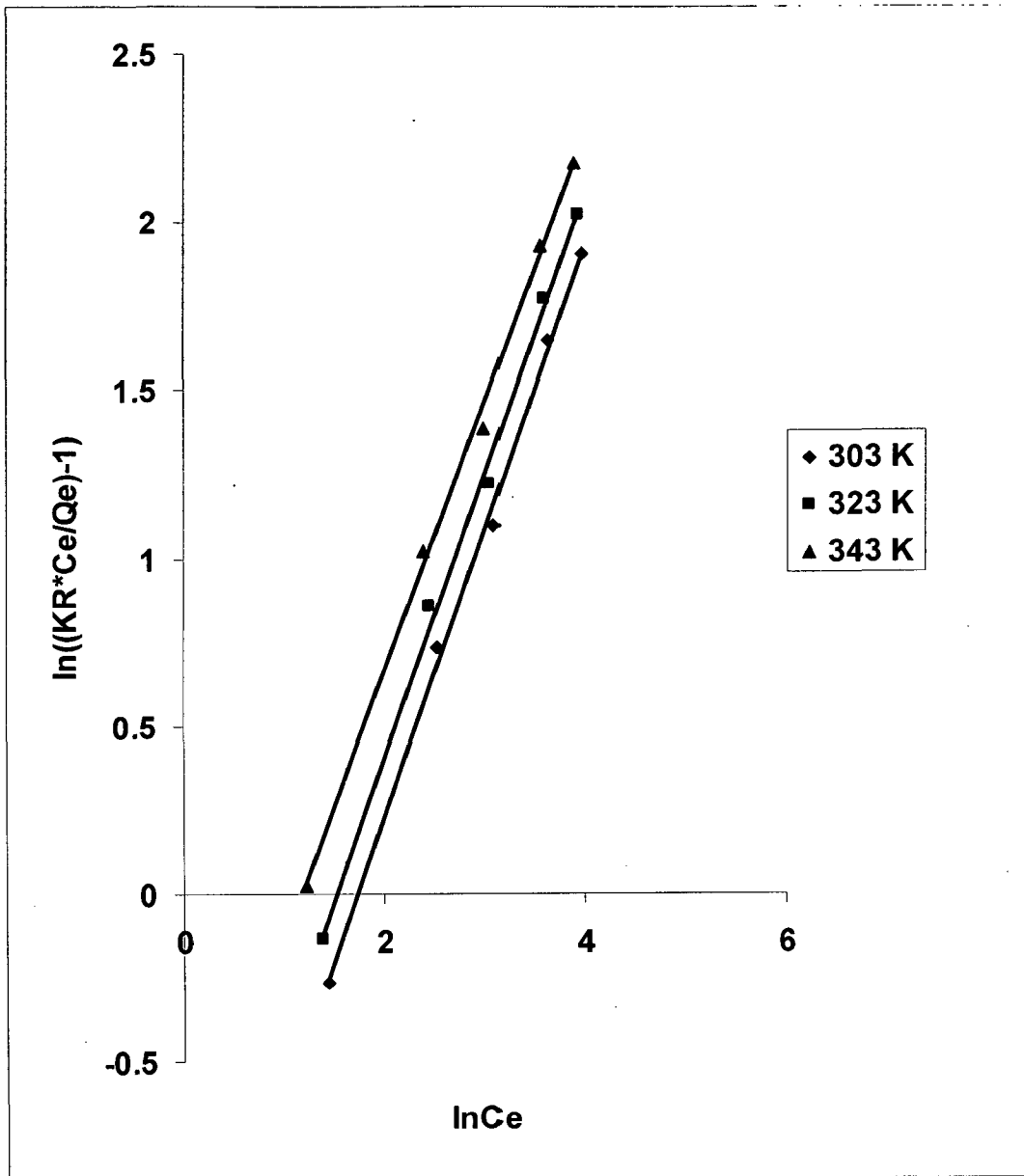


Fig. B - 38: Redlich-Peterson isotherm plots for the removal of Pb(II) for CAC

($t=4$ h, dose = 1 g/l, pH=4.2, $C_0 = 20, 40, 60, 80$ and 100 mg/l).

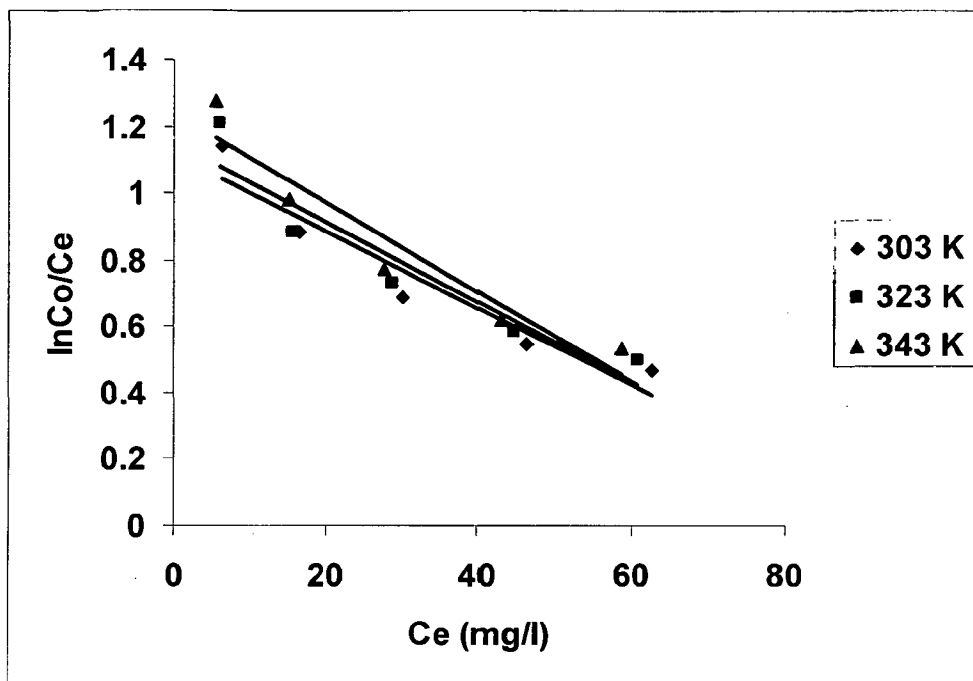


Fig. B - 39: Thermodynamic equilibrium constant values at different temperatures for CJAC
 (t=4 h, dose = 1 g/l, pH=5).

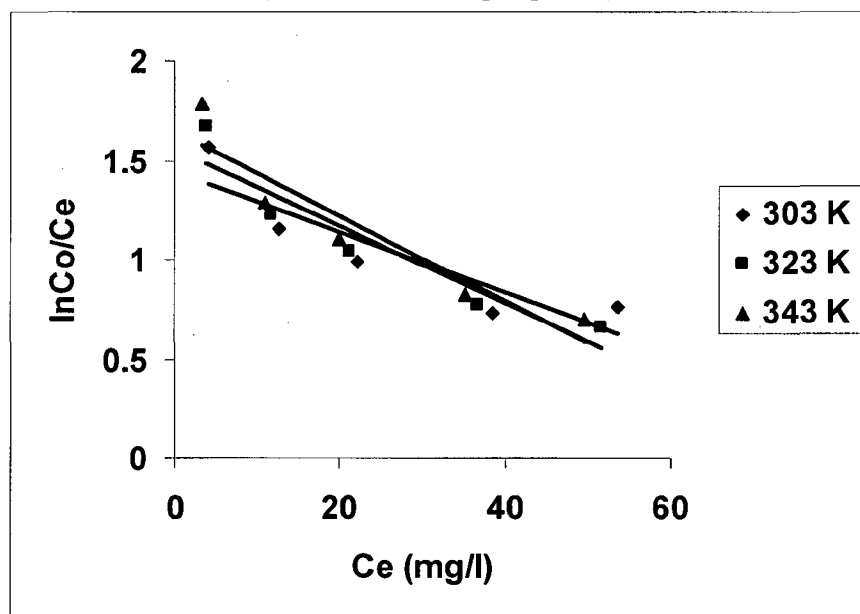


Fig. B - 40: Thermodynamic equilibrium constant values at different temperatures for CAC
 (t=4 h, dose = 1 g/l, pH=4.2).

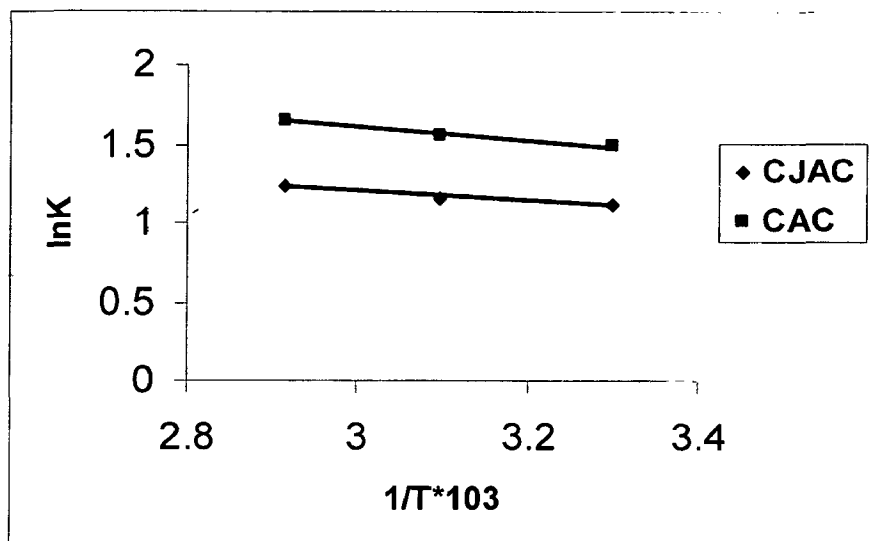


Fig. B- 41: Vant Hoff's plot

APPENDIX – C

Table C - 1: Characteristics of Coconut Jute Activated Carbon

Proximate Analysis		Physical Properties
Moisture Percentage	0.188	Bulk density (Kg/m ³) 318.90
Ash Percentage	0.032	
Volatile matter Percentage	0.209	
Fixed carbon Percentage	0.571	

Table C - 2: Characteristics of Commercial Activated Carbon

Proximate Analysis		Physical Properties
Moisture Percentage	0.082	Bulk density (Kg/m ³) 268.70
Ash Percentage	0.164	
Volatile matter Percentage	0.043	
Fixed carbon Percentage	0.711	

Kinetic parameters for the removal of Pb(II) from waste water by CJAC ($pH_0 = 5$, $T = 303$ K, $C_0 = 20, 40, 60, 80$ and 100 mg/l, dose = 1 g/l) and CAC ($pH_0=4.2$, $T=303$ K, $C_0= 20, 40, 60, 80$ and 100 mg/l, dose = 1 mg/l).

Table C - 3: Pseudo-first-order model

Pseudo-first-order model					
Adsorbent	Initial Concentration (mg/l)	k_f (min^{-1})	q_e (mg/g)		R^2
			q_e (Cal)	q_e (Exp)	
CJAC	20	0.0258	8.8145	13.6250	0.9844
	40	0.0233	11.8522	23.4500	0.8759
	60	0.0205	12.0642	29.9000	0.7571
	80	0.0179	16.1622	33.8000	0.8201
	100	0.0168	21.7220	37.2500	0.8864
CAC	20	0.0205	11.5931	15.8320	0.8892
	40	0.0235	12.2885	27.4300	0.8808
	60	0.0230	13.6500	37.6500	0.7917
	80	0.0237	19.1778	41.5600	0.8874
	100	0.0196	21.5179	46.4500	0.9103

Table C - 4 : Pseudo-second order model

Adsorbent	Conc(mg/l)	$q_{e,exp}$ (mg/g)	$q_{e,cal}$ (mg/g)	h (mg/g.min)	k_s (g/mg.min)	R^2
CJAC	20	13.625	14.6627	1.0081	0.0047	0.9983
	40	23.45	26.1780	1.3428	0.0019	0.9843
	60	29.9	33.5570	1.6377	0.0014	0.9773
	80	33.8	37.3734	1.8241	0.0013	0.9818
	100	37.25	40.9836	1.7504	0.0010	0.9860
CAC	20	15.832	16.5837	0.9199	0.0033	0.9910
	40	27.43	29.4118	2.2717	0.0026	0.9943
	60	37.65	40.9836	2.8281	0.0017	0.9885
	80	41.56	44.2478	3.5373	0.0018	0.9942
	100	46.45	49.0196	3.9385	0.0016	0.9974

Table C - 5 : Weber-Morris Intra-particle diffusion model

Adsorbent	Conc (mg/l)	$k_{id,I}(\text{mg/g} \cdot \text{min}^{1/2})$	C,I (mg/g)	R^2,I	$k_{id,II}(\text{mg/g} \cdot \text{min}^{1/2})$	C,II (mg/g)	R^2,II
CJAC							
	20	1.8269	0.1989	0.8759	0.2452	10.0880	0.8849
	40	5.5486	-11.3840	0.8529	0.2111	20.2630	0.9760
	60	7.8934	-18.0320	0.8304	0.2470	26.1350	0.9940
	80	7.4974	-14.8340	0.8073	0.3694	28.0030	0.9811
	100	8.4642	-18.2760	0.9594	0.6914	26.5210	0.9377
CAC							
	20	1.9894	0.2805	0.9970	0.5570	7.5790	0.9493
	40	5.3995	-6.7319	0.8800	0.2061	24.284	0.9288
	60	8.6167	-15.0390	0.8328	0.2018	34.6040	0.9447
	80	7.5004	-6.8208	0.8108	0.3627	36.0630	0.9279
	100	8.9857	-10.3220	0.9844	0.6259	36.9800	0.9733

Table C - 6: Bangham's model

Adsorbent	Conc (mg/l)	$k_r(\text{mg/g} \cdot \text{min})$	1/m	R^2
CJAC				
	20	3.9700	0.2419	0.8844
	40	4.3924	0.3371	0.7423
	60	5.2264	0.3523	0.7084
	80	6.0940	0.3415	0.7532
	100	5.5706	0.3763	0.7811
CAC				
	20	4.0973	0.2557	0.9345
	40	7.5910	0.2577	0.7605
	60	9.1432	0.2863	0.7166
	80	12.3481	0.2420	0.7621
	100	13.2404	0.2494	0.7824

Isotherm parameters for the removal of Pb(II) from waste water by CJAC ($pH_0 = 5$, $T = 303\text{ K}, 323\text{ K}, 343\text{ K}$, dose = 1 g/l) and CAC ($pH_0=4.2, T=303\text{ K}, 323\text{ K}, 343\text{ K}$, dose = 1 mg/l).

Table C - 7: Langmuir Constants (CJAC)

Adsorbent	Constant	T=303 K	T=323 K	T=343 K
CJAC				
	$K_L(\text{l/mg})$	0.0631	0.0641	0.0656
	$q_m(\text{mg/g})$	46.0829	48.5437	51.0204
	R_L	0.4421	0.4382	0.4395
	$R^2(\text{linear})$	0.9988	0.9981	0.9974
	$R^2(\text{non-linear})$	0.9994	0.9991	0.9987

Table C - 8: Langmuir Constants (CAC)

Adsorbent	Constant	T=303 K	T=323 K	T=343 K
CAC				
	$K_L(\text{l/mg})$	0.0806	0.0926	0.0989
	$q_m(\text{mg/g})$	55.5555	57.4713	59.5238
	R_L	0.3655	0.3506	0.3358
	$R^2(\text{linear})$	0.9957	0.9953	0.9943
	$R^2(\text{non-linear})$	0.9978	0.9976	0.9972

Table C - 9: Freundlich Constants (CJAC)

Adsorbent	Constant	T=303 K	T=323 K	T=343 K
CJAC				
	$K_F((\text{mg/g})/(\text{mg/l})^{1/n})$	6.6.3949	6.7087	7.0696
	n	2.2826	2.2635	2.2527
	$1/n$	0.4381	0.4418	0.4439
	$R^2(\text{linear})$	0.9794	0.9822	0.9846
	$R^2(\text{non-linear})$	0.9896	0.9911	0.9823

Table C - 10: Freundlich Constants (CAC)

Adsorbent	Constant	T=303 K	T=323 K	T=343 K
CAC				
	$K_F((\text{mg/g})/(\text{mg/l})^{1/n})$	9.0739	9.7406	10.4793
	n	2.3552	2.3769	2.4067
	$1/n$	0.4246	0.4207	0.4155
	$R^2(\text{linear})$	0.9757	0.9782	0.9810
	$R^2(\text{non-linear})$	0.9878	0.9892	0.9904

Table C-11: Tempkin Constants (CJAC)

Adsorbent	Constant	303 K	323 K	343 K
CJAC				
	B	10.2950	10.8190	9.1554
	K_T (l/mg)	0.5911	0.6065	1.3093
	R^2 (linear)	0.9996	0.9996	0.9806
	R^2 (non-linear)	0.9998	0.9998	0.9995

Table C - 12: Tempkin Constants (CAC)

Adsorbent	Constant	303 K	323 K	343 K
CAC				
	B	12.0660	12.3550	12.6140
	K_T (l/mg)	0.8702	0.9516	1.0565
	R^2 (linear)	0.9897	0.9919	0.9897
	R^2 (non-linear)	0.9948	0.9949	0.9948

Table C - 13: Redlich-Peterson Constants (CJAC)

Adsorbent	Constant	303 K	323 K	343 K
CJAC				
	a_R (l/mg)	0.3363	0.3864	0.4951
	K_R (l/mg)	5.1100	5.8500	7.0500
	β	0.7469	0.7338	0.7073
	R^2 (linear)	0.9969	0.9976	0.9974
	R^2 (non-linear)	0.9985	0.9986	0.9987

Table C - 14: Redlich-Peterson Constants (CAC)

Adsorbent	Constant	303 K	323 K	343 K
CAC				
	a_R (l/mg)	0.2317	0.2949	0.3924
	K_R (l/mg)	6.7200	8.0600	10.0010
	β	0.8463	0.8227	0.7969
	R^2 (linear)	0.9970	0.9972	0.9973
	R^2 (non-linear)	0.9985	0.9986	0.9986

Values of five different error analyses of isotherm models for adsorption of Pb(II).

Table C - 15: Error Analysis for CJAC

303 K					
	SSE	HYBRID	MPSD	ARE	SAE
Freundlich	9.3658	-0.0931	4.3414	4.8132	6.2803
Langmuir	0.7292	0.1912	1.4015	1.4152	1.7562
R-P	2.3533	0.0019	2.0909	2.3818	3.2286
Temkin	0.1351	-0.0114	0.4476	0.4220	0.6225
323 K					
	SSE	HYBRID	MPSD	ARE	SAE
Freundlich	9.0917	-0.0863	4.1163	4.5725	6.2111
Langmuir	1.2496	0.3146	1.8706	1.8555	2.3367
R-P	2.0861	-0.0731	1.9505	2.2397	3.0963
Temkin	0.1791	0.0226	0.5372	0.6196	0.8818
343 K					
	SSE	HYBRID	MPSD	ARE	SAE
Freundlich	8.7638	-0.0643	3.9028	4.3385	6.1191
Langmuir	1.9948	0.3623	2.3520	2.3252	2.9944
R-P	2.3975	0.0003	1.9780	2.2538	3.2836
Temkin	21.56	-4.6832	10.5326	8.1067	8.1205

Table C - 16: Error Analysis for CAC

303 K					
	SSE	HYBRID	MPSD	ARE	SAE
Freundlich	25.7860	-0.8266	5.9184	6.2935	10.0320
Langmuir	6.4960	0.3502	3.6970	3.9019	5.5365
R-P	5.7629	-0.0439	2.5531	2.3235	4.0381
Temkin	6.1671	-0.0334	2.8840	2.8090	4.4519
323 K					
	SSE	HYBRID	MPSD	ARE	SAE
Freundlich	21.6030	-0.2149	4.6092	5.0066	8.9456
Langmuir	16.8420	-1.9063	5.0109	5.1100	7.8228
R-P	4.7483	-0.1060	2.2643	2.1075	3.7593
Temkin	5.3396	0.0304	2.7915	2.8859	4.5415
343 K					
	SSE	HYBRID	MPSD	ARE	SAE
Freundlich	23.0630	-0.1081	4.5444	4.7888	8.9804
Langmuir	10.4310	0.5600	4.9820	4.7971	6.7575
R-P	6.6281	-0.0458	2.5783	2.3453	4.3337
Temkin	7.4915	0.0532	3.3059	3.4337	5.4884

Table C - 17: Thermodynamic parameters for adsorption of Pb(II) by CJAC and CAC

Adsorbent	$-\Delta G^0$ (kJ/mol K)			ΔH^0 (kJ/mol)	ΔS^0 (J/mol K)
	303 K	323 K	343K		
CJAC	2.8209	3.0971	3.5327	2.5441	17.6350
CAC	3.754	4.1949	3.4611	3.4611	23.7780

Fig. B-19	Effect of temperature on removal of lead on percent removal by CJAC	89
Fig. B-20	Effect of temperature on removal of lead on percent removal by CAC	89
Fig. B-21	Effect of temperature on removal of lead on amount adsorbed by CJAC	90
Fig. B-22	Effect of temperature on removal of lead on amount adsorbed by CJAC	90
Fig. B-23	First order kinetics for removal of lead by CJAC	91
Fig. B-24	First order kinetics for removal of lead by CAC	91
Fig. B-25	Pseudo second order plot for removal of lead by CJAC	92
Fig. B-26	Pseudo second order plot for removal of lead by CAC	92
Fig. B-27	Weber Morris plot for removal of lead by CJAC	93
Fig. B-28	Weber Morris plot for removal of lead by CAC	93
Fig. B-29	Bangham's plot for removal of lead by CJAC	94
Fig. B-30	Bangham's plot for removal of lead by CAC	94
Fig. B-31	Freundlich Isotherm plot for lead with CJAC	95
Fig. B-32	Freundlich Isotherm plot for lead with CAC	96
Fig. B-33	Langmuir Isotherm plot for lead with CJAC	97
Fig. B-34	Langmuir Isotherm plot for lead with CAC	98
Fig. B-35	Temkin Isotherm plot for lead with CJAC	99
Fig. B-36	Temkin Isotherm plot for lead with CAC	100
Fig. B-37	Redlich-Peterson Isotherm plot for lead with CJAC	101
Fig. B-38	Redlich-Peterson Isotherm plot for lead with CAC	102
Fig. B-39	Thermodynamic equilibrium constant values and different temperatures for CJAC	103
Fig. B-40	Thermodynamic equilibrium constant values and different temperatures for CAC	103
Fig. B-41	Van't Hoff's plot for various isotherm models.	104